SEPTEMBER 2014 M.Sc. IN MECHANICAL ENGINEERING AHMED IBRAHEEM RAHEEM

UNIVERSITY OF GAZIANTEP

GRADUATE SCHOOL OF

NATURAL & APPLIED SCIENCES

PRESSURE GRADIENT PREDICTION OF OIL-WATER TWO PHASE FLOW THROUGH HORIZONTAL PIPE

M.Sc. THESIS

IN

MECHANICAL ENGINEERING

BY

AHMED IBRAHEEM RAHEEM

SEPTEMBER 2014

Pressure Gradient Prediction of Oil-Water Two Phase Flow through Horizontal Pipe

M.Sc. Thesis

In

Mechanical Engineering

University of Gaziantep

Supervisor

Prof. Dr. M. Yaşar GÜNDOĞDU

Co-supervisor

Assist. Prof. Dr. Fuat YILMAZ

By

Ahmed Ibraheem RAHEEM

September 2014

T.C.

UNIVERSITY OF GAZİANTEP
GRADUATE SCHOOL OF
NATURAL & APPLIED SCIENCES
MECHANICAL ENGINEERING DEPARTMENT

Name of the thesis: Pressure Gradient Prediction of Oil-Water Two-Phase Flow through Horizontal Pipe

Name of the student: Ahmed Ibraheem RAHEEM

Exam date: 16/09/2014

Approval of the Graduate School of Natural and Applied Sciences

Assoc. Prof. Dr. Metin BEDİR
Director

I certify that this thesis satisfies all the requirements as a thesis for the degree of Master of Science.

Prof. Dr. M. Sait SÖYLEMEZ
Head of Department

This is to certify that we have read this thesis and that in our opinion it is fully adequate, in scope and quality, as a thesis for the degree of Master of Science.

Prof. Dr. M. Yaşar GÜNDOĞDU
Supervisor

Assist. Prof. Dr. Fuat YILMAZ
Co-supervisor

Examining Committee Members

Prof. Dr. Melda ÇARPINLIOĞLU .....

Prof. Dr. M. Yaşar GÜNDOĞDU .....

Assist. Prof. Dr. Murtaza YILDIRIM .....

I hereby declare that all information in this document has been obtained and presented in accordance with academic rules and ethical conduct. I also declare that, as required by these rules and conduct, I have fully cited and referenced all materials that are not original to this work.

Ahmed Ibraheem RAHEEM

ABSTRACT

PRESSURE GRADIENT PREDICTION OF OIL-WATER TWO PHASE FLOW THROUGH HORIZONTAL PIPE

RAHEEM, Ahmed Ibraheem

M.Sc. In Mechanical Engineering

Supervisor: Prof. Dr. M. Yaşar GÜNDOĞDU

Co-supervisor: Assist. Prof. Dr. Fuat YILMAZ

September 2014, 116 pages

In this thesis, stratified and stratified wavy flow regimes have been investigated numerically for the oil (1.57 m Pa s viscosity and 780 kg/m^3 density) and water two-phase flow in small and large horizontal steel pipes with a diameter between 0.0254 to 0.508 m by ANSYS Fluent software. Volume of fluid (VOF) with two phases flows using two equations family models (Realizable k-**ε** and Shear Stress Transport k–ω (SST)) in turbulence modeling is applied used to simulate flow to obtain the hydrodynamic parameters effect of velocities in the range of 0.2-1.2 m/s, volume fraction of water in the range of 20-80 %; and diameters on the pressure gradient. The results show that the pipe diameter has a large effect on the pressure gradient. Furthermore, it was found that at 40 % and 60 % water volume fraction for large diameters, where stratified wavy flow patterns prevail, there is a peak in the pressure gradient during phase inversion. The pressure gradient is found by Shear Stress Transport k–ω turbulence model better than those found by Realizable k-**ε** turbulence model according to compare with published experimental studies.

Keywords: *CFD, two-phase flow, pressure gradient, volume of fluid, large diameter, horizontal pipe, oil-water stratified and stratified wavy flow.*

ÖZET

YATAY BORU KULLANARAK

YAĞ VE SU İKİ-FAZLI AKIŞ BASINÇ GRADİYENTİ TAHMİNİ

RAHEEM, Ahmed Ibraheem
Yüksek Lisans Tezi, Makine Mühendisliği Bölümü
Tez danışmanı: Prof. Dr. M. Yaşar GÜNDOĞDU
Eş-danışman: Yard. Doç. Dr. Fuat YILMAZ
Eylül 2014, 116 sayfa

Bu tez çalışmasında, tabakalı ve tabakalı dalga akış rejimleri ANSYS Fluent yazılımı kullanılarak yağ (1.57 mPa s viskozite ve 780 kg/m^3 yoğunluk) ve su iki-fazlı akışı için 0.0254 ve 0.508 metre arasında bir çapa sahip küçük ve büyük yatay çelik borularda sayısal olarak ortaya konmuştur. İki fazlı akışkan hacimleri (AH) yöntemi ile beraber Realizable k- ε ve Shear Stress Transport k- ω (SST) türbülans modelleri akışı sayısal olarak çözümlemek için kullanılmış, hidrodinamik parametrelerin (0.2-1.2 m/s aralığında hızların, 20-80 % aralığında suyun hacimsel oranının, ve boru çapının) basınç gradiyenti üzerindeki etkileri elde edilmiştir. Elde edilen sonuçlar boru çapının basınç gradiyenti üzerinde etkisinin oldukça kuvvetli olduğunu göstermiştir. Tabakalı dalga akış rejiminde, suyun hacimsel oranının 40 % ve 60 % olduğu büyük çaplı borularda basınç gradiyentinde akış rejimi dönüşümü sırasında bir zirveye ulaştığı gözlemlenmiştir. Ayrıca, Shear Stress Transport k-ω türbülans modeli kullanılarak elde edilen sonuçlar, Realizable k-ε türbülans modeli kullanılarak elde edilen sonuçlara göre, literatürde bulunan deneysel sonuçlarla genelde daha uyum içerisindedir.

Anahtar kelimeler: Hesaplamalı akışkanlar dinamiği (HAD), iki fazlı akım, basınç gradiyenti, sıvı miktarı, büyük çap, yatay boru, Yağ-su tabakalı ve tabakalı dalgalı akım.

This thesis is dedicated to my beloved wife and my kids for their endless love, support and encouragement.

ACKNOWLEDGEMENT

First and foremost, I would like to thank the GOD for his guidance and rewards toward me and my family. Then, I'd like to express my deepest respect and most sincere gratitude to my supervisor, Prof. Dr. M. Yaşar Gündoğdu and Co-supervisor: Assist. Prof. Dr. Fuat YILMAZ, for their guidance and encouragement during all stages of this mutual work. I will always be grateful for their valuable advice and insight supervision and encouragement to me during this research.

Finally, I would like to express my deepest regards and respects to my roommate, a graduate student Mr. Dilshad A. KAREEM for his encouragement and support throughout my thesis study.

CONTENTS

LIST OF FIGURES

LIST OF TABLES

LIST OF SYMBOLS

A	Area (m^2)
b	Body force per unit volume (N/m^3)
D	Diameter of pipe (m)
d_h	Hydraulic diameter (m)
e	Roughness of pipe (m)
F	Force (N)
f	Force per unit volume (N/m^3)
G	Mass flux (kg /s)
g	Acceleration (m/s^2)
k	Kinetic energy (J)
h	Enthalpy (J)
j	Volumetric flux (m/s)
L	Length (m)
I	Turbulent intensity
M	Mass (kg)
m	Mass flow rate (kg/s)
p	Pressure (N/m)
Q	Volumetric flow rate (m^3 /s)
q	Volumetric flow rate per unit width (m^2 /s)
Re	Reynolds number
R	Relative roughness

S	Entropy (kJ/kg K)
t	Time (s)
u	Local velocity (m/s)
V	Unperturbed component velocities (m/s)
υ_1, υ_2	Component velocities (m/s)
W	Mass flow rate (kg/ s)
w	Work (kg m/ s^2)
x	Quality
z	The length in the direction of motion (m)
ρ	Density (kg/m^3)
ρ_m	Mixture density (kg/m^3)
τ	Shear stress (N/m^2)
μ	Viscosity (kg/m s)
μ_m	Mixture viscosity (kg/m s)
ω	Frequency
ε	Dissipation rate (J/m)
$\int$	Friction factor
γ	Surface tension (N/m)
α	Volume of fraction (%)
θ	Angle to vertical

Subscripts

1	Component
2	Component
o	Oil
w	Water

CHAPTER 1

INTRODUCTION

1.1 GENERAL

Two-phase stratified flow through a gathering pipe line is defined as the co-current or countercurrent simultaneous motion of the gases and immiscible liquids in a pipe.

Generally, the multiphase flow can be classified into three categories according to the position of principal axis:

1- Horizontal flow.
2- Inclined flow (upward or downward).
3- Vertical flow (upward or downward).

Two–phase flows occur in a wide spread domain of environmental condition and occur extensively in industrial plants. Multiphase flow is especially in air-conditioning, refrigerators, tubular boilers, heat exchangers, condensers, distillation columns, desalination, nuclear reactors, rocket motors, chemical reactors, oil and gas transportation pipelines and natural gas liquefaction.

The existence of flow patterns or flow regimes in a two-phase flow is the basic difference between single-phase flow and two-phase flow. Flow patterns belong to the large scale distribution of the phases in the pipe. When a mixture of oil and water flows simultaneously in a pipe, both phases can diffuse themselves in a

variety of flow configuration or flow patterns. Flow patterns are creating because of the difference in characteristics such as density and viscosity. Flow regimes in any system depend on the geometrical variables such as pipe diameter, roughness and inclination, operational variables such as flow rate of phase and the fluid physical properties such as density, viscosity and surface tension.

The pressure gradient through a two-phase liquid-liquid flow is highly influenced by the material of the pipe. The pressure gradient in all situations is higher, typically up to 100% in the steel pipe than in other materials (Angeli and Hewitt, 1998). Flow pattern map is gathered for the air-water two-phase flow in large-diameter horizontal pipelines. The transmission differs basically from those for-small diameter pipes and is not predicted rightly by any theoretical models. An increase in the superficial liquid velocity is necessary in order to reach slug flow (Jepson and Taylor, 1993). Pressure drop will play a significant role and is a very important point in the design and running of oil–water flow systems (Xuan Xu, 2007). As a high mixture velocity increases the pressure gradients, in the same way, mixture velocity also influence the viscosity of the working two-phase flow. In working fluid, the mixture velocity can directly affect the viscosity diminish of pressure gradients (Yuling, 2012). In liquid-liquid flow, the buoyancy effect is generally small and capacity of the momentum transfer is large. Ratio of the density usually varies between 0.7 and 1.1 and viscosity ratio varies in the range of 0.3 to 104 in a liquid-liquid system (Valls, 2000). Stratified flow is one of the two-phase flow patterns. In this flow pattern, the oil-water phases flow as layers with the lower (heavier) phase, usually water with the upper (lighter) phase, usually oil. At the interface, some waviness can be observed.

A scientific and technological interest are in both accurate predictions of the

pressure gradient and void fraction in stratified oil-water flow. The development of high-speed computers and the advanced turbulence models, allows to simulate stratified oil-water two-phase flow by using CFD.

A mesh independent study was carried out to obtain optimum mesh size to be used in the simulation process (Al-Yaari and Abu-Sharkh, 2011). By using a volume of fluid model with renormalization group of k-ε turbulence model, the stratified oil-water two-phase turbulent is simulated flow through a horizontal pipe. A first order upwind momentum equation is solved throughout the domain (Gao, 2002). If the concentration of water (volume fraction) changes in flow in a horizontal steel or acrylic pipes, the flow regimes are different from stratified flow and reached up to fully mix condition. Generally, the mixed flow regime was seemed to have higher velocities in acrylic pipes than the steel pipe (Angeli and Hewitt, 1999). To test the effects of the type of models on a complex geometry, the best way is the use of computational fluid dynamics to simulate the liquid-liquid flow in a horizontal tube. For example, volume of fluid model with k-ε turbulence model of homogeneous flow can be successfully implemented (Hussain and Khuan, 2009). In CFD code FLUENT a simple mixing-length turbulence model is used to sophisticate a 2D model for fully–developed, turbulent-turbulent oil-water stratified flow, which is based on a numerical solution of the requisite governing differential equations by a finite-volume method in a dipolar coordinate system (Al-Yaari et al., 2009).

Our main aim in this thesis is to develop models for prediction of the hydrodynamics of oil-water two-phase flow and compare them with experimental data in literuture. The advantages and other reasons for using CFD FLUENT 14.0 program to simulate oil-water stratified flows through different diameters of a

horizontal pipe are as follows:

- Provides more time and effort: thus, if the research is done in a normal lab, it takes more time for its implementation and being in a lab continuously means to consume more efforts.
- More economical: in the way, the price of providing lab is much greater than the price of a modern computer.

Finally, pressure gradient prediction of a stratified and stratified wavy two-phase flow in a horizontal pipe at different hydrodynamic parameters will be investigated in the evaluation of characteristic flow parameters such as velocity, water volume fraction and diameters. In literature, almost studies carried by CFD methods is limited to oil-water stratified flow through a small diameter pipe and use only one turbulence model. However, if industrial facility application such as chemical reactors, oil and gas transportation pipelines and natural gas liquefaction related with oil-water two-phase flow are examined, the reality is that these flows include large diameters more than 0.1 m, different velocities and different water volume fraction ratio. Therefore, our study is mainly directed to determine pressure gradient prediction oil-water two-phase stratified flow through horizontal small and large diameters of steel pipe by CFD methods.

1.2 Dissertation Structure

The aim of this thesis is to analyze two-phase oil-water stratified flow. The software which used for this purpose is FLUENT V 14.0 in ANSYS WORKPANCH (engineering simulation software). The skeleton outline of the dissertation with respect to chapters is as follows:

Chapter 1: Introduction, gives general information about two phase oil-water stratified flow, and aim of this study also.

Chapter 2: literature survey, presents a detailed literature review about two phase flow regimes in gathering pipe line as experimental and theoretical, flow pattern in vertical and horizontal pipe, stratified two phase flow theory, experimental studies on stratified flow, analytical studies on stratified flow, CFD studies on stratified flow and conclusion.

Chapter 3: Test case, present a geometrical effect (material, roughness and diameters of pipe), density, viscosity, surface tension and velocity effects on the flow, mesh size effects on study results, Reynolds number range, turbulent intensity and modeling studies of two-phase oil-water flow (homogenous oil-water flow models) also the conclusion.

Chapter 4: CFD programming chapter, pre processing (geometry, mesh), analytical processing (setup, solution) and post processing (results).

Chapter 5: Results and discussion of velocity profile and pressure gradient at different diameters will be given and several other relations such as water volume fraction-pressure gradient and table for turbulence models at the velocity. Diameters difference will be also included.

Chapter 6: Conclusion, the main conclusion from this study is given. The results of the pressure gradient will be compared with theoretical and experimental data in literature.

CHAPTER 2

LITERATURE SURVEY

2.1 Background

A phase can be either a gas, a liquid, or a solid. Multiphase flow is defined as the co-current or countercurrent simultaneous flow of several phases. Multiphase system especially oil-water stratified flow has become widely used in power generation, nuclear reactors, fields of oil wells, chemical reactors, and the oil industrial facilities, most researchers focus on it. Generally, the description of two-phase flow in a horizontal pipe is complicated because of the existence of an interface in a wide variety of forms, depending on the flow rates and the physical properties of the phase, and on the geometry and inclination of the pipe. The different interfacial structures are called flow patterns or flow regimes. These flow patterns, which are created because of the interaction between the phases, exhibit characteristic pressure drop. So, it is important to predict these flow patterns in order to predict the pressure drop in most cases the oil-water flow in a horizontal pipes.

Any fluid is forced to flow through a pipe. Effected by the physical properties of the phases, densities, viscosities and surface tension, the relative flow rate, and inclination, geometry of the pipe as diameter, roughness and material of pipe. In order to control the behavior of two-phase oil-water, it is important to understand some of its properties and most necessary. A broad understanding of the fundamentals of two-phase oil-water flow in a horizontal pipe is the primary goal of this chapter.

Mostly, during oil production in worldwide, a high ratio of water is extracted with oil in horizontal pipes. Flow regime maps and their identification methods, are also included and discussed in this chapter.

By study in the literature survey, we can find some good experimentally, analytically and numerically studies on stratified flow some amendment is also available in different ways.

2.2 Two – Phase Flow Regimes and Their Maps in Gathering Line

The term morphological arrangements or geometrical distribution is the most necessary criteria for two-phase flow through a pipe when the flow is simultaneous. This geometric distribution or morphological arrangements of the two-phase under flowing conditions are often termed as flow regime or flow pattern. These regimes may be represented as an area on a graph, the coordinates of the graph are the superficial phase velocities or generalized parameters containing these velocities. Usually, these maps are presented as a plot of superficial velocity of water against oil.

The presence of the variety of flow regimes is detected as a main problem in analyzing two-phase flow, it is important to predict which flow pattern is likely to happen for any combination of phase properties.

2.2.1 Experimental Flow Regime Maps

The flow pattern of a particular fluid of a given pipe can be represented graphically to evaluate a flow pattern map by plotting experimental data as superficial phase velocities versus dimensionless groups or by using video recording.

2.2.2 Theoretical Flow Regime Maps

It is considered that the evaluated flow pattern shows the main characteristics of two-phase flow. Prediction of the theoretical flow pattern map is based on the physical phenomenon effect on transition boundaries of flow regimes. Therefore, the prediction of flow patterns has accepted as a central problem in two-phase flow in a pipe.

Several approaches are available for the study of the two-phase flow models in pipes (Ityokumbul et al., 1994). Direct visual observation through a transparent pipeline is the easiest and the most common using strategy of flow pattern determination. However, clear visual observations of flow regimes are not easy for high mixture flow rates. If the pattern becomes indistinct, visual methods of video and/or photographic techniques generally are used. In stratified turbulent two-phase flows, the multiple interfaces react and reflect light in such a way that it is impossible to see beyond the region near the wall of the pipe, especially at the high flow rates. Clarification of such cases can often be obtained by using flash X-radiography.

De Schepper et al., (2008) studied the flow pattern change occurred in horizontal lines for a long time ago. Quantitative prediction of flow a regime is considered to start with the pioneering work of Baker. Backer's flow pattern map has been used for a long time despite the limit data which it was based on. It is the oldest and perhaps the most durable map for two-phase gas-liquid flow. It is generally used by petroleum industries. Proposed experimental flow pattern map of Backer is generally composed of seven regimes for two-phase, gas liquid flow in horizontal pipes as shown in Figure 2.1. These flow regimes are called as dispersed, bubble, slug, plug, stratified, wave and annular.

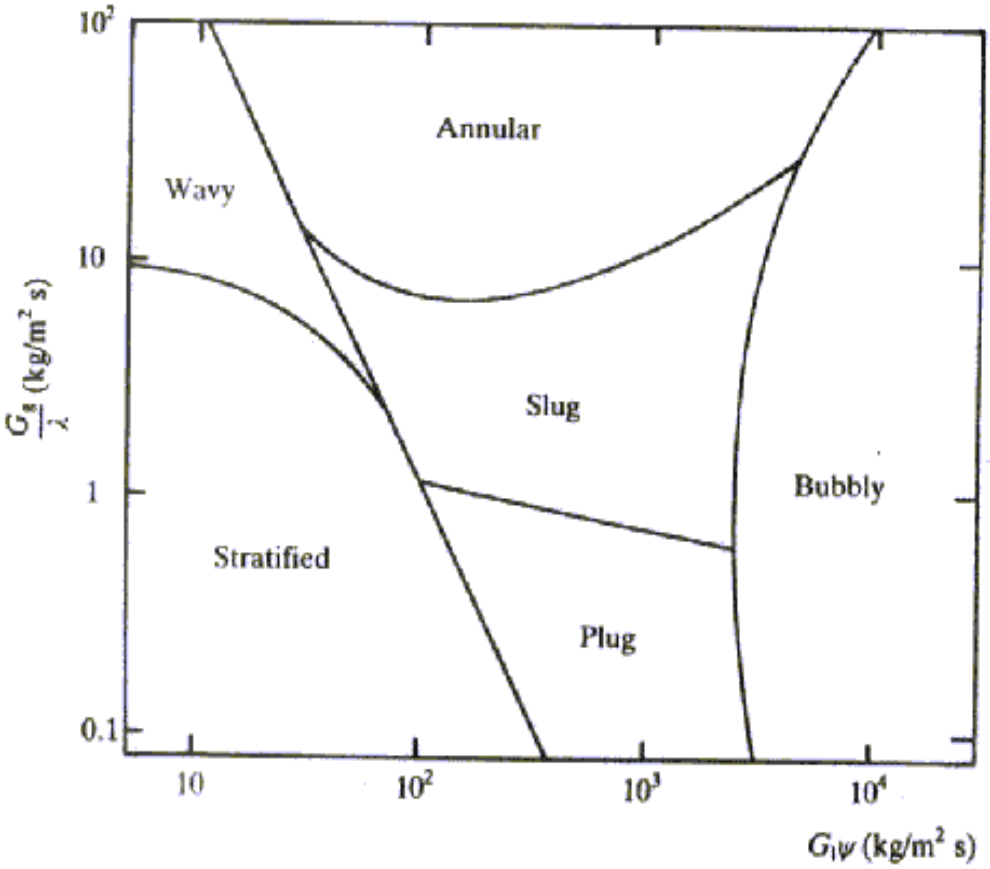

Figure 2.1 Baker chart for a two-phase flow pattern correlation

Another experimental method of obtaining flow pattern maps has been suggested in the study of Taitel and Dukler (2004) for horizontal gas-liquid flow. The changeover strategy based on physical concepts and generalization of the flow regime map has been defined in the study of Banderas et al., (2005). A good agreement with experimental data is found on both horizontal and inclined pipes in the range 0 to 10^o (Taitel and Dukler (2004); Banderas et al., (2005)).

2.3 Flow Pattern in a Vertical Pipe

Five gas-liquid main flow patterns which are for the particular case of upwards in vertical pipe as show in Figure 2.2 are suggestes by Hewitt and Taylor, (1970):

i. Bubble flow: It is one of the familiar flow patterns of two-phase flow and

characterized by the gas phase being dispersed randomly in the form of deformed spheres bubble in a liquid continuous phase.

ii. Slug or plug flow: When the concentration of the bubbles becomes high in a gas-liquid flow, large bubbles form that span most of the pipe diameters. So bubble adhesion occurs. Further coalescence results in the deformation of the bubbles or plugs. Plug flow then consists of plugs or Taylor bubbles as gas phase, separated by regions of bubbly flow, commonly called slugs. The plugs of gas are surrounded by a thin liquid film which flows vertically down wards.

iii. Churn flow: This region sometimes belongs to semi-annular or slug-annular flow in which churn flow formed by breaking dawn of the large gas bubbles in slug flow that is a highly confused flow regime in the vertical motion of the liquid that is wobbling.

iv. Wispy annular flow: The liquid film is created by small gas bubble, and entered liquid phase in the central gas core appears as large droplets which have agglomerated into long irregular filaments or wispy in this regime. The think liquid film along the pipe walls slowly flows and the gas flows along the center of the pipe with agglomeration of liquid droplets (wisps) in it.

v. Annular flow: The liquid film flow along the walls of the pipe, and the gas phases along the center of the pipe as continuous phase which that is partially separated droplets in the center gas core.

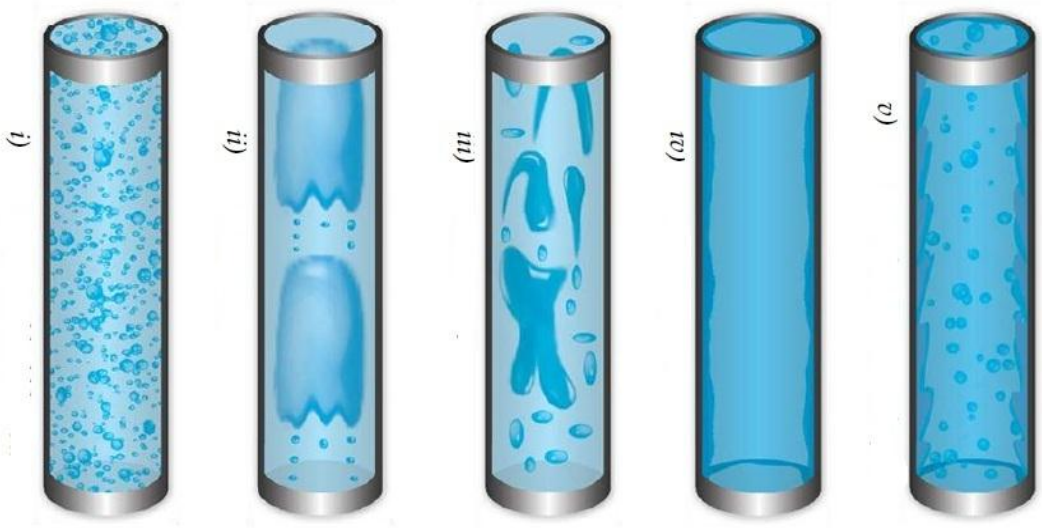

Figure 2.2 Flow patterns through a vertical pipe.

2.4 Flow Pattern in a Horizontal Pipe

The flow patterns in a horizontal flow through the pipes are comparable to those in vertical flow, but the gravity has an impact on the distribution of the liquid that acts to stratify the heavy phase (water) to the bottom of the pipe and the lighter phase (oil) to the top by (Thome, 2010). The flow pattern types of co-current flow are shown in Figure 2.3 and classified as follows for a gas-liquid in a horizontal pipe.

i. Bubble flow: Here, the liquid phase flow as a continuous phase with discrete small gas bubbles flowing at the upper half of the pipe as gas phase flow.
ii. Plug flow: The liquid phase flow as continuous liquid slugs with bullet-shaped, elongated gas bubbles.
iii. Stratified flow: In this regime, the two-phase flow is separated with a comparatively smooth interface. Because of gravity, the liquid phase flows at the bottom part of the pipe, while the gas phase flows at the top part of the pipe. This pattern occurs at very low velocities of liquid and gas.

iv. Wave flow: As velocity of the gas is increased the interface becomes troubled by wavy traveling in the direction of flow.

v. Slug flow: An increase in gas velocity causes the waves on the interface to be picked up. Then the wave peaks are sufficiently high to reach the top of the pipe, after that the flow is a slug flow (large gas bubbles with liquid slugs).

vi. Annular flow: In this pattern, a continuous liquid film on the walls of the pipe flows, while along the center of the pipe, the gas flow as a continuous phase.

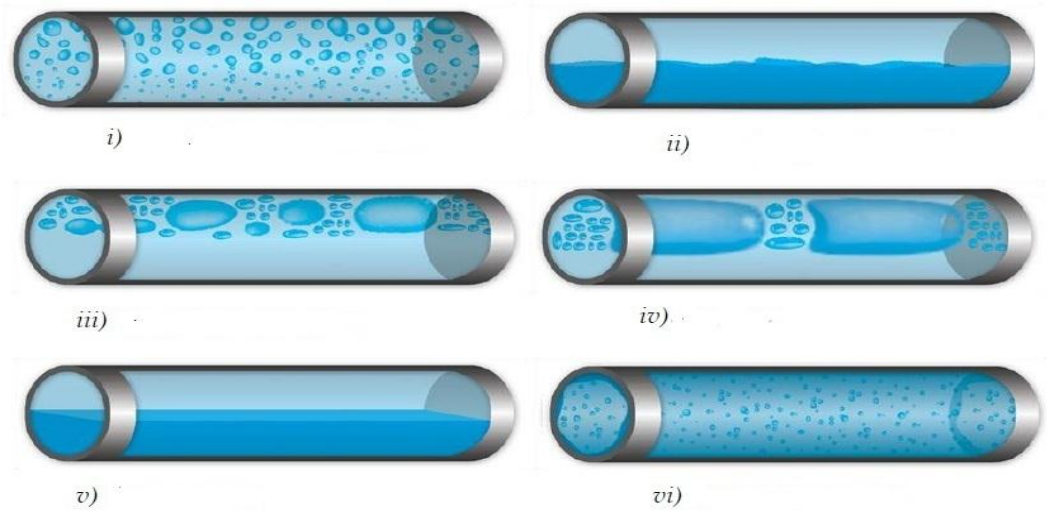

Figure 2.3 Flow patterns through a horizontal pipe

2.5 Stratified Two-Phase Flow Theory

One of the two-phase flow patterns is the stratified flow. Generally, in this flow regime, the oil-water phases flow as layers, full separation of the two-phases occurs at low velocities. These two-phase are segregated by gravity with an undisturbed horizontal interface. Many researchers have described the transition between stratified and non-stratified two-phase gas-liquid and liquid-liquid flow in

terms of stability analyses.

The stratified flow is classified as three-section according to velocity of gas-liquid flow(Abdulkadir, 2011). The gas and liquid phases flow smoothly through a pipe at low velocities. At higher velocity of the gas, the shearing action on the gas at the interface generates small 2-Dimensional waves (wavy stratified flow). At even higher velocities, large amplitude waves are seen on the liquid surface. These waves cause the liquid drop entrainment in the gas. The transition of stratified flow to slug or annular flow pattern depends uniquely on the liquid height of the stratified layer.

2.6 Experimental Studies on Stratified Flow

A lot of experimental studies have been published on gas-liquid and liquid-liquid (particularly oil-water) stratified flow using an overall average macroscopic bulk approach, including volume fractions and pressure gradient.

The research of Lockhart and Martinelli, (1949) is one of the early approaches describing two-phase flow, and it is fundamentally experimental in nature. This study is very appropriate for oil-water two-phase separated stratified flow. They presented that practical relationships exist between the pressure gradient and liquid holdup, the Lockhart and Martinelli parameter for horizontal pipe flow, X, is defined as the square root of the ratio of the liquid superficial pressure gradient to the gas superficial pressure gradient. Depending on experimental data, correlations were made for the prediction of the pressure gradient and the liquid holdup.

Angeli and Hewitt, (1998) measured the pressure gradient through the co-current flow of oil (ρ= 801 kg/m^3 and μ= 0.0016 kg/m.s) and water (ρ= 998.2 kg/m^3 and μ= 0.001003 kg/m.s) through 2.54 cm diameter horizontal stainless steel and

acrylic resin pipes. Mixture velocities from 0.3 m/s to 3.9 m/s and volume fraction of water between 0 to 100 % are used in the study of Angeli and Hewitt, (1998). The large differences amoung the results are observed due to the roughness and wettability phenomenon of stainless steel and acrylic resin pipe. At high mixture velocities, where dispersed flow patterns prevail, there is a peak in pressure gradient during phase inversion and an apparent drag reduction effect when oil is the continuous phase. The results of this study are compared with both phenomenological and empirical models. These models have demonstrated poor agreement with the results.

Al-Yaari et al., (2009) measured the drag-reduction for oil–water flows in a horizontal 0.0254 m diameter and 1.1 m long of pipe with a water volume fraction range from 10 to 90 %. The geometry, wetting properties at the wall surface and the liquid physical phenomenon have effects on flow regimes map. Optical monitoring based method is used to classify the flow patterns. By using of the observation in this study, flow regimes as shown Figure 2.4 are defined as follows, stratified wavy flow (SW), stratified wavy-drops (SWD), stratified mixed / water layer (SMW), stratified mixed / oil layer (SMO), three layers flow, and dispersed flow. In the study of (Al-Yaari et al., 2009), the stratified flow pattern is clearly observed for 0.5 m/s mixture velocity and all range of input volume fraction. The mixture velocity was increased to 1 m/s with increasing water volume fraction of 0.35, 0.55, 0.75, the stratified flow regime changed to stratified wavy with drops, three layers and stratified mixed-water layer flow pattern respectively.

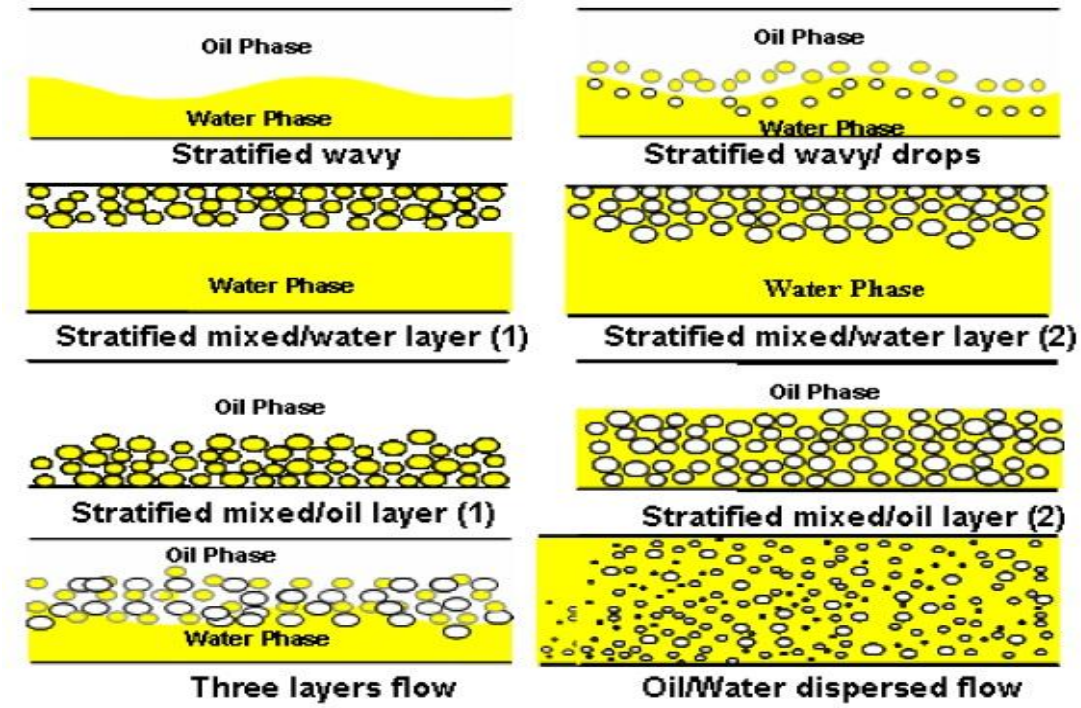

Figure 2.4 Oil–water flow patterns in a 0.0254 m diameter horizontal pipe (Al-Yaari et al., 2009)

A pressure gradient correlation based on other researcher investigations was developed for oil–water separated flow (stratified and dual continuous flows) through a diameter between 14 mm to 82.4 mm for horizontal pipe made out of glass, perspex, acrylic and stainless steel (Al-Wahaibi, 2012). In this study, eleven-pressure gradient data source in the literature was used to obtain the pressure gradient correlation. This study is the first one to publish a broad range of pressure gradient database containing operational cases, properties of fluid, materials and diameters of pipe for oil-water flow. This correlation was tested against the two-phase model and had a higher accuracy.

Venkatesan et al., (2011) investigated the small pipe diameter effect (0.6, 1.2, 1.7, 2.6 and 3.4 mm) on the frictional pressure drop for an air-water two-phase flow. Segregate two-phase model, is used with superficial velocities of gas between 0.01 to

50 m/s and the superficial velocities of water between 0.01 to 3 m/s in this study. High-speed camera was used to record flow pattern map. By using the homogenous model, only bubbly flow pattern is predicted well. However, all other patterns are considerably deviated. For smaller pipe diameters, unique flow patterns were observed. Pressure drop measured and compared with available model such as homogeneous model and Lockhart–Martinelli model.

Angeli and Hewitt, (2000) investigated the structure of flow occurring through the co-current flow of water (ρ= 998.2 kg/m^3 and μ= 0.001003 kg/m.s) and oil (ρ= 801 kg/m^3 and μ= 0.0016 kg/m.s) by using two horizontal stainless steel and acrylic resin pipe with 2.54 cm diameter, mixture velocities between 0.2 m/s to 3.9 m/s and changing input water volume fraction ratio between 6% to 86%. At this condition ranges, different flow regimes were observed in the range from stratified to oil-water mixture. The flow pattern is obtained by the two methods. While one is used a conductivity needle probe, the other one is used high-speed video recording to determine the local phase fraction. At lower mixture velocities, the mixed flow pattern is appeared in the steel pipe.

Lovick and Angeli, (2004) used an impedance and a conductivity probe to identify boundaries of the dual continuous flow pattern by using water (ρ_{water}= 998.2 kg/m^3 and μ_{water}= 0.001003 kg/m.s) and oil ρ_{oil}= 828 kg/m^3 and μ_{oil}= 0.006 kg/m.s) as working fluids. Measurements were taken for mixture velocities from 0.8 to 3 m/s and input water volume fraction from 10 to 90 %. Dual continuous flow was observed between stratified and dispersed flows and resulted in pressure gradient less than that of single-phase oil flow. The pressure gradient appeared a minimum at high oil fraction when the mixture velocities become higher.

2.7 Analytical Studies on Stratified Flow

The stratified flow model is one of the two-phase flow patterns. Each phase can have different velocities and properties. The equations of continuity, momentum and energy for stratified or separated flow can be written for each phase to solve simultaneously. From these equations, we can describe the interaction between phases and interaction with walls of the pipe.

2.7.1 Steady two-phase flow

The conservation laws of mass, momentum and energy during homogeneous flow can be derived in expression of the velocity for each phase υ_1 and υ_2 (Wallis, 1969).

Continuity equation:

$$W = W_1 + W_2 \qquad 2.1$$

$$W_1 = \rho_1 \upsilon_1 A_1 \qquad 2.2$$

$$W_2 = \rho_2 \upsilon_2 A_2 \qquad 2.3$$

Momentum equation:

For a homogeneous flow through a round pipe:

$$-\frac{dp}{dz} = \frac{4\tau\omega}{D} + G\frac{d}{dz}[x\upsilon_2 + (1-x)\upsilon_1] + \alpha\rho_2 + (1-\alpha)\rho_1]\cos\theta \qquad 2.4$$

Energy equation:

$$\frac{1}{W}\left(\frac{dq}{dz} - \frac{dw}{dz}\right) = \frac{d}{dz}[xh_2 + (1-x)h_1] + \frac{d}{dz}\left[x\frac{v_2^2}{2} + (1-x)\frac{v_1^2}{2}\right] + g\cos\theta \qquad 2.5$$

2.7.2 Separated or stratified flow

For stratified flow, it is necessary to use equations to relate most of the variables (Wallis, 1969). This can be made by writing equations for each component and the entire mixture.

Continuity equation:

Generally, the equations of continuity can be written in a differential form:

$$\frac{\partial}{\partial t}[\rho_1(1-\alpha)] + \nabla .\ [\rho_1(1-\alpha)v_1] = S_{12} + S_1 \qquad 2.6$$

$$\frac{\partial}{\partial t}(\rho_2\alpha) + \nabla .(\rho_2\alpha v_2) = -S_{12} + S_2 \qquad 2.7$$

After integration of equations 2.6 and 2.7, following one-dimensional formula can be obtained for the first phase:

$$\frac{\partial}{\partial t}[\rho_1(1-\alpha)A] + \frac{\partial}{\partial Z}[\rho_1(1-\alpha)v_1A] = \int(S_{12} + S_1)dA \qquad 2.8$$

and for the second phase:

$$\frac{\partial}{\partial t}(\rho_2\alpha A) + \frac{\partial}{\partial Z}[\rho_2\alpha v_2 A] = \int(-S_{12} + S_1)dA \qquad 2.9$$

Momentum equation:

The equation of motion for two-phase flow can be written for each phase in the form of

$$\rho_1\left(\frac{\partial v_1}{\partial t} + v_1.\nabla v_1\right) = b_1 + f_1 - \nabla p \qquad 2.10$$

$$\rho_2 \left(\frac{\partial V_2}{\partial t} + v_2 . \nabla v_2\right) = b_2 + f_2 - \nabla p \qquad 2.11$$

2.8 CFD Studies on Stratified Flow

Computational fluid dynamic models are widely used to study different multiphase flow regimes, including stratified flow in any internal horizontal and vertical pipe. In addition to provision time and effort, the FLUENT program provides the flexibility in selecting discretization schemes for pressure gradient, momentum, volume fraction of fluid, energy equation, etc., and uses the segregated solution method to obtain a good numerical solution for stratified and stratified wavy flow through a horizontal pipe.

Walvekar, (2009) simulated dispersed oil-water two-phase turbulent flow in a horizontal tube by using commercial CFD package FLUENT 6.2 in conjugation with multiphase model. They applied standard k-ε turbulent model to describe the turbulence in continuous phase and Eulerian–Eulerian approach model to analyze the interaction between dispersed phase and continuous phase. They reported numerical results in expressions of distribution of the phase and average phase hold-up.

Torres, (2006) applied finite-volume method in a bipolar coordinate system for fully-developed, turbulent-turbulent oil-water stratified flow by using a simple mixing-length turbulence model. The proposed models based on a numerical solution (solution of the basic governing differential equations including a modified turbulent diffusion model simplify significantly the flow pattern map for liquid-liquid flow. The results are in satisfactory agreement with a large number of experimental data sets.

Newton and Behnia, (2000) attempted to present a variety of objects

concerning numerical calculations of axial pressure gradient, liquid delay, and turbulence flow fields in stratified gas-liquid pipe flow. This model embodied the wall humidity, functions. Obviously, normal standard wall functions have special generality to be applied for the two-phase that is considered here. This conclusion contrasts with the poor outcome performance of generally used single-phase flow relationships to model both walls and cut interaction stresses, as shown by the recent calculations. Since the present pattern does not depend on such a data, it is obvious that it may have considerable value in this study into more common stratified two-phased flows. The results showed that such tuning had a small effect, and was in good agreement with experimental data.

Al-Yaari and Abu-Sharkh, (2011) used the volume of fluid multiphase model, RNG k-ε turbulence model to simulated oil-water two-phase stratified flow through 2.54 cm diameter of a horizontal pipe by FLUENT 6.2 from ANSYS package. Their calculations were performed by computational fluid dynamic to predict the stratified flow and optimum mesh size independent on it to decide which one used in the simulation process. By CFD simulation, they predicted the wavy interface of oil water system, and the clear segregated oil layer, but were not able to predict fully of separation of the water layer. Many results of CFD simulation are verified by experimental data in literature.

Hussain and Khuan, (2009) applied standard k-ε turbulent model and Eulerian–Eulerian approach model to simulate the oil-water flow through 0.0254 m internal diameter and 9.7 m a length horizontal pipeline. The flow is considered homogeneous. They compared their results with previous numerical research and found that the oil and water distribution in the horizontal pipe is found to be

impartially uniform and well dispersed in the system.

Desamala et al., (2013) numerically investigated the transition boundaries of different flow regimes for two-phase oil-water flow (density ratio 0.89, viscosity ratio 107, and surface tension of 0.032N/m) through a 0.025 m diameter and 7.16 m length horizontal pipeline. A total of 47037 elements of quadrilateral was selected for the geometry of the horizontal pipeline. The computation has been performed by constant liquid properties, unsteady flow and immiscible liquid. Their simulation predicted the transition boundaries of wavy stratified to stratified mixed flow. Simulated data has been verified with their own experimental data in literature.

Newton and Behnia, (2001) applied k-ε turbulence model with low Reynolds number to solve the steady axial momentum equation and amended the model of turbulence to accommodate the irregular geometry of stratified flow through the pipe. A set of boundary conditions was devised for the stratified wavy gas-liquid flow from empirical consideration. Predictions of pressure drop and flow quantities (velocity and wall shear stress) to compared favorably with experimental data and showed acceptable agreement.

Sampaio et al., (2008) experimentally and numerically investigated the fully developed stratified gas–liquid two-phase flow in horizontal circular pipes (2.10 and 5.12 cm diameters). The Reynolds averaged Navier–Stokes equations (RANS) with the k-ω turbulence model was numerically solved. The interface surface was assumed smooth without considering the influence of the interfacial waves. Their numerical results with available experimental results in literature indicates that the k-ω model can be uses for the numerical CFD simulation of stratified gas–liquid two-phase flow.

2.9 Conclusion

It is obvious that there are several efficient studies on using ANSYS Fluent package to simulate oil-water two-phase stratified and stratified wavy flow by volume of fluid model. A finite number of studies found on the pressure gradient prediction for a wide range of diameter, especially at the large diameter above 0.1 m by Realizable k- ε and Shear Stress Transition k- ω turbulence models. However, several mixture velocities between 0.2 to 1.2 m/s, volume fraction of water in the range 20 to 80 %, and different pipe diameters between 0.0254 to 0.508 m will be used in this study. There is a very limited study in the literature.

CHAPTER 3

TEST CASE

3.1 Introduction

Generally, a test case consists of a set of variables such as diameters, water volume fraction and velocities. From these parameters, we can obtain required flow parameters by a CFD software. ANSYS Fluent is one of the most popular software in this branch

3.2 Effect of Geometry

Several parameters are strongly effects on the flow pattern such as the physical phenomenon (density, viscosity, surface tension, velocity, volume fraction of oil or water, diameter, pipe roughness and pipe material (Al-Yaari et al., 2009).

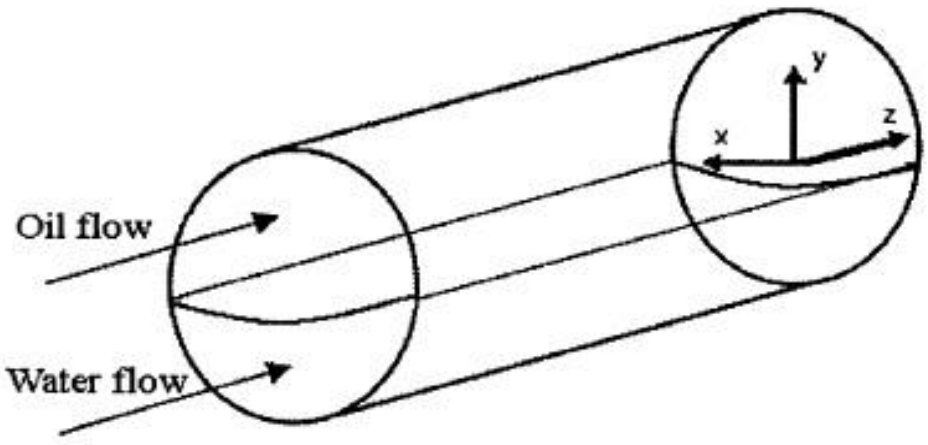

Figure 3.1 Oil-water stratified flow through a horizontal pipe

3.2.1 Material and Roughness of Pipe

The pipe roughness is a very important impact on the flow rates and the pressure gradient for fluids passing through it. Generally, the pipe roughness is an expression in units of length. However, the absolute roughness of the pipe material is dimensionless.

$$r = \frac{e}{d_h} \qquad 3.1$$

The roughness of pipe, e, for a commercial or welded steel is 0.000045 m. It is one of the required data to entry in FLUENT program.

Table 3.1 Relative Roughness values for different pipe diameters

Diameter (m)	Relative Roughness
0.0245	0.001771
0.127	0.00035
0.254	0.0001771
0.508	0.0000885

The geometry includes a horizontal steel pipe used for high pressure transmission system, and it widely used in pipeline transmission in industrial facilities. Several years ago when drawing any geometry in ANSYS package we needed more time to execute it by attachment GAMBIT program, but now by ANSYS package with FLUENT 14.0 program the process does not take long time for drawing any geometry after fixed data.

3.2.2 Diameters of Pipe

Pipe diameter impact is very important on the results of this thesis and strongly influences on the transition of flow patterns. Pipe diameters cover a range between 0.0245 m and 0.508 m. Length of pipe is selected according to fully develop length equation. The data about a large diameter such as 0.127, 0.254 and 0.508 m is very little in literature, and these data are becoming increasingly significant, because many offshore facilities are requiring that large pipe diameter.

Different diameter and length are used by researchers as shown in Table 3.2 to compare their results with experimental results in the literature.

Table 3.2 Diameter and length of pipe from different sources for horizontal oil–water flow

Pipe diameter m	Pipe length m	Reference
0.0243	9.7	(Angeli, and Hewitt, 1998)
0.0254	2.2	(Al-Yaari and Abu-Sharkh, 2011)
0.0557	8	(Hui Gao et al., 2002)
0.0254	9.7	(Hussain and Khuan, 2009)
0.1	40	(Shi et al., 1999)
0.025	7.16	(Desamala et al., 2013)
0.101	40	(Wallis, 1969)

3.2.3 Density Effect

Density is one of the physical properties of matter, as each compound and element have a unique density related with it. Density defined in a specific style as the measure of the relative weightiness of an objects with a constant volume. It is the

ratio of mass to volume, and the usual term is

$$\rho = \frac{M}{V} \tag{3-2}$$

Density for a single-phase flow is a function of pressure and temperature. For two-phase liquid-liquid flow, the density difference has an essential effect on the flow regime. Two immiscible liquids with different densities head for stratify when flowing through a horizontal pipeline. Thus, it is perhaps difficult to produce a scattered flow regime when the density difference is high.

The major density for one-dimensional two-phase homogeneous flow can be crossed in diverse ways (Wallis, 1969). In expression of void fraction, it is

$$\rho_m = \alpha\rho_2 + (1-\alpha)\rho_1 \tag{3-3}$$

In terms of the quality, it is

$$\frac{1}{\rho_m} = \frac{x}{\rho_2} + \frac{1-x}{\rho_1} \tag{3-4}$$

and in terms of volume fraction or quality

$$x\rho_m = \alpha\rho_2 \tag{3-5}$$

$$(1-\mathrm{x})\rho_\mathrm{m} = (1-\alpha)\rho_1 \tag{3-6}$$

Densities of oil (Kerosene $C_{12}H_{23}$) and water are 780 kg/m^3 and 998.2 kg/m^3 respectively.

3.2.4 Viscosity Effect

Generally, viscosity is a resistance of fluid to flow. A fluid becomes less viscous as the liquid's temperature increases, becoming more viscous as the liquid is temperature decreases get cooler.

When oil and water are flowing together through a pipe, the obvious viscosity of the individual phases is lower than the mixture viscosity. The apparent viscosity of oil-water is influenced by many factors such as mixture velocity and interfacial tension (Fritz and Russ, 2001).

The viscosity effects for oil-water flows appear little or no effect on the observed flow regimes (Russell et al,. 1959). Generally, the viscosity has a paired influence on the flow: (1) increase of viscosity can cause an increase in instability due to the different of velocity profiles, and (2) at the same time it helps to waste the energy that causes instability (Yih, 1967). Some joint terms for two-phase flow are

$$\mu_m = \alpha\mu_2 + (1-\alpha)\mu_1 \qquad \text{(Bankoff, 1960)} \qquad 3\text{-}7$$

$$\frac{1}{\mu_m} = \frac{x}{\mu_2} + \frac{1-x}{\mu_1} \qquad \text{(Mc Adams, 1942)} \qquad 3\text{-}8$$

Viscosities of oil (Kerosene $C_{12}H_{23}$) and water are 0.0024 kg/m.s and 0.001003 kg/m.s respectively.

3.2.5 Surface Tension Effect

The surface tension is another required data for entry in ANSYS Fluent 14.0 to complete analysis data model. Volume of fluid (VOF) approach has been employed to predict the flow pattern by including surface tension effect. Density,

viscosity and geometry have also an impact on flow patterns. Generally, it is defined the quantity of the force (measured by Newton) exerted parallel to the surface of any liquid to the length (meter) of the line over which the force acts:

$$\gamma = \frac{F}{L} \qquad 3\text{-}9$$

The surface tensions of oil and water at 20^{o} C are 0.027 N/m and 0.073 N/m respectively, and interfacial tension between oil and water is 0.017 N/m.

3.2.6 Velocity Effect

In any flow system, a single flow or a two-phase flow, velocity is a very important parameter that affects on design. It affects the flow pattern transition and it is one of the parameters to specify the type of flow (laminar, transition and turbulent) in a horizontal pipe in addition to diameter and kinematic viscosity.

There are significant velocities to make a precise study of two-phase flow (Vallejo and Reiriz, 2011):

1. Actual velocity**:** Actual velocities of the phases (u_{oil} and u_{water}) are also called true average velocities by which the phases indeed travel. The cross sectional average true velocities are determined by the volumetric flow rates of the oil and water, $\dot{Q}oil$ and $\dot{Q}water$.

$$u_o = \frac{\dot{Q}_o}{A_o} = \frac{\dot{Q}_o}{\alpha.A} = \frac{G.x}{\rho_o \alpha} \qquad 3\text{-}10$$

$$u_w = \frac{\dot{Q}_w}{A_w} = \frac{\dot{Q}_w}{(1-\alpha).A} = \frac{G.(1-x)}{\rho_w (1-\alpha)} \qquad 3\text{-}11$$

where A is the section of the pipe and G is the mass velocity of the flow

$$G = \frac{\dot{m}}{A} \quad 3\text{-}12$$

and $\dot{m}$ is the total mass flow rate

$$\dot{m} = \dot{m_o} + \dot{m_w} \quad 3\text{-}13$$

2. Superficial velocity: **S**uperficial velocities or volumetric fluxes of oil and water phases are defined as the volumetric flow rate of the phase, $\dot{Q}_o$ and $\dot{Q}_w$ (m^3/s). It also might be expressed as the phase velocity if it flowed alone in the entire cross section. Thus:

$$j_o = \frac{\dot{Q}_o}{A} = \frac{G.x}{\rho_o} = \alpha.u_o \quad 3\text{-}14$$

$$j_w = \frac{\dot{Q}_w}{A} = \frac{G}{\rho_w}(1-x) = (1-\alpha).u_w \quad 3\text{-}15$$

The total superficial velocities are defined as:

$$j = j_o + j_w \quad 3\text{-}16$$

Mixture velocities are used between the range of 0.2 m/s to 1.2 m/s in this study. Most of the researchers, mixture velocities are used between the range of 0.3 to 3.9 m/s (Angeli and Hewitt, 1998), 0.5 to 3.5 m/s (Al-Yaari and Abu-Sharkh, 2011), 1.05 m/s (Hui Gao et al., 2002), 1.8 to 2.76 m/s (Hussain and Khuan, 2009), 0.4 to 3 m/s (Shi et al., 1999), 0.1 to 1.1 m/s (Desamala et al., 2013) and 0.4 to 3 m/s (Wallis, 1969).

Al-Yaari and Abu-Sharkh, (2011) observed the stratified flow pattern at very low mixture velocity 0.3 to 0.75 m/s with the different range of the input water volume fraction, if the mixture velocity increased to 1 m/s the pattern changes from stratified to stratified wavy flow.

3.3 Mesh Effect

One of the main principal of engineering simulation is mesh generation. The existence of many cells of mesh may result in long solver runs, and few cells of mesh may give inaccurate results. Technology of meshing in ANSYS is based on the strengths a stand-alone, class-leading, meshing tool, which leads to balance.

Hussain and Khuan, (2009) meshed the flow domain of a horizontal pipe with a diameter of 0.0254 m and a length of 9.7 m into 227,820 elements with 164,306 tetrahedrons, 58,333 of prisms and 5181 of pyramids. Al-Yaari and Abu-Sharkh, (2011) used coarse and fine mesh (63,493, 82,933, 104,533 and 147,733 cells by CFD package FLUENT 6.2) to show the mesh independence of the solution.

The computational mesh properties of this study are shown in Table 3.3. These different meshes are used to select the optimum size of the mesh by using the mesh independence study.

Table 3.3 Mesh properties

For 0.0254 m diameter, V_m= 1.2 m/s and α_w= 40 %		
Mesh number	Number of elements	Pressure
1	425015	91.0209
2	665028	94.8277
4	845215	111.136
5	915453	111.177
For 0.127 m diameter, V_m= 0.2 m/s and α_w= 20 %		
1	246519	224.184
2	308902	226.488
3	404322	226.649
4	621576	226.062
For 0.254 m diameter, V_m= 0.5 m/s and α_w= 60 %		
1	425184	194.599
2	523998	198.537
3	616121	196.037
4	716384	197.421

For 0.508 m diameter, V_m= 0.8 m/s and α_w= 80 %		
1	876428	703.785
2	981996	701.817
3	1064252	703.362
4	1230880	714.639

3.4 Reynolds Number

Reynolds number must be known to determine the regime of flow (laminar or turbulent). The characteristic length of geometry, average velocity and fluid properties are effecting the transition from laminar flow to turbulent flow. Generally, Re can be expressed as for single-phase flow

$$Re = \frac{Inertial\ forces}{viscous\ forces} = \frac{VD}{v} = \frac{\rho VD}{\mu} \qquad 3\text{-}17$$

and for two-phase flow

$$Re = \frac{Inertial\ forces}{viscous\ forces} = \frac{VD}{v} = \frac{\rho_m VD}{\mu_m} \qquad 3\text{-}18$$

The flow regime classification according to the Reynolds number for a circular pipe is given below

Laminar flow $Re \leq 2300$

Transitional flow $2300 \leq Re \leq 4000$

Turbulent flow $Re \geq 4000$

Table 3.4 Reynolds numbers obtained from Equation 3-18			
Diameter (m)	Velocity (m/s)	Water volume fraction (%)	Reynolds numbers
0.0245	0.2	20	2872.51
		40	3280.06
		60	3762.79
		80	4343.57
	0.5	20	7181.26
		40	8200.16
		60	9406.96
		80	10858.93
	0.8	20	11490.02
		40	13120.26
		60	15051.14
		80	17374.29
	1.2	20	17235.03
		40	19680.39
		60	22576.71
		80	26061.44
0.127	0.2	20	14362.53
		40	16400.32
		60	18813.93
		80	21717.86
	0.5	20	35906.32
		40	41000.80
		60	47034.82
		80	54294.66
	0.8	20	57450.11
		40	65601.29
		60	75255.71
		80	86871.46
	1.2	20	86175.16
		40	98401.93
		60	112883.56
		80	130307.19
0.254	0.2	20	28725.05
		40	32800.64
		60	37627.85
		80	43435.73
	0.5	20	71812.63
		40	82001.61
		60	94069.64
		80	108589.32
	0.8	20	114900.21
		40	131202.57
		60	150511.42
		80	173742.92

	1.2	20	172350.32
		40	196803.86
		60	225767.13
		80	260614.37
0.508	0.2	20	57450.11
		40	65601.29
		60	75255.71
		80	86871.46
	0.5	20	143625.26
		40	164003.22
		60	188139.27
		80	217178.65
	0.8	20	229800.42
		40	262405.15
		60	301022.84
		80	347485.83
	1.2	20	344700.63
		40	393607.72
		60	451534.26
		80	521228.75

3.4.1 Turbulent Intensity

It is one of the turbulence parameters that refer to level of turbulence. It is defined as the ratio of the root-mean-square of the turbulent velocity to the mean free stream velocity.

$$I = \frac{u'}{\overline{u}} \qquad 3\text{-}19$$

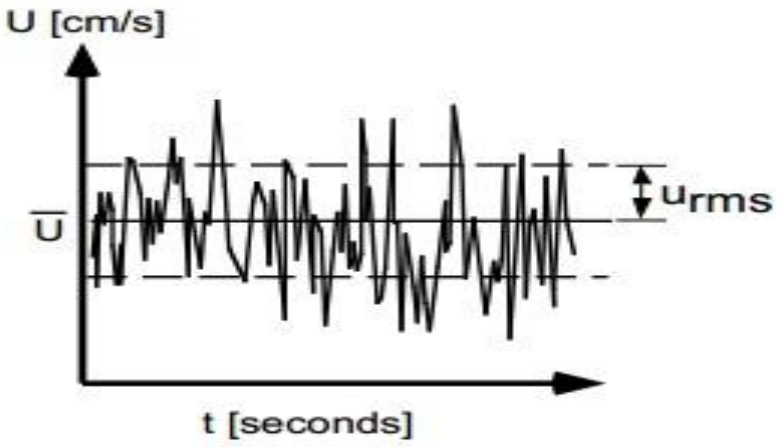

Figure 3.2 Turbulence intensity diagram

When setting boundary conditions in CFD simulation, it is often necessary to assess the turbulence intensity for the inlet and outlet boundary condition in Fluent 14.0 software. The incoming turbulence intensity is high for heat exchanger between the ranges of 5 % to 20 %, is medium for large pipe between the range of 1 % to 5 %, and is less than 1 %for external flow (www.esi-cfd.com, 2014). Only Reynolds number used to estimate it. For fully developed two phases flow through a pipe, the turbulence intensity in the core can be estimated as (White, 1997):

$$I = 0.16\, R_e^{-\frac{1}{8}} \qquad 3\text{-}20$$

Table 3.5 Relative turbulence intensity obtained from equation 3-20

Diameter (m)	Velocity (m/s)	Water volume fraction (%)	Reynolds numbers	Turbulence intensity
0.0245	0.2	20	2872.51	0.059
		40	3280.06	0.058
		60	3762.79	0.057
		80	4343.57	0.056
	0.5	20	7181.26	0.053
		40	8200.16	0.052
		60	9406.96	0.051
		80	10858.93	0.050
	0.8	20	11490.02	0.050
		40	13120.26	0.049
		60	15051.14	0.048
		80	17374.29	0.047
	1.2	20	17235.03	0.047
		40	19680.39	0.046
		60	22576.71	0.046
		80	26061.44	0.045
0.127	0.2	20	14362.53	0.048
		40	16400.32	0.048
		60	18813.93	0.047
		80	21717.86	0.046
	0.5	20	35906.32	0.043
		40	41000.80	0.042
		60	47034.82	0.042
		80	54294.66	0.041
	0.8	20	57450.11	0.041
		40	65601.29	0.040
		60	75255.71	0.039

		80	86871.46	0.039
	1.2	20	86175.16	0.039
		40	98401.93	0.038
		60	112883.56	0.037
		80	130307.19	0.037
0.254	0.2	20	28725.05	0.044
		40	32800.64	0.044
		60	37627.85	0.043
		80	43435.73	0.042
	0.5	20	71812.63	0.040
		40	82001.61	0.039
		60	94069.64	0.038
		80	108589.32	0.038
	0.8	20	114900.21	0.037
		40	131202.57	0.037
		60	150511.42	0.036
		80	173742.92	0.035
	1.2	20	172350.32	0.035
		40	196803.86	0.035
		60	225767.13	0.034
		80	260614.37	0.034
0.508	0.2	20	57450.11	0.041
		40	65601.29	0.040
		60	75255.71	0.039
		80	86871.46	0.039
	0.5	20	143625.26	0.036
		40	164003.22	0.036
		60	188139.27	0.035
		80	217178.65	0.034
	0.8	20	229800.42	0.034
		40	262405.15	0.034
		60	301022.84	0.033
		80	347485.83	0.032
	1.2	20	344700.63	0.033
		40	393607.72	0.032
		60	451534.26	0.031
		80	521228.75	0.031

3.5 Modeling Studies of Two-Phase Oil-Water Flow

Oil-water flows through a horizontal pipe like any two-phase flow model follow all the fundamental of fluid mechanics. However, due to a difference between properties of oil and water causes slipping at the interface between phases. The equations are more complex and more numerous than single-phase flow.

Homogeneous and segregated models are widely used for obtain theoretical and experimental results and to predict parameters of design. In the present study, homogeneous model is used.

3.5.1 Homogeneous Oil-Water Flow Models

It is the simplest model for analyzing two-phase flows. This model assumes that the two phases are intimately mixed or two phases travel at the same velocity and flow as like a single phase. The basic problem is to get the characteristic of the pseudo-fluid. Once those properties are obtained, then all equations of single-phase fluid flow can be used.

The total pressure gradient equation for single-phase flow is the sum of the frictional, acceleration and gravitational components (Wallis, 1969).

$$\left(\frac{dp}{dz}\right) total = \left(\frac{dp}{dz}\right) F + \left(\frac{dp}{dz}\right) A + \left(\frac{dp}{dz}\right) G \qquad 3\text{-}21$$

where the pressure gradient due to friction loss,

$$\left(\frac{dp}{dz}\right) F = \frac{P}{A}\tau_w \qquad 3\text{-}22$$

the pressure gradient due to acceleration,

$$\left(\frac{dp}{dz}\right) A = \frac{W}{A}\frac{dv}{dz} \qquad 3\text{-}23$$

and pressure gradient due to gravitational forces are given respectively.

$$\left(\frac{dp}{dz}\right) F = \rho_m g \cos\theta \qquad 3\text{-}24$$

The fanny friction factor in laminar flow is a function of only Reynolds's number, and is given by

$$f = \frac{16}{R_e} \quad 3\text{-}25$$

In the case of turbulent flow, fanny friction factor is a function of both the Reynolds's number and the roughness of the pipe. If the flow is turbulent for smooth pipe, it is given by:

$$f = 0.079 R_e^{-0.25} \quad 3\text{-}26$$

The effective properties for a homogeneous flow model, the two-phase oil-water mixture are usually expressed by using simple mixing rules:

$$u_m = u_o + u_w \quad 3\text{-}27$$

The mixture density, the mixture viscosity and the Reynolds's number are commonly calculated by Equations (3-3), (3-7) and (3-18) respectively, and for steady flow, the void fraction and quality are given as:

$$\alpha = \frac{Q_w}{Q_o + Q_w} = \frac{j_o}{j} \quad 3\text{-}28$$

$$x = \frac{\dot{m}_o}{\dot{m}_w + \dot{m}_o} = \frac{G_o}{G} \quad 3\text{-}29$$

For homogeneous steady oil-water flows, the pressure gradient can be predicted by using previous Equations (3-21), (3-22) and (3-23).

3.6 Conclusion

Prediction of the pressure gradient of the oil-water stratified flow through a horizontal pipe by computational fluid dynamics is the aim of the present thesis. The oil-water stratified and stratified wavy flow is simulated by volume of fluid (VOF)

multiphase with Realizable k-ε model and Shear Stress Transition k-ω model then discussing the results numerically and experimentally with those in literature.

CHAPTER 4

CFD METHOD AND TURBULENCE MODELING

4.1 Introduction

Bakker et al., (2001) is one of the first adopters of Computational Fluid Dynamics (CFD) in the field of the automotive, aerospace and nuclear industries. CFD is a technique based on the numerical solution of the fundamental fluid mechanics equations. CFD needs a good processor and a big memory to simulate and analyze fluid motion. A collection of mathematical equations that characterize the flow is, firstly, structured for any numerical model. This set of equations will be then dissolved using of a computer program such as ANSYS FLUENT in getting the fluid parameter along the flow domain. It is used in a broad range of industrial application areas, such as:

- In the field of mechanical works: combustion system in gas turbines and engines, refrigeration and air conditioning systems, transmission system in gas and oil through pipeline gathering.
- In the field of chemical engineering: nuclear energy plants, mixing and separating of gas-liquid, solid-liquid and liquid-liquid chemical material.
- In the field of environmental engineering: environmental pollution.
- In the field of medical science: nervous system, circulatory, the blood flow.

Codes in CFD can supply very large volumes of results with effectively low costs to execute parametric studies (Versteeg and Malalasekera, 2007). There are

some advantages of CFD method over experiment-based methods to fluid system designs, such as low cost, speed, effort, and the applicability to simulate both danger and troublesome conditions.

4.2 CFD Simulation Process

Three basic steps are necessary to input problem variables advanced user interfaces and test the results of CFD codes.

4.2.1 Pre-processor

The first step must be a definition of the geometry of the computational domain. Mesh and grid should be generated. The problem specification should be also provided by appropriate physical, chemical phenomena and boundary conditions. The mesh independence studies are very important to specify and provides better conversion and accuracy of the CFD solution. Unknown flow properties such as velocity, pressure and water volume fraction are solved at nodes inside each cell.

The geometry and grid generation processes are executed using specialized computer-aided drawing (CAD) and mesh generation software, for example, GAMBIT program. The definition of the domain of the geometry and mesh for any fluid problem in CFD project is required more than half time of the project. All CFD software such as FLUENT, PHONENICS, CFX/ANSYS and Star-CD are equipped with their own CAD-style interface or the facilities to import data from proprietary surface modelers and mesh generators.

4.2.2 Numerical solver

The numerical solver or solution is a very important and the second step of the CFD process. The solution of the equations governing of the fluid flow problem is obtained using a CFD code after discretizing and iterations until convergence is achieved. In another word, a solution algorithm involves the following steps:

- Convert the variety of unknown flow parameter for any model to a simple function.
- Replacement the function of unknown flow parameters to the mathematical manipulation in order to be discrete.
- Finally, solve all equations by an iterative method.

Therefore, this section also contains the definition of fluid properties (density, viscosity, velocity, etc....) and the selection of flow models, for example, volume of fluid (VOF).

4.2.3 Post-processing

This final step contains explaining and analyzing the results obtained from above solution steps. For example, the geometry and mesh generation of whole domain, vectors, the surfaces 2D and 3D, rotating domain, translation, scaling, view sections, surfaces, separating the regions of domain by color and XY plots and graphs of results are possible to obtain in accordance with the requests.

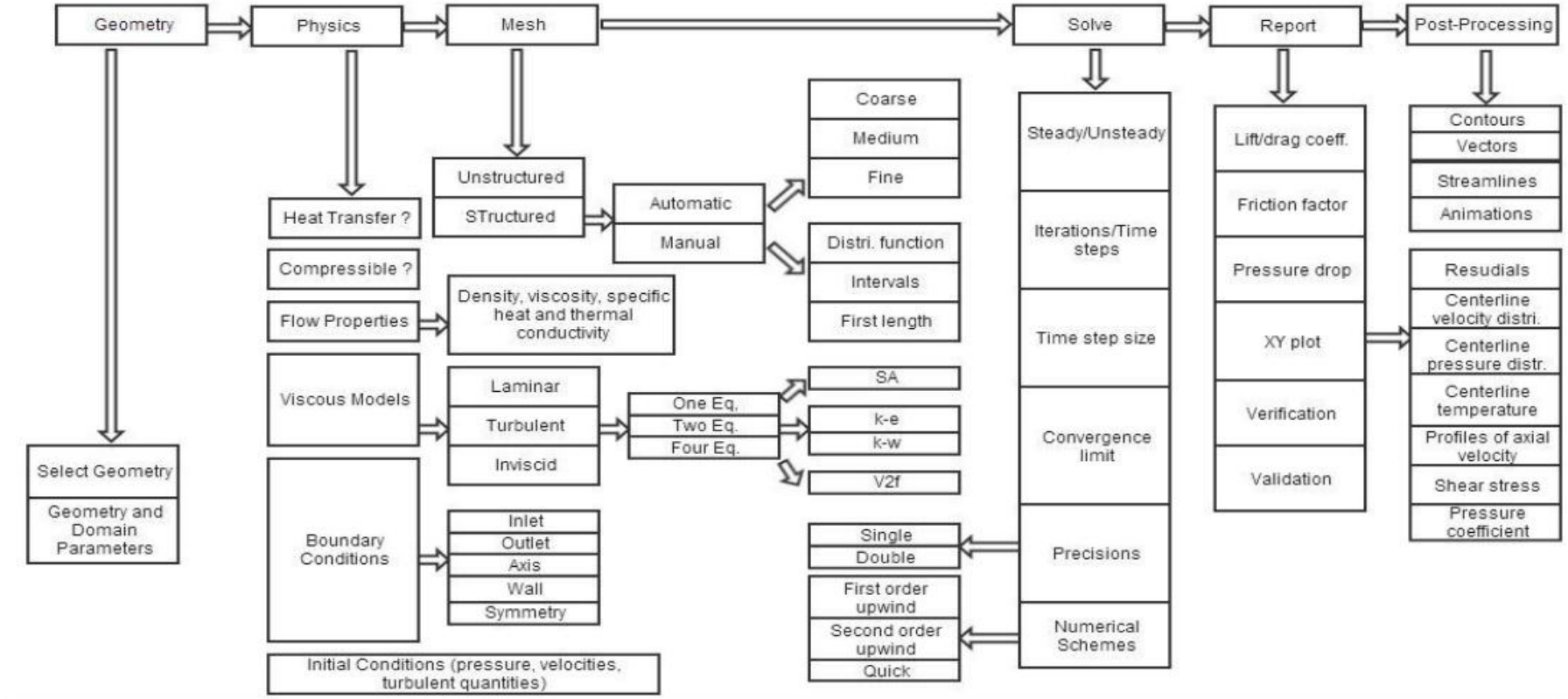

Figure 4.1 The methodology of CFD work

4.3 Turbulence

Turbulence causes the appearance of eddies in the flow with a wide range of length and time scales that interact in a dynamically complex way. In general, Reynolds number is the main way to determine the dominating force between inertial and viscous force.

$$Re = \frac{Inertial\ forces}{viscous\ forces} = \frac{VD}{v} = \frac{\rho VD}{\mu} \qquad 4\text{-}1$$

The viscous forces are small compared to the initial forces in turbulent flows.

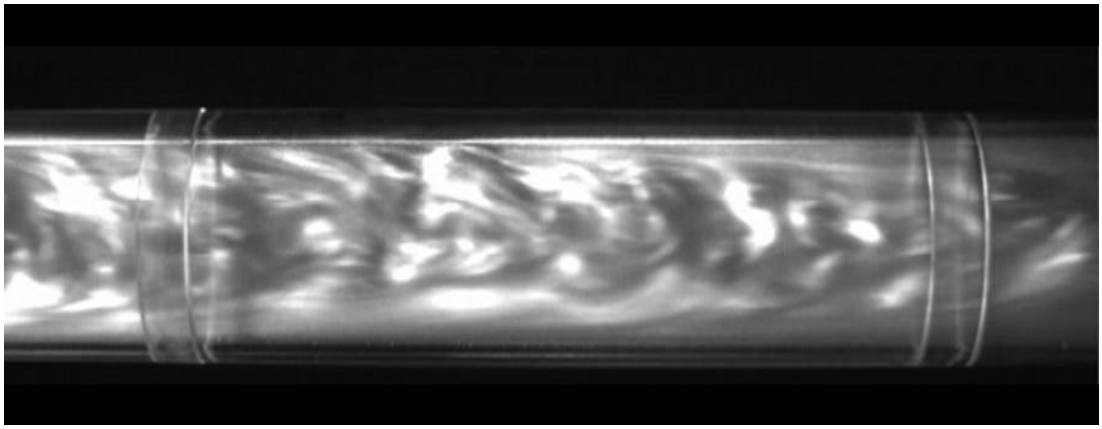

Figure 4.2 A view of turbulence in a pipe (Manchester Center for Nonlinear Dynamics, 2013)

4.4 Turbulence Models in CFD

CFD modeling can be applied for all types of fluid flow (laminar or turbulent). Analyzing of a laminar flow is easy in comparison with a turbulent flow which needs some special considerations for modeling. The ANSYS FLUENT software provides different options of multiphase models such as Volume of Fluid (VOF), Mixture and Eulerian model, which contain below turbulence models

- The Spalart-Allmaras Model.

- k-ε models, (k = turbulence kinetic energy, ε = turbulence dissipation rate)
- k-ω models, (k = turbulence kinetic energy, w = specific dissipation rate).
- The v2–f model.
- The Reynolds Stress Models.
- Detached Eddy Simulation (DES) model.
- Large Eddy Simulation (LES) model.

The select any one of the above turbulence model depend on type of fluid problem and type of flow pattern. For stratified and stratified wavy flow pattern or free surface flow, the Volume of Fluid (VOF) model should be used (ANSYS package help, 2011). In VOF, the flow domain is divided into a grid involving a large number of cells. For any cell, if occupied only with water, $\alpha_w = 1$; otherwise α_w=0, while for the cells occupied by both water and oil $0 < \alpha_w < 1$. So the flow properties in each cell can be fixed according to the local volume fraction, for example, the density in each cell is calculated depending on volume fractions of phases according to the Equation. 3-3.

4.4.1 The k-ε model

The accuracy of the CFD results for turbulent two-phase flows can be influenced by the turbulence modeling. The k-ε model solves two further differential equations for kinetic energy k and dissipation ε. As authenticated by Versteeg and Malalasekera (2007) and Pope (2000), it is recognized that the select of a turbulence model to include the influence of turbulence in the time-averaged mean-flow equations represents one of the principal sources of uncertainty of CFD predictions. The non-linearity in the discretized equations caused turbulence effects on these equations (Pope, 2000). The k-ε model has become the most widely used turbulence

model in the engineering industry (DeJesus, 1974).

K-ε model is one of the two equation models. It contains two further transport equations to represent properties of the turbulent of the flow. The rate of production and dissipation of turbulent flows in the k-ε turbulence model are assumed in near-balance with energy transfer, so that the dissipation rate of the energy, ε, is given as,

$$\varepsilon = \frac{k^{\frac{3}{2}}}{L} \qquad 4\text{-}2$$

where k is the kinetic energy of the flow and L is the involved length.

K-ε models in ANSYS package version 14.0 are standard k-ε model, RNG k-ε model and realizable k-ε model (Fluent User Services Center, 2013).

4.4.1.1 The standard k-ε model

The terms k and ε refer to the turbulence kinetic energy which is the variance of fluctuations in velocity. ε is the dissipation rate of k. It is powerful and rationally accurate in results. Therefore, it is the most widely used turbulence model for industrial engineering applications.

4.4.1.2 The RNG k- ε model

The renormalize group (RNG) k- ε model is commonly used for incompressible flows, but contains some advantages according to the standard k- ε model as follows:

- There is an additional term in the ε equation to improve the accuracy in results.
- It is used for flows, including high strain rates, swirl, and separation.

- The performance of this model better than the standard k- ε model for more complex shear flows.

4.4.1.3 The realizable k- ε model

The realizable means that the model satisfies appointed mathematical constraints on the Reynolds stresses, proportional to the physics of turbulent flows. Improvements and advantages in the realizable k- ε model are:

- Improvements of the ε equation.
- Variable Cμ is used.
- More accurately, prediction of flows involving planer and around jets, and passes good performance for flows involving rotation, boundary layers under strong adverse pressure gradients, separation and recirculation.

4.4.2 The k–ω Turbulence Models

Two different types of the k- ω model are described in this section. Standard k–ω (SKW) and Shear Stress Transport k–ω (SSTKW) models use similar transport equations for k and ω. However, the SST model differs from the SKW model in some point. Both models are widely used because:

- The k–ω turbulence model equations do not involve expressions, which are undefined at the wall.
- They are accurate in results and sturdy for a wide range of boundary layer flows with pressure gradient.

4.4.2.1 Standard k–ω (SKW) model

FLUENT code uses a standard k-ω model developed by Wilcox (1998) that

was formulated to compute better for low-Reynolds number flows. The terms k (turbulent kinetic energy) and ω (turbulent frequency) stand for two transport equations. It is frequently used in the fields of aerospace and turbo-machinery communities. Several options of k–ω model are compressibility effects, transitional flows and shear-flow corrections. The results are computed based on the concept of eddy-viscosity.

4.4.2.2 Shear Stress Transport k–ω (SSTKW) model

The shear stress k–ω model was developed by Florian (1994) using the standard k-ω model and a transformed k-ε model. It uses a blending function to progressively transition from the (SKW) model near the wall and a high Reynolds number version of the k–ε model in the outer portion of the boundary layer. It involves a modified turbulent viscosity model to account for the transport influence of the principal turbulent shear stress.

4.5 Simulation of Oil-Water in a Horizontal Pipe

This part involves the modeling and simulation procedure of the domain of oil-water in a horizontal pipe from the first point of pre-processing to the results or post-processing stage. Initially, describe and specify data to input to the ANSYS CFD FLUENT program. The normal analytical procedure is used to validate the model. Typical modeling is substantial to obtain the valid selection in all simulations, in order to end or at least reduce the complication to the problem retaining the important properties. The flow problem specification and formulation required in a computational domain must be considered by the physical and chemical properties of oil-water flow. Experimental and computational studies in literature must be used to prove the accuracy of any study. Figures 4.3 and 4.4 give a comparison of

experimental data taken from (Al-Wahaibi, 2012) and (Al-Yaari et al., 2009) respectively with computational data obtained with k-ε and k-ω turbulence models in this study. Generally, the pressure gradient is found by the Shear Stress Transport k-ω model better than those found by Realizable k-**ε** turbulence model. The results are in good agreement with the most recent experimental data over a large domain of the pressure gradient.

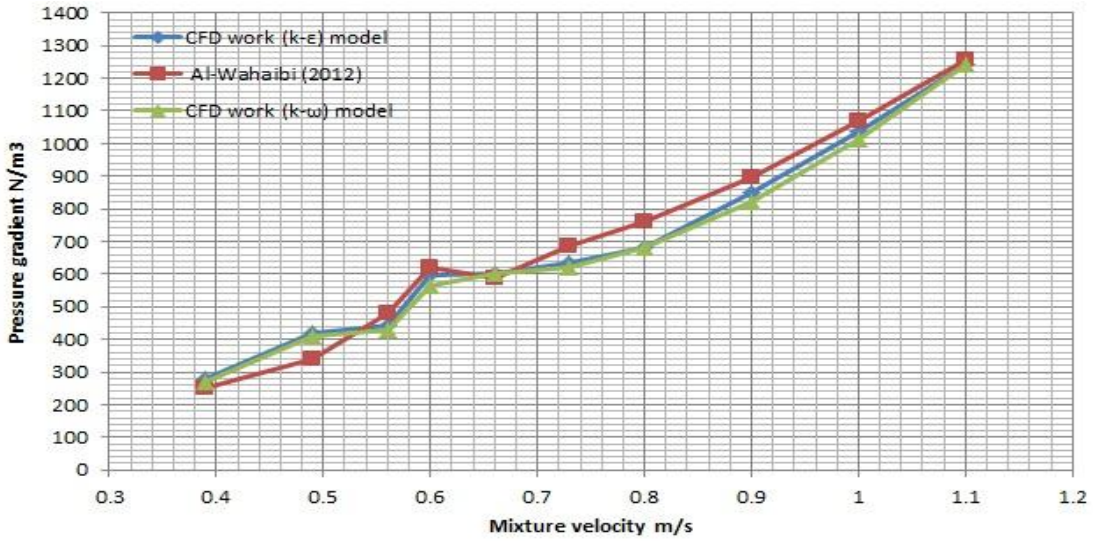

Figure 4.3 A comparison of computational results to experimental data taken from (Al-Wahaibi, 2012)

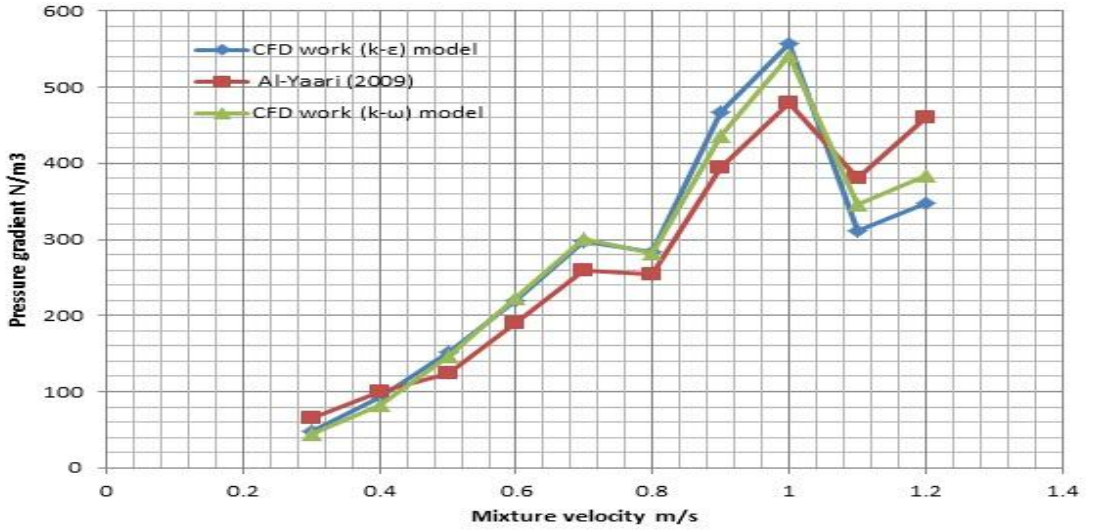

Figure 4.4 A comparison of computational results to experimental data taken from (Al-Yaari et al., 2009)

4.5.1 Modeling and Simulation Procedure

A CFD code such as ANSYS-FLUENT requires definition of geometry, mesh, and solver settings in order to compute the required results. The procedure of the modeling and simulation step by step from pre-processing, to post-processing stages are described respectively. ANSYS- FLUENT version 14 on a Core i7 Computer Dell is used in the present study. A series of CFD simulations as a parametric study is used as a study methodology to determine the effects of changing geometry parameters such as diameters, length, and flow parameters such as velocities and volume fraction of water.

4.5.1.1 Pre-processing

For any simulation, model is a very important step of the study, because it involves the preliminary idea and generation of the model. Model is created by Design modular in ANSYS Workbench in this study. The geometry is then meshed using ANSYS meshing platform. The physical properties such as density, viscosity, and boundary conditions such as velocity and volume fraction of water are defined.

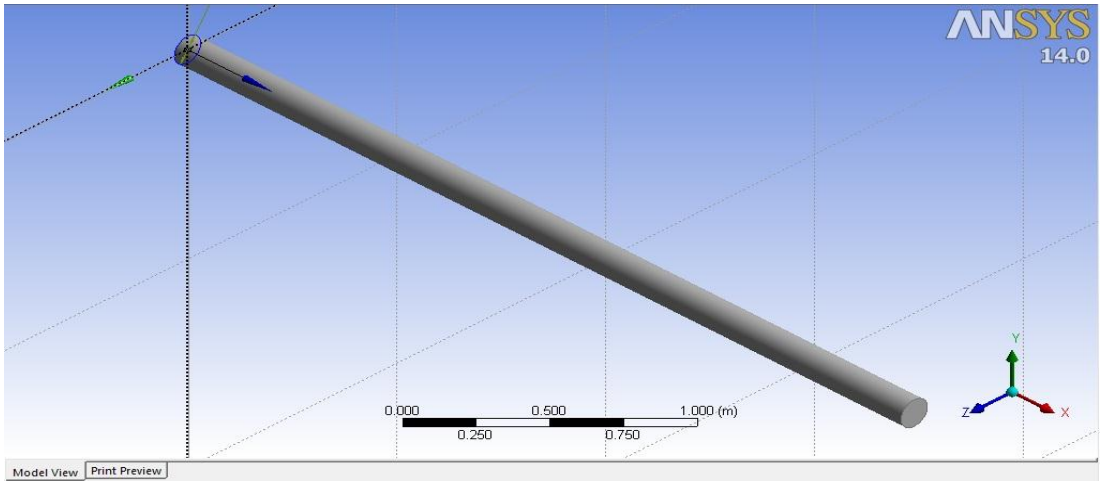

Figure 4.5 The whole domain of the pipe

4.5.1.1.1 Creating the model and defining the geometry

The first step in simulating any engineering flow is the creation of the flow geometry, which can be created by using ANSYS Design Modular in ANSYS workbench, or any CAD software, and then exporting it to ANSYS workbench. For the present study, the geometry was created by using ANSYS Design Modular in ANSYS workbench application. There are two steps to create geometry regions. A circular sketch, firstly, created on base plane YZ since the flow is accepted in X direction. The four circle diameters are used between 0.0245 to 0.508 m. This circular sketch is then extruded to represent a horizontal pipe flow domain with different length 0.4245 to 25.9034 m according to the Equation 4.3 (White, 1997) to obtain the fully developed region before the test section. The second step is a creation of a slice on ZX plane to define the oil and water region in the pipe was shown in Figure 4.6. The creation of these two conduits according to oil and water volume fraction ratios makes an advantage for entering some boundary condition into the CFD solver (Mouza et al., 2001).

$$\frac{L}{D} = 1.6\, R_e^{\frac{1}{4}} \qquad 4.3$$

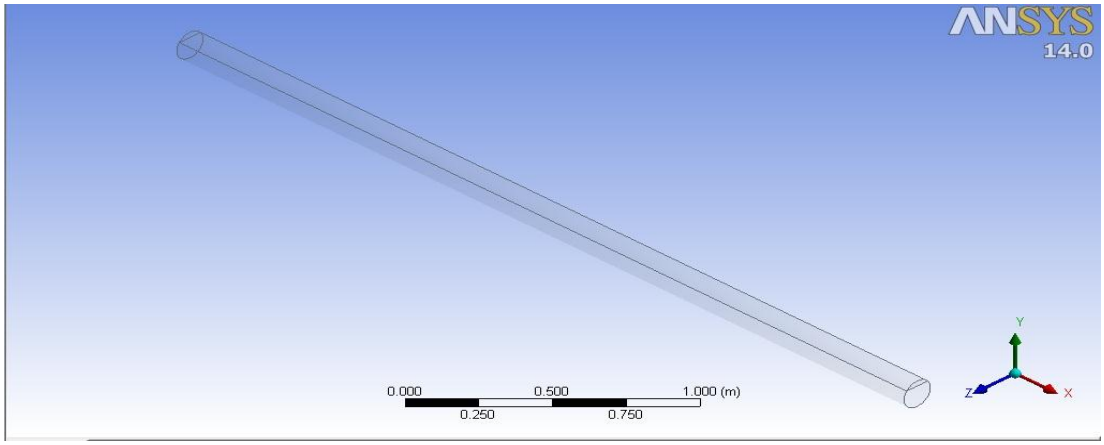

Figure 4.6 The oil-water flow domain

Table 4.1 Dimensions of the pipe in Figure 4.6

Length (m)	3.4828
Diameter (m)	0.127
Water volume fraction (%)	0.8
Oil volume fraction (%)	0.2

4.5.1.1.2 Creating mesh and the boundary layer

The optimum mesh size is selected by the mesh independence study. The minimum size of mesh is set to be less than the first layer thickness near the wall of the pipe. For the present study, the first layer thicknesses from the wall of the pipe are 0.001, 0.005, 0.01 and 0.015 m for 0.0254, 0.127, 0.254 and 0.508 m diameter pipes respectively. The minimum mesh sizes are set to 0.00001, 0.00005, 0.0001 and 0.00015 m to avoid incorrect automatic mesh generation in FLUENT. Finally, the ratio of the mesh size between two neighboring elements should be no greater than 1.5 (Berger and Stockstill, 1999). On this basis, the grow rate between two neighboring meshes has been set to 1.2 meaning that 5 layers are required to achieve the near-maximum side mesh size..

ANSYS-FLUENT contains a new technique, the sweep method, to capture the free surface flow profile for Stratified flow. The purpose of this technique is to refine the mesh size along the direction normal to the flow direction. It may also be used as an alternative to inflation techniques to make appropriate refinements near the wall of the pipe, to maintain first layer thickness. For this purpose, the inlet of the pipe is set as a source for the sweep method, and the outlet as a target, so the sweep starts from the inlet to the end of the pipe outlet. For the present study, the first inflation layer thickness is set as 0.001, 0.005, 0.01 and 0.015 m for 0.0254, 0.127,

0.254 and 0.508 m diameter pipes respectively.

When the mode is defined, mesh is updated and generated. Pipe domain is divided into a number of cells for accuracy and control of the results. On the other hand, all boundaries such as inlet, walls and outlet are defined.

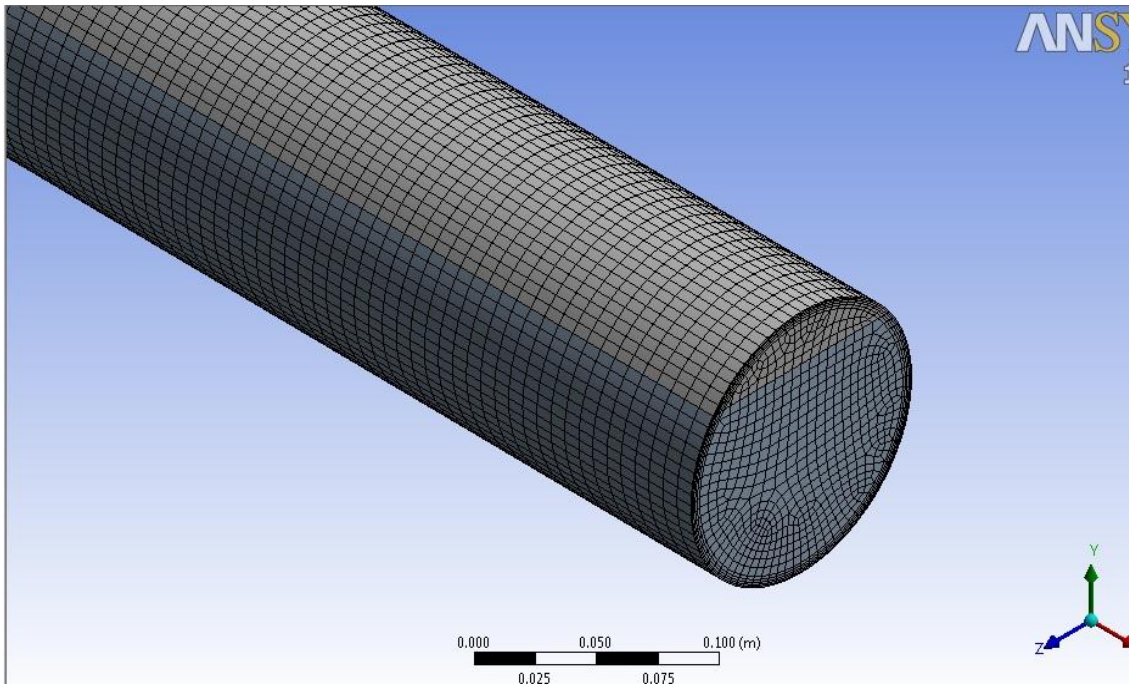

Figure 4.7 Mesh of pipe

In this study, the model is divided into nodes and elements according to diameter and length of pipe, Table 4.2 shows the mesh metric of the created mesh.

Table 4.2 The mesh metric

Diameter of the pipe	Length region of the pipe	Element
0.0254	0.5007-0.7196	208464-239512
0.127	3.2405-4.8767	404322-632800
0.254	7.3228-11.2143	366272-568936
0.508	16.6476-25.9034	826964-1161300

Different views of meshing are given in Figures 4.7 to 4.9.

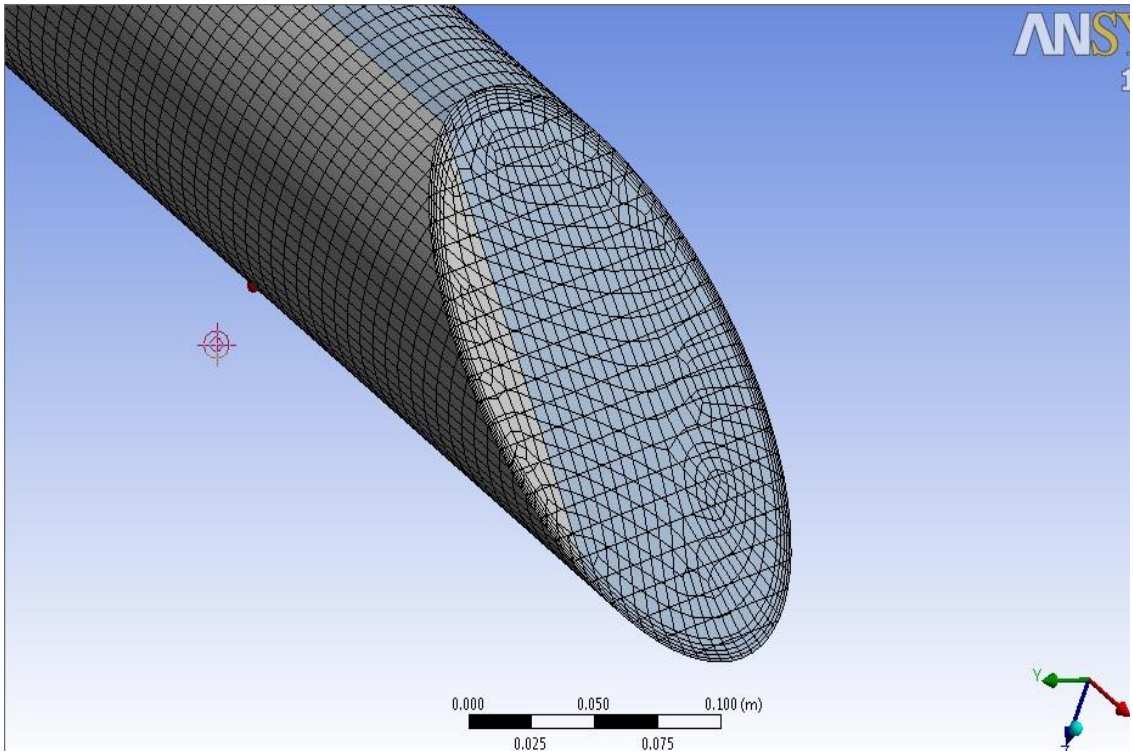

Figure 4.8 The cross-section of the mesh

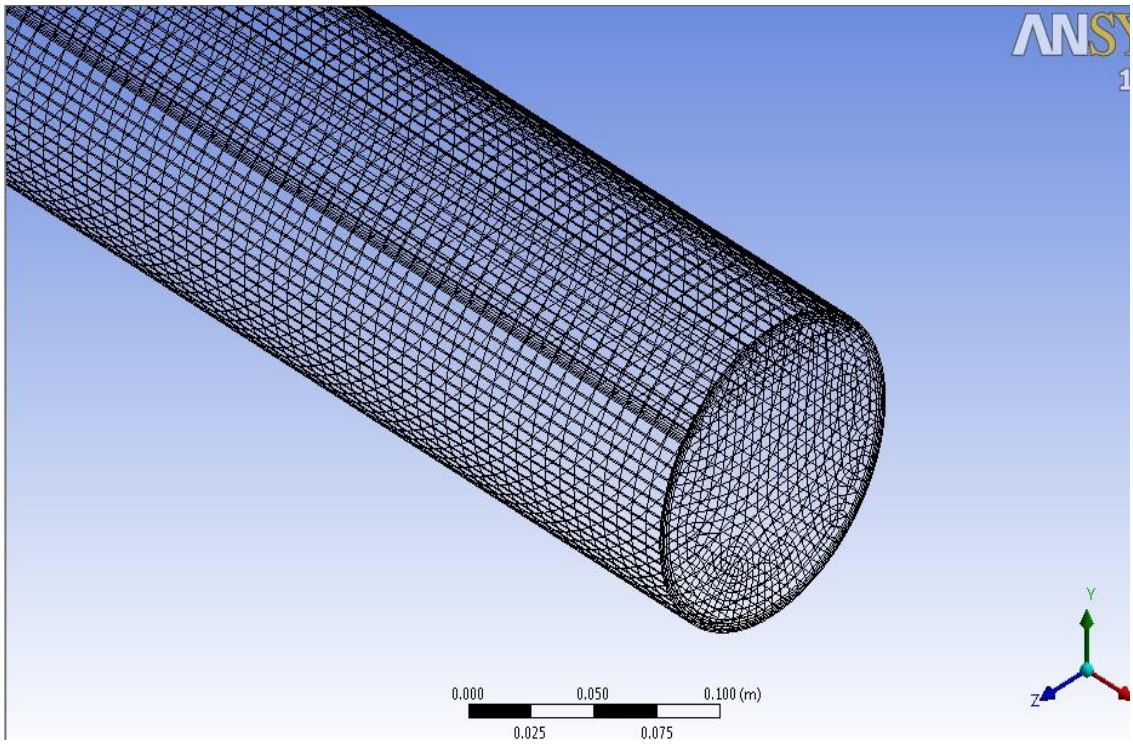

Figure 4.9 The wire frame of the mesh

4.5.1.2 Simulation

The quality of the mesh is checked after the mesh generated in the FLUENT software with entering the boundary layer conditions and properties. Simulation steps of the model are defined in the following sub-topics.

4.5.1.2.1 The physical procedure

Separate solver and implicit formulation are selected in this study. The gravity vector is depend with a magnitude of 9.81 m/s in the y-direction. A multiphase 3D Volume of Fluid model is used. Two turbulent models which are the εrealizable k-ε model and Shear Stress Transition k-ω model with standard wall functions are used to simulate the characteristics of the two-phase stratified and stratified wavy flow.

4.5.1.2.2 Defining the fluid properties

The oil is selected as primary phase if fraction volume in oil-water mixture is higher than 0.5. The water is selected as a secondary phase. The fluid properties of each phase are given in Table 4.3.

Table 4.3 Fluid properties of oil and water

Property	Water	Oil
Density	998.2 kg/m^3	780 kg/m^3
Viscosity	0.001003 kg/ms	0.00157 kg/ms

4.5.1.2.3 Specification of boundary conditions

No-slip is used for both phases. A pressure outlet boundary conditions is imposed at the exit of the pipe. Two-cell zones are used. Table 4.4 shows all boundary conditions.

Table 4.4 The boundary conditions

Surface	Boundary conditions
Inlet	Velocity inlet
Outlet	Pressure outlet
Wall	Wall

4.5.1.3 Initialization and solving the model

Here, the turbulence properties are introduced and defined. The inlet is taken as reference to initialize the solution. The active reference frame is chosen relative to the cell zone. The input velocity in the X-direction is introduced as 0.2 m/s to 1.2 m/s. In the present calculations, 10^6 values residual is set for continuity, volume fraction, turbulent kinetic energies, turbulent dissipation energies and velocity components. The number of iterations is set as 1000 for good conversion. At this stage, it is important to save the results in order to prevent from any problem with computer. Figure 4.10 shows the residuals vs. the number of iterations.

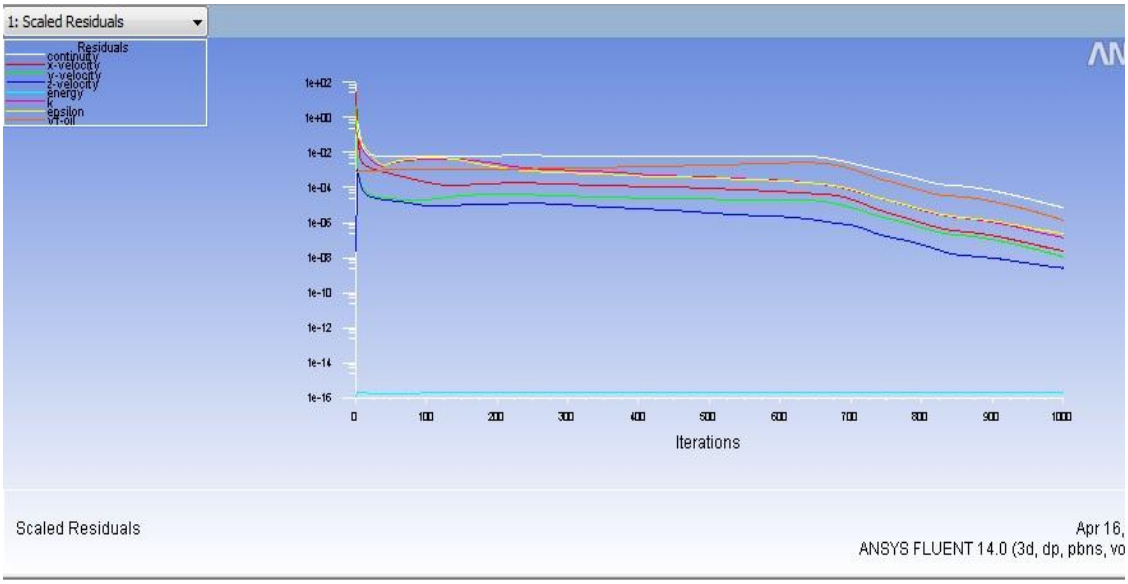

Figure 4.10 The residuals versus the number of iterations

4.5.1.4 Post-processing

In the post-processing stage, the required results such as pressure gradient, volume of fraction of each phase and velocity of each phase can be screened. The vector or contour plot type in different styles can be obtained. The post-processing results of this study is given in Chapter 5.

CHAPTER 5

RESULTS AND DISCUSSIONS

5.1 Introduction

The simulation results of water volume fraction, pressure gradient and other physical properties are presented in this chapter. The reasonable simulation results by CFD gave detailed visualizations with a lower cost than experimental tests.

This chapter contains the results of two different turbulence models realizable k-ε and shear stress transport k-ω, for all diameters between the 0.0254 m and 0.508 m, all water volume fractions between the 20 % and 80 % and all mixture velocities between the 0.2 m/s and 1.2 m/s.

5.2 Test section

The lengths of the pipes used in simulations are different from each other, the length of the pipe is equal to the sum of the length of fully develop flow entrance length according to the Equation 4.3 and 8 times diameter (8D). The test section consists from two points. The first section point is at a distance of the sum of the length of fully develop flow and 5 times diameter and the second section point is at 6 times diameter after the fully develop flow length away from the inlet.

Figures 5.1 to 5.4 plot the pressure gradient dependency upon Reynolds number (Re) for different pipe diameters and volume fractions of water by Realizable k-ε and Shear Stress Transport k-ω turbulence models.

5.3 Pressure gradient

The procedure of calculating a pressure gradient through a horizontal pipe in a single-phase flow is also applied to the two-phase flow. ANSYS Fluent program provides flexibility in selecting discretization schemes for the solution model to obtain the pressure gradient. The discretized equations, along with the initial condition and boundary conditions, were solved using the pressure-velocity coupling solution method to obtain a numerical solution. While SIMPLE discretization scheme was used for pressure, second order upwind discretization scheme was used for the momentum equation, volume fraction, turbulent, kinetic and turbulent dissipation energy. The volume of fluid is directly proportional to the pressure gradient. The other conditions that affect this flow are the pipe length, pipe diameter and pipe roughness. Pressure gradient in a horizontal steel pipe changes according to the used turbulence model, diameter, water volume fraction and mixture velocity.

In this study, four different diameters as 0.0254, 0.127, 0.254 and 0.508 m; two different turbulence models for each model as Realizable k-ε and Shear Stress Transport k-ω (SST); four different water volume fractions as 20, 40, 60 and 80 %; and four different mixture velocities as 0.2, 0.5, 0.8 and 1.2 m/s are used.

5.3.1 Effect of the water volume fraction on the pressure gradient

The effect of the water volume fraction in oil–water stratified flow and stratified wavy flow on the pressure gradient in the volume fraction range of 20 % to 80 % is studied for each diameter. Figures.5.1 to 5.4 show the pressure gradient results of oil–water stratified flow versus Reynolds number for four different diameters as (0.0254, 0.127, 0.254 and 0.508 m) and water volume fractions.

Pressure gradient for 20 % water volume fraction is increased with Reynolds

numbers between the diameter range of 0.0254 and 0.127 m as shown in Figures 5.1a and 5.1b. However, the pressure gradient is dropped between the diameter range of 0.254 and 0.508 m with Reynolds numbers increasing to 71812.63 for 0.254 m diameter pipe and 229800.42 for 0.508 m diameter pipe. After that pressure gradient is increased back again with Reynolds number as shown in Figures 5.1c and 5.1d.

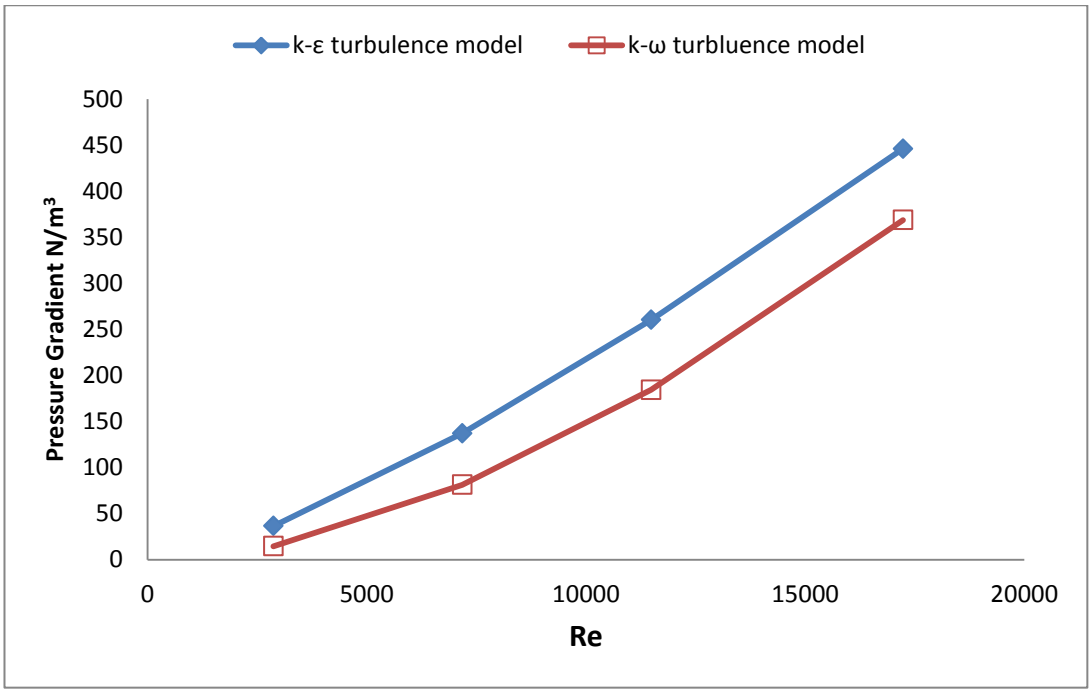

a) for 0.0254 m diameter pipe

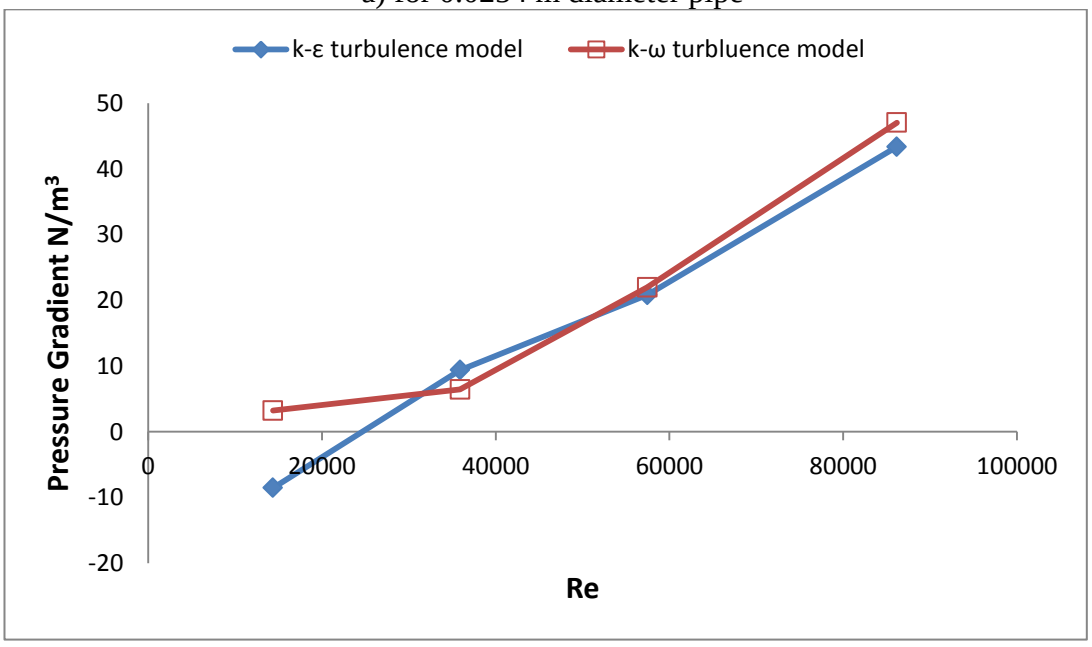

b) for 0.127 m diameter pipe

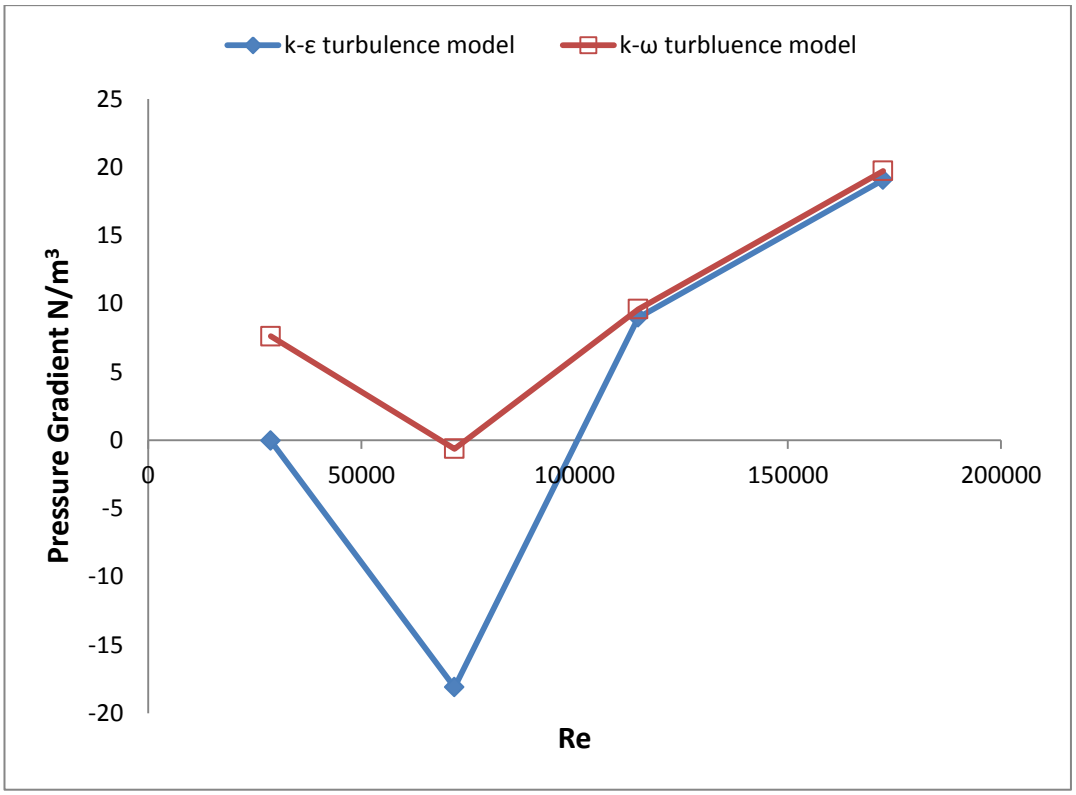

c) for 0.254 m diameter pipe

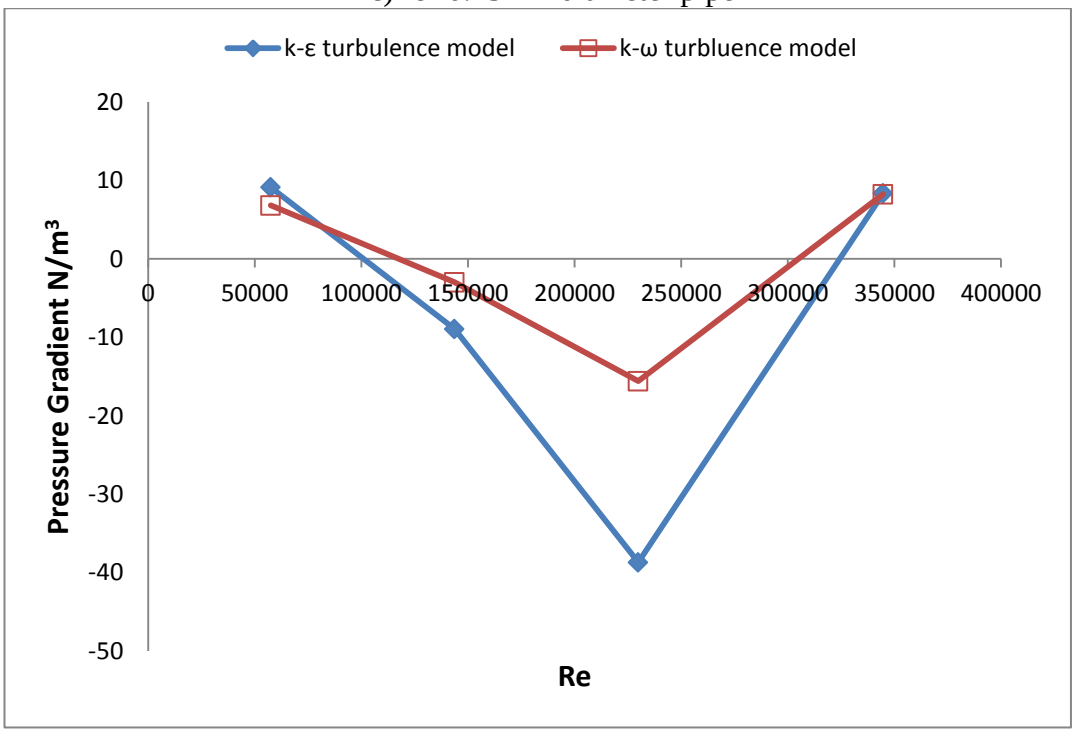

d) for 0.508 m diameter pipe

Figure 5.1 Pressure gradient versus Reynolds number for 20 % water volume fraction

Pressure gradient for 40 % water volume fraction is increased with Reynolds numbers for 0.0254 m diameter pipe as shown in Figures 5.2a. However, the pressure

gradient a little different for 0.127 m diameter pipe which is dropped with Reynolds number increasing to 41000.8. After that the pressure gradient is increased back again with Reynolds number as shown in Figures 5.2b. The pressure gradient increased for 0.254 m diameter pipe with Reynolds number to 82001.61 and after that the pressure gradient is dropped with Reynolds numbers increasing to 131202.57, and then the pressure gradient is increased with Reynolds number as shown in Figure 5.2c. The pressure gradient for 0.508 m diameter pipe increased with Reynolds number to 262405.15 and after that it dropped with Reynolds number increasing to 393607.7 for Shear Stress Transport k-ω model. However for Realizable k- ε model, the pressure gradient at same parameters is different. So, the pressure gradient, firstly, is dropped with Reynolds numbers increasing to 164003.22 then it raises with Reynolds number increasing to 262405.15, and then the pressure gradient is decrease with Reynolds number increasing to 393607 as shown in Figure 5.2d.

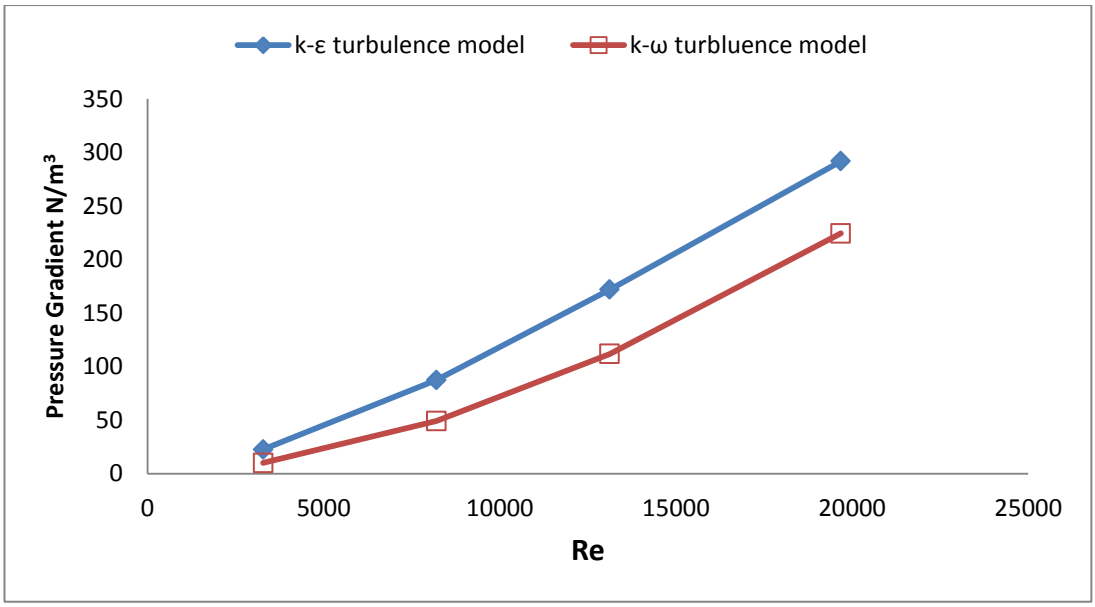

a) for 0.0254 m diameter pipe

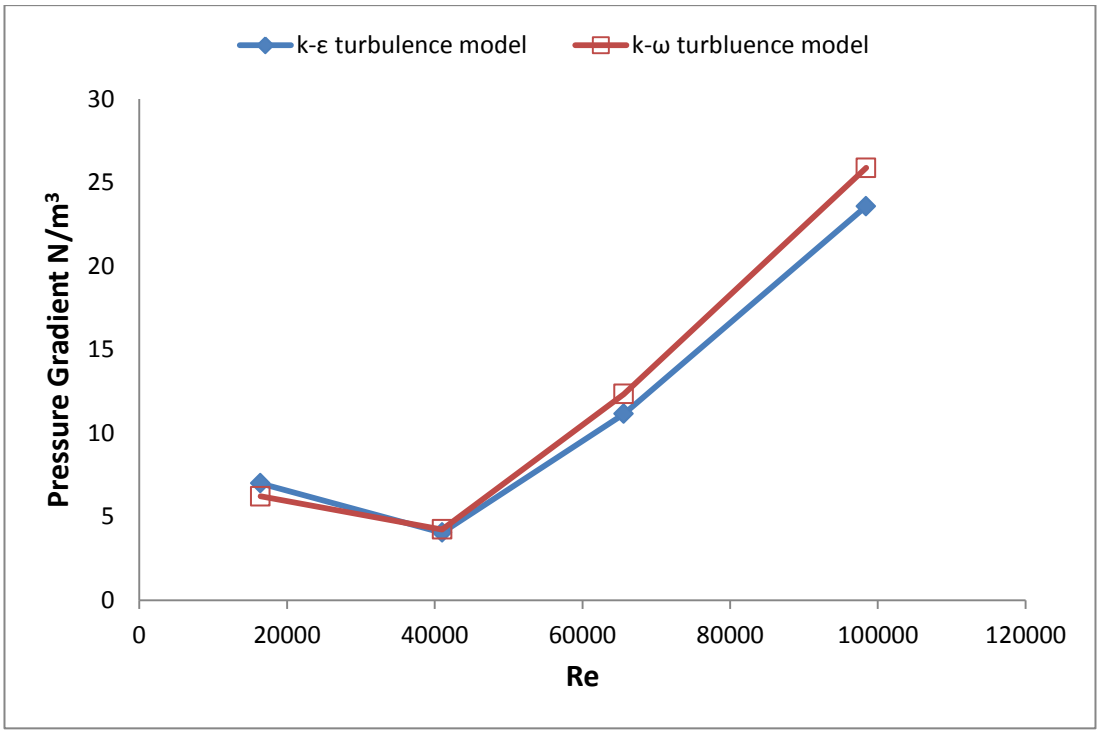

b) for 0.127 m diameter pipe

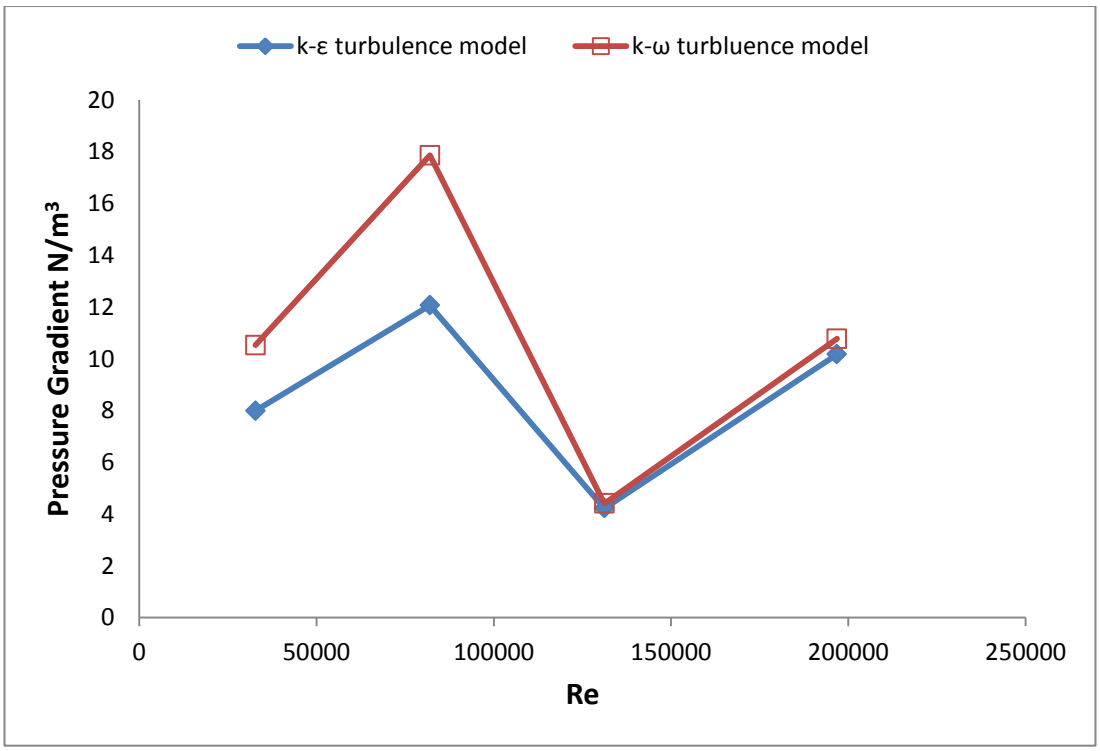

c) for 0.254 m diameter pipe

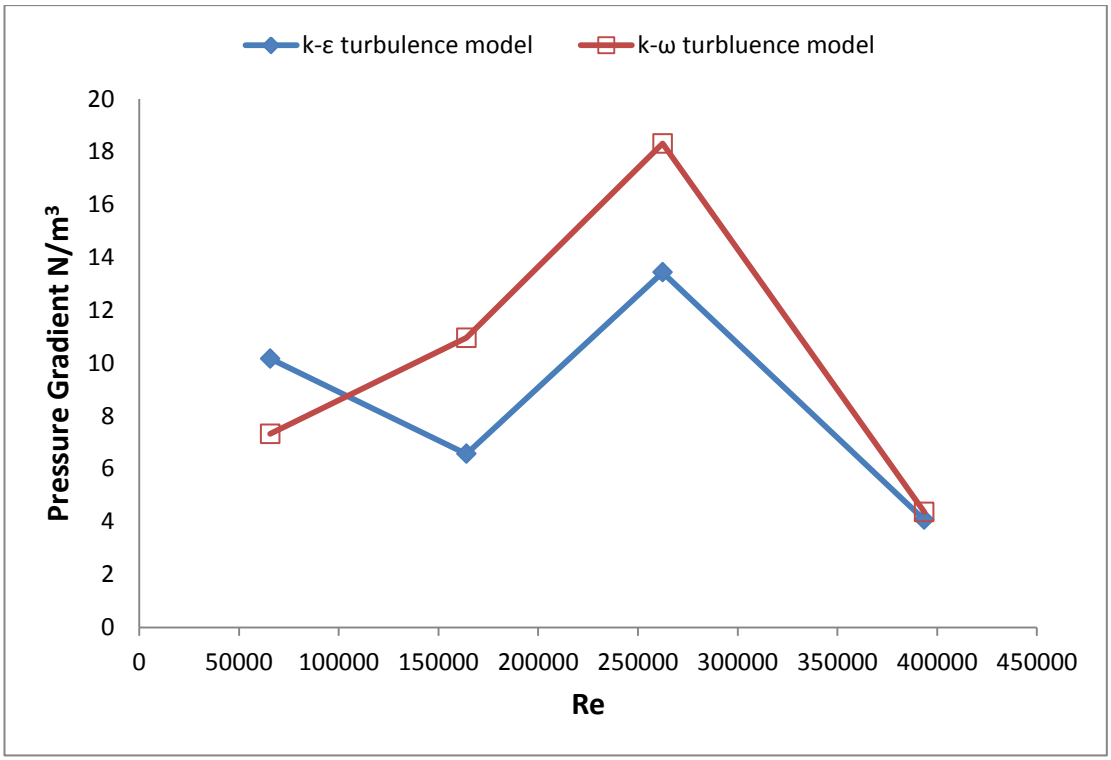

d) for 0.508 m diameter pipe

Figure 5.2 Pressure gradient versus Reynolds number for 40 % water volume fraction

Pressure gradient for 60 % water volume fraction is increased with Reynolds number for 0.0254 m diameter pipe as shown in Figure 5.3a. However, the pressure gradient a little different for 0.127 m diameter pipe is dropped with Reynolds number increasing to 54294.66. After that the pressure gradient increased with Reynolds number for 98401.93 as shown in Figure 5.3b. The pressure gradient for 0.254 m diameter pipe is dropped with Reynolds number increasing of to 150511.42, and then it rises again with Reynolds number increasing to 225767.13 as shown in Figure 5.3c. The pressure gradient is increased for 0.508 m diameter pipe with Reynolds numbers increasing up to 188139.27 and after that it is dropped with Reynolds numbers increasing of to 301022.84, and then the pressure gradient is increased with Reynolds numbers as shown in Figures 5.3d.

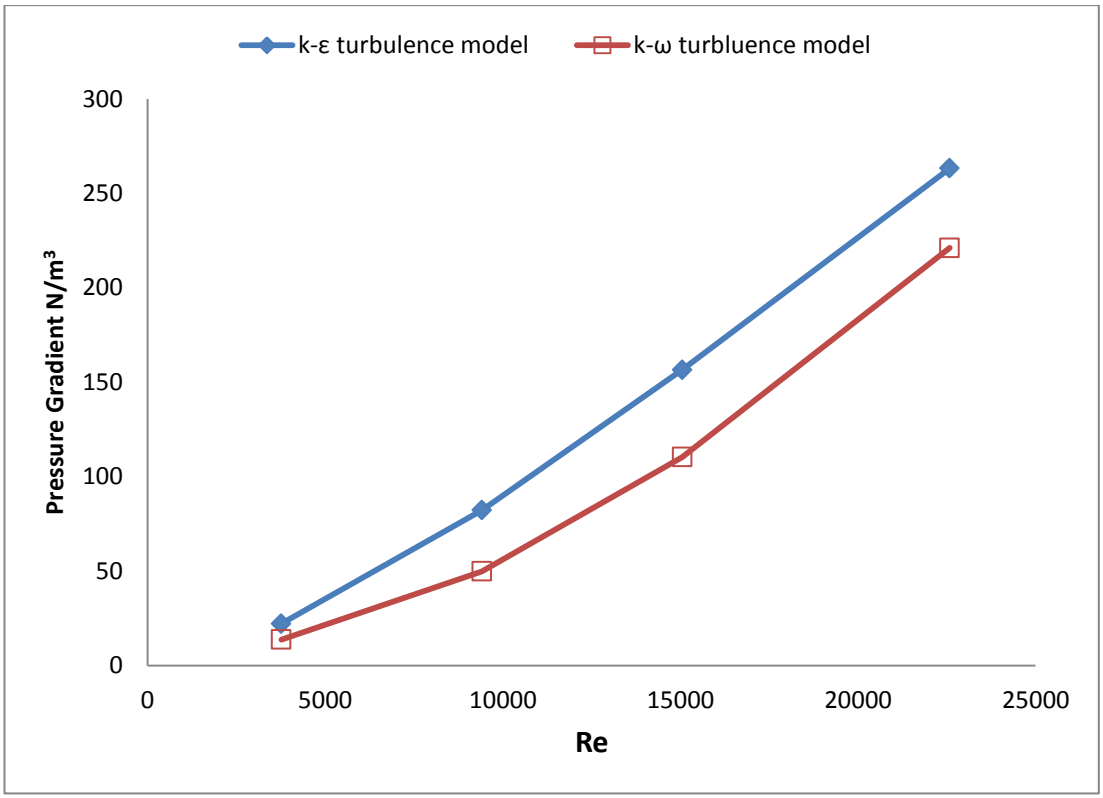

a) for 0.0254 m diameter pipe

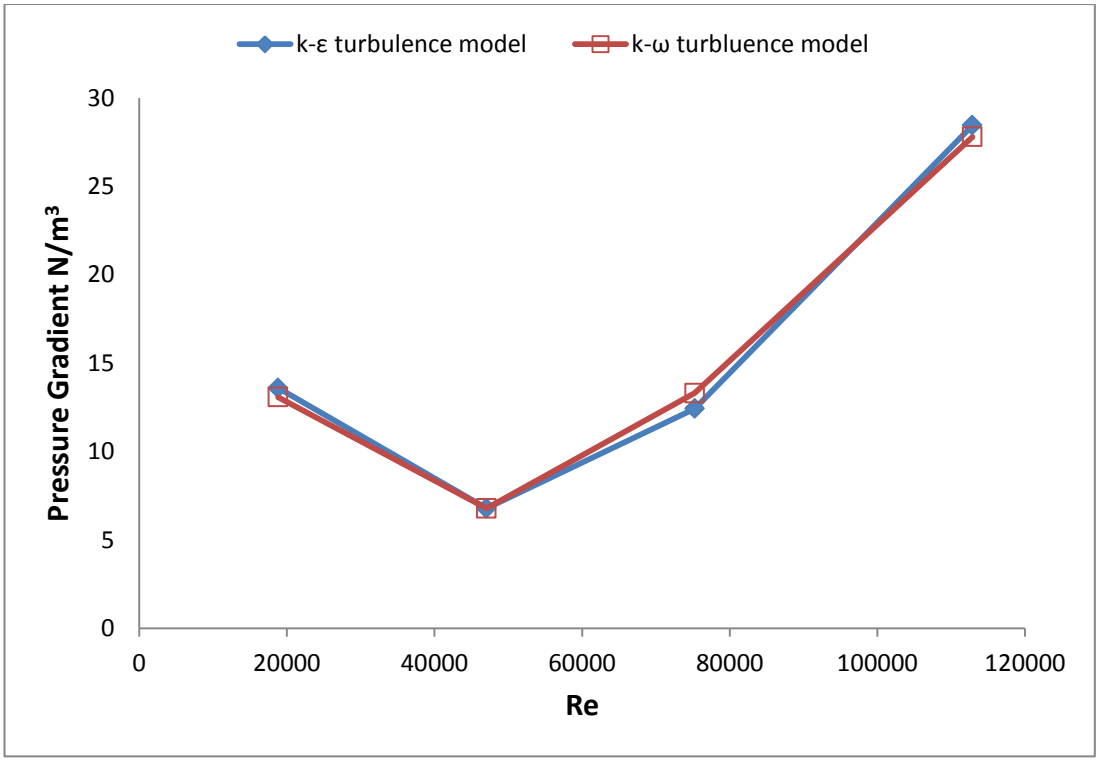

b) for 0.127 m diameter pipe

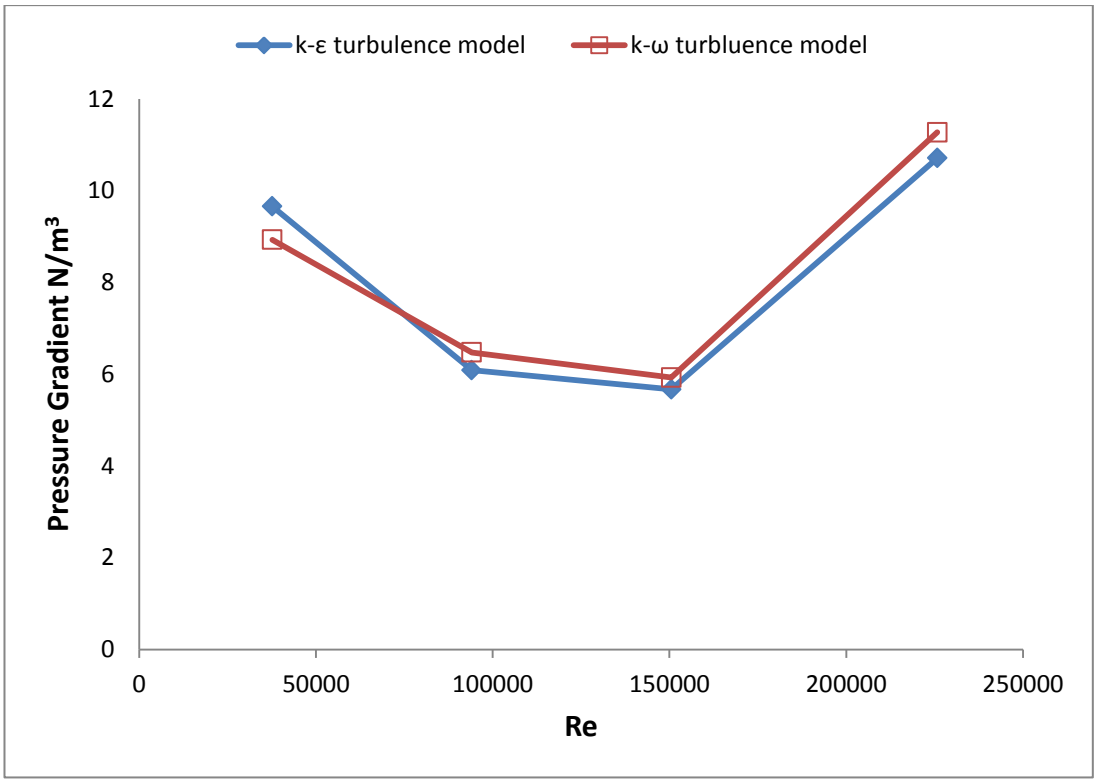

c) for 0. 254 m diameter pipe

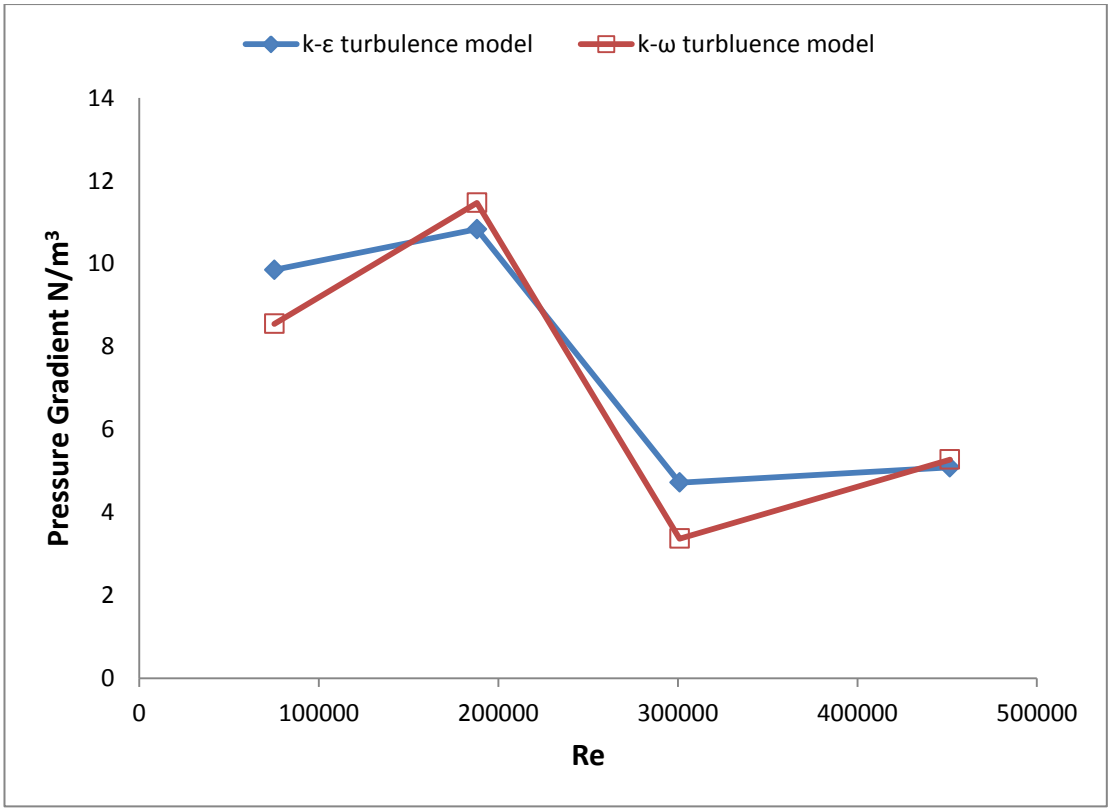

d) for 0.508 m diameter pipe

Figure 5.3 Pressure gradient versus Reynolds number for 60 % water volume fraction

Pressure gradient for 80 % water volume fraction is increased with Reynolds numbers between the diameter range 0.0254 m and 0.127 m as shown in Figures 5.4a and 5.4b. The pressure gradient is dropped for 0.254 m diameter pipe with Reynolds number increasing to 108589.32. After that it is increased with Reynolds number for 260614 as shown in Figure 5.3c. The pressure gradient is dropped for 0.508 m diameter pipe with Reynolds number increasing to 217178.65. After that it is increased back again with Reynolds number 521228.75 as shown in Figure 5.3d.

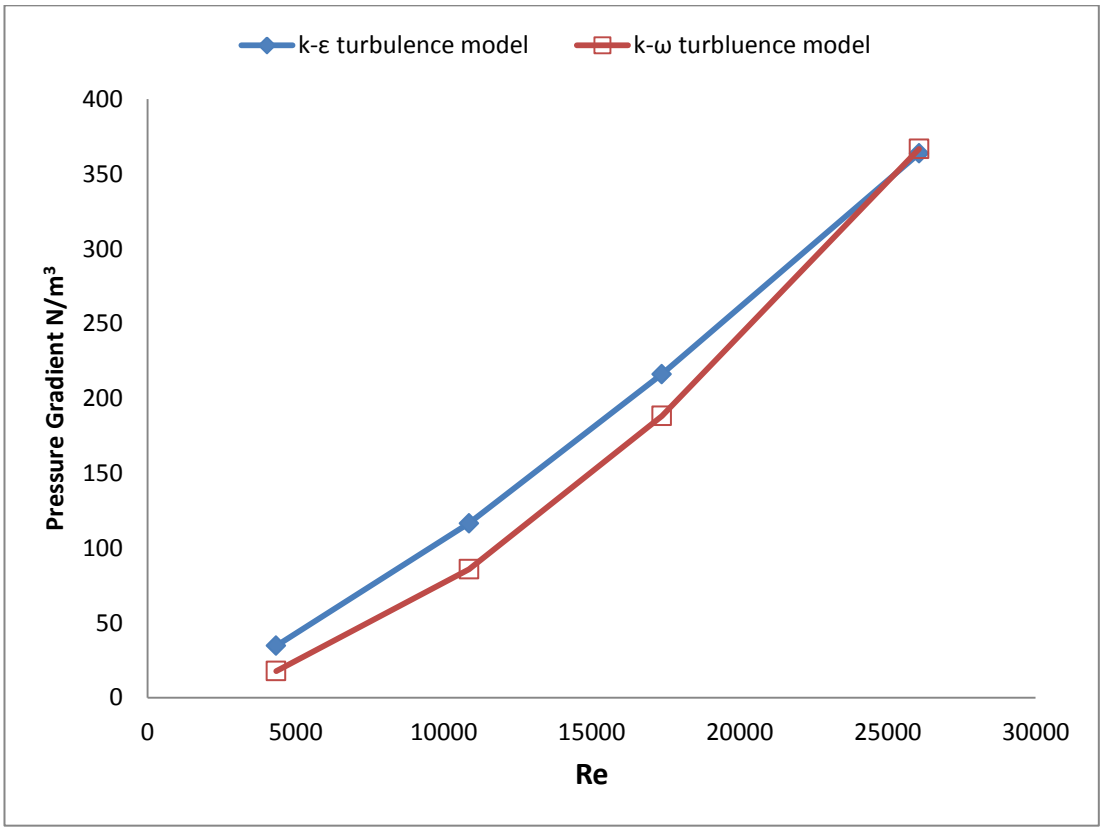

a) for 0.0254 m diameter pipe

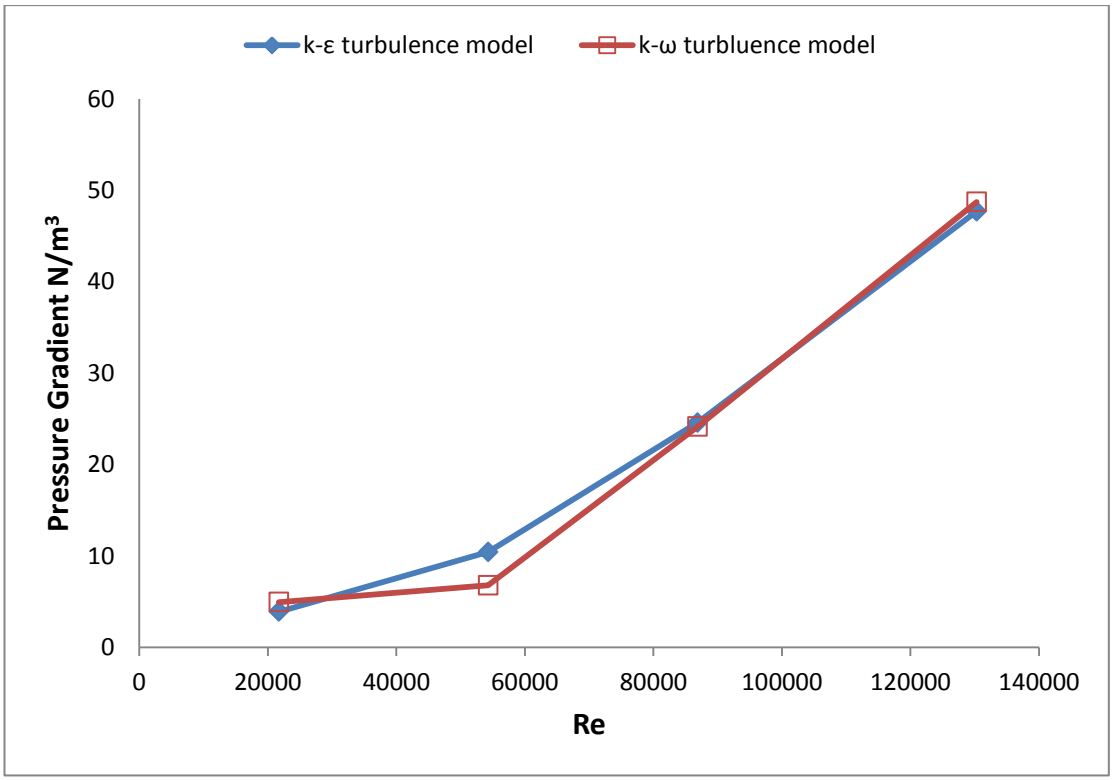

b) for 0.127 m diameter pipe

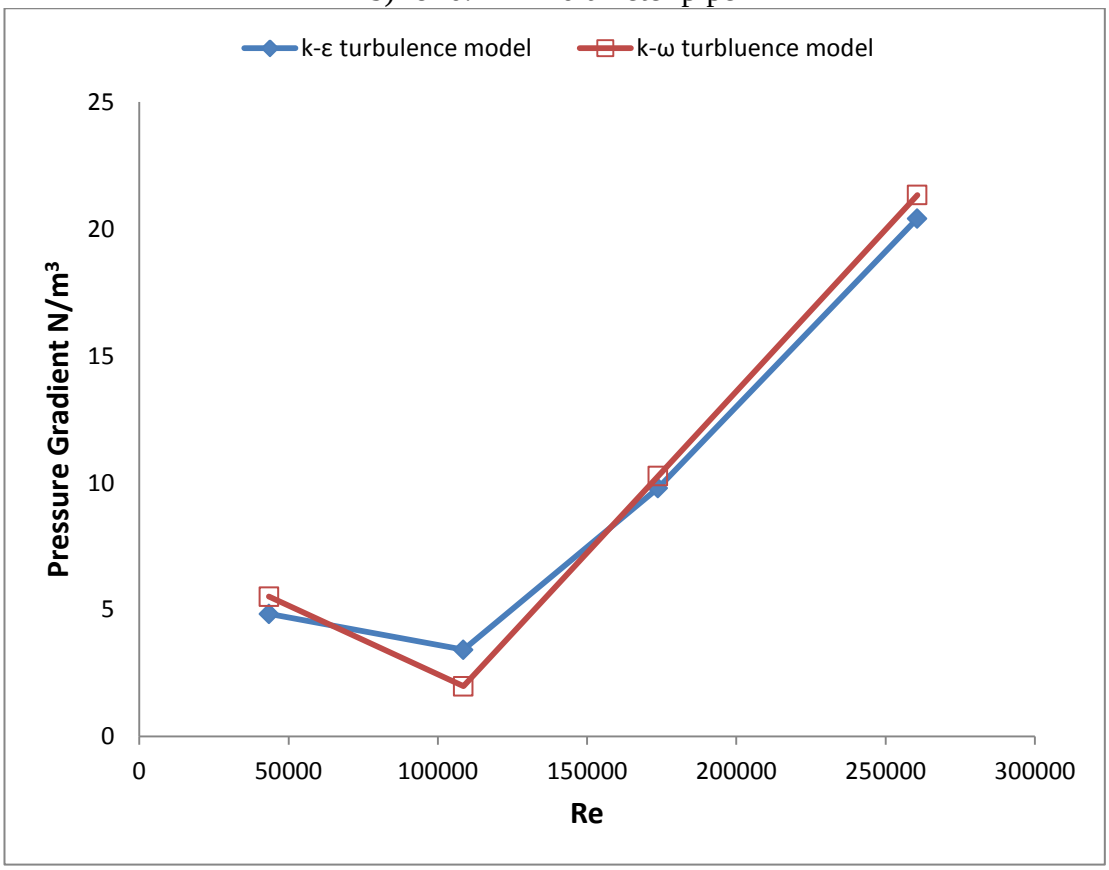

c) for 0.254 m diameter pipe

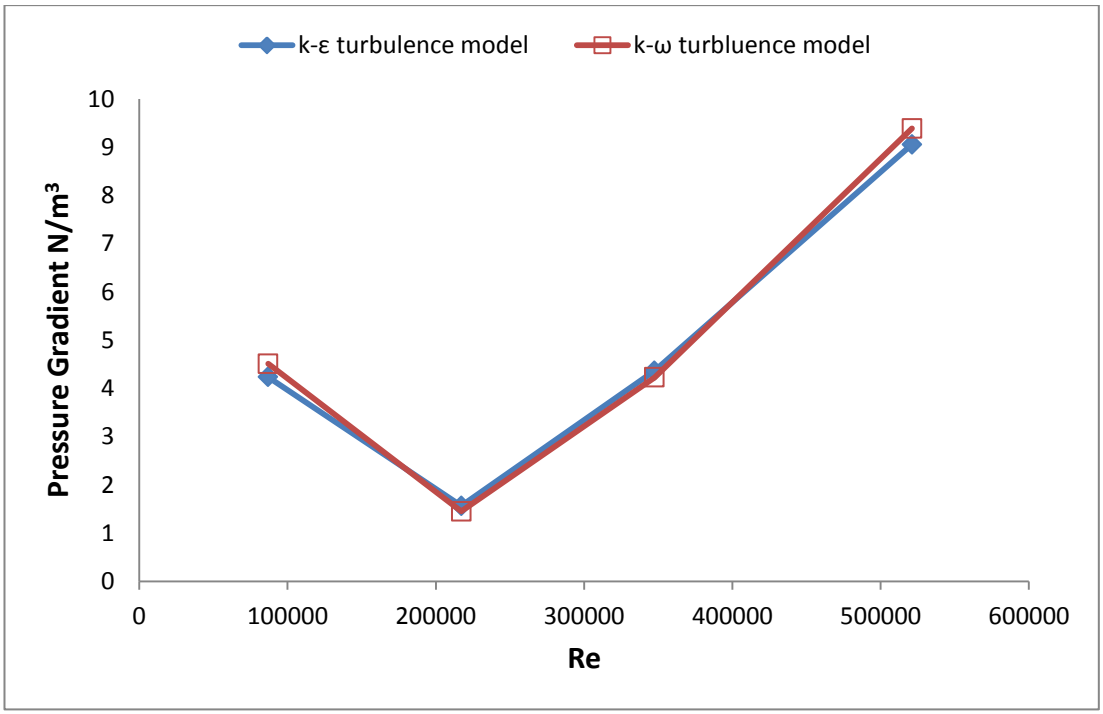

d) for 0.508 m diameter pipe

Figure 5.4 Pressure gradient versus Reynolds number for 80 % water volume fraction

Figures 5.1 to 5.4 present the pressure gradient in the 0.0254, 0.127, 0.254 and 0.505 diameters pipe and 20, 40, 60 and 80 % water volume fraction for Realizable k-**ε** and Shear Stress Transport k-ω (SST) turbulence model. Mostly, the pressure gradient value increases with Reynolds number increasing, that is normal and logical for small diameter such as 0.0254 m with increasing mixture velocity and this result agree with the (Angeli and Hewitt, 1999) and (Al-Yaari et al., 2009). For large diameters more than 0.127 m also the pressure gradient increases with Reynolds number increasing, but at the some cases that the effect of water volume fraction on pressure gradient is significant especially for 40 % the pressure gradient decreases, that could be associated with local phase inversion from water phase continuous to oil phase continuous in the pipe.

5.3.2 Effect of diameter, length and mixture velocity on pressure gradient

Two-phase stratified flows in a horizontal pipe were numerically studied on oil–water mixture test cases. Pipe diameters are 0.0254, 0.127, 0.254, and 0.508 m. The lengths of the pipe are in the range of 0.5007 to 25.9034 m according to fully developed length Equation (4.3). The mixture velocities are used as 0.2, 0.5, 0.8 and 1.2 m/s.

The effects of mixture velocity and diameter of pipes on the pressure gradient are shown in Figures 5.5 to 5.8. The pressure gradient of 0.0254 m diameter pipe is higher than the other pipe diameters for all mixture velocities and water volume fractions. In another word, the pressure gradient decreases with increasing of the pipe diameter. There is a large pipe diameter such as 0.254 m and 0.508 effects on flow pattern from stratified to stratified wavy flow especially at o.5 m/s and 0.8 m/s as shown in figures 5.21 and 5.22. This result of the pressure gradient agrees well and the same trends as described by (Jepson and Taylor, 1993), (Al-Yaari et al., 2009) and (Venkatesan et al., 2011)

The pressure gradient increases as predictable for a small diameter pipe such as 0.0254 m with increasing mixture velocity. However, the pressure gradient for a large diameter pipe more than 0.127 m decreases and stabilizes with high mixture velocities. This is caused by the flow in a large diameter and longer length of pipe. Generally, the pressure gradient is founded by the Shear Stress Transport k-ω model better than those found by Realizable k-**ε** turbulence model. In figures 5.5 to 5.8, L is the developed length belonging to the and D is the different pipe diameter

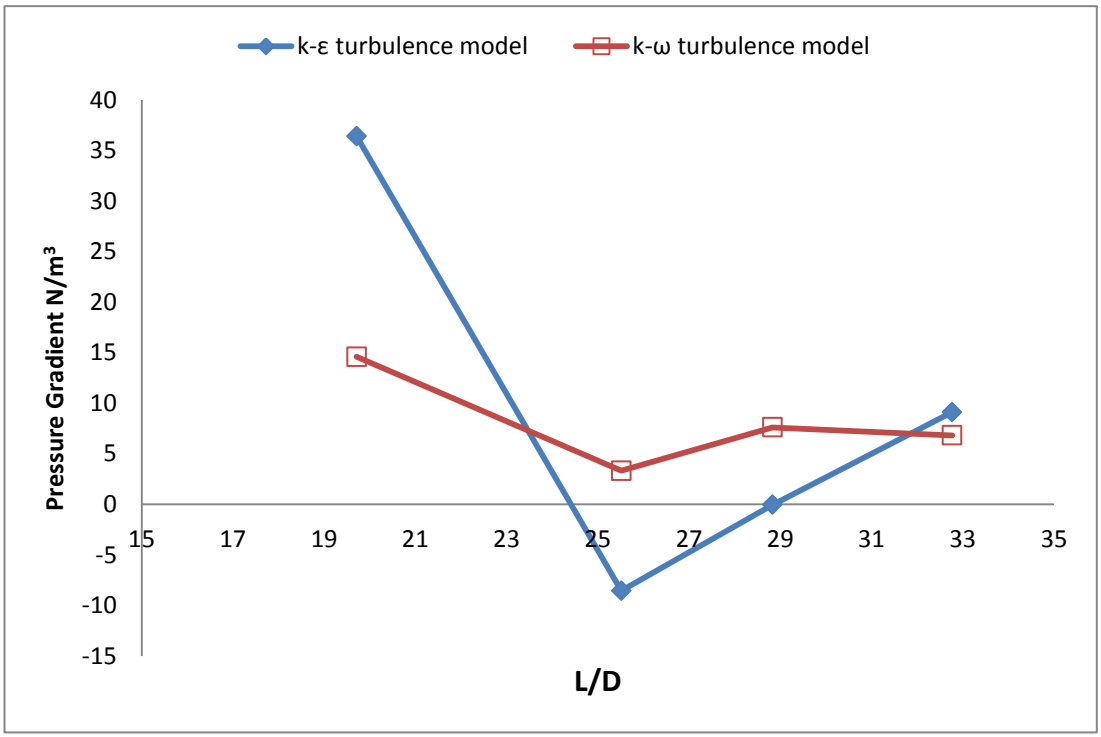

a) for 20 % water volume fraction

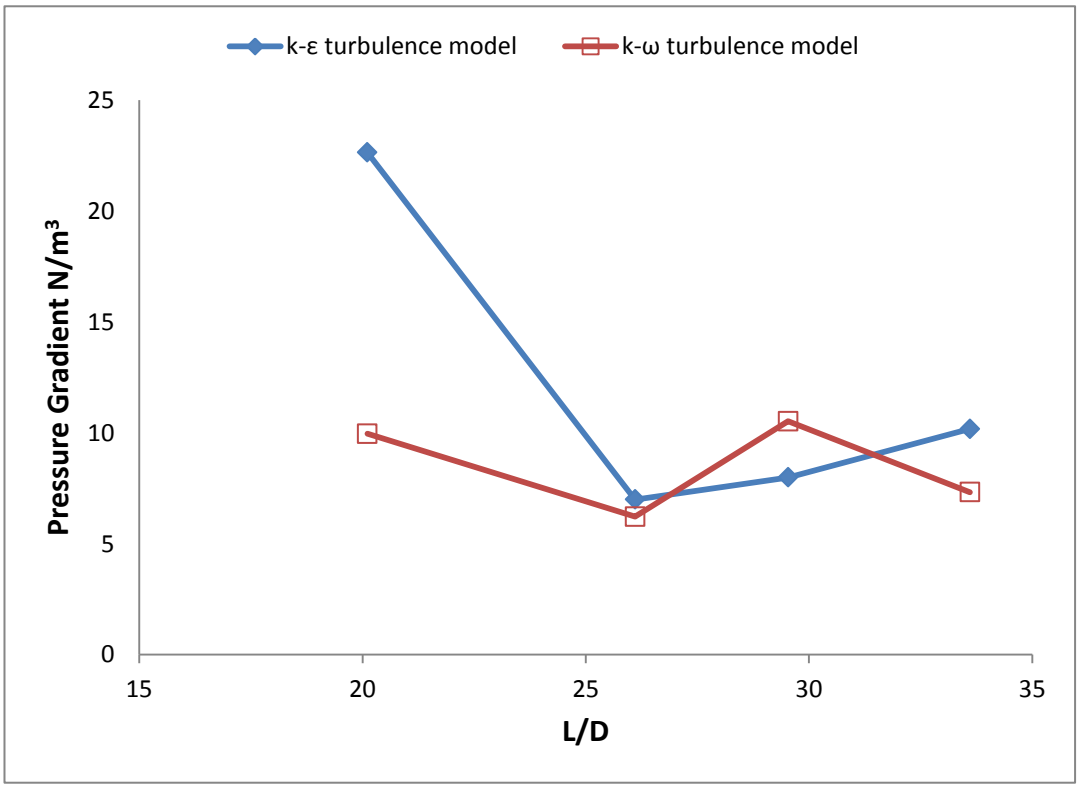

b) for 40 % water volume fraction

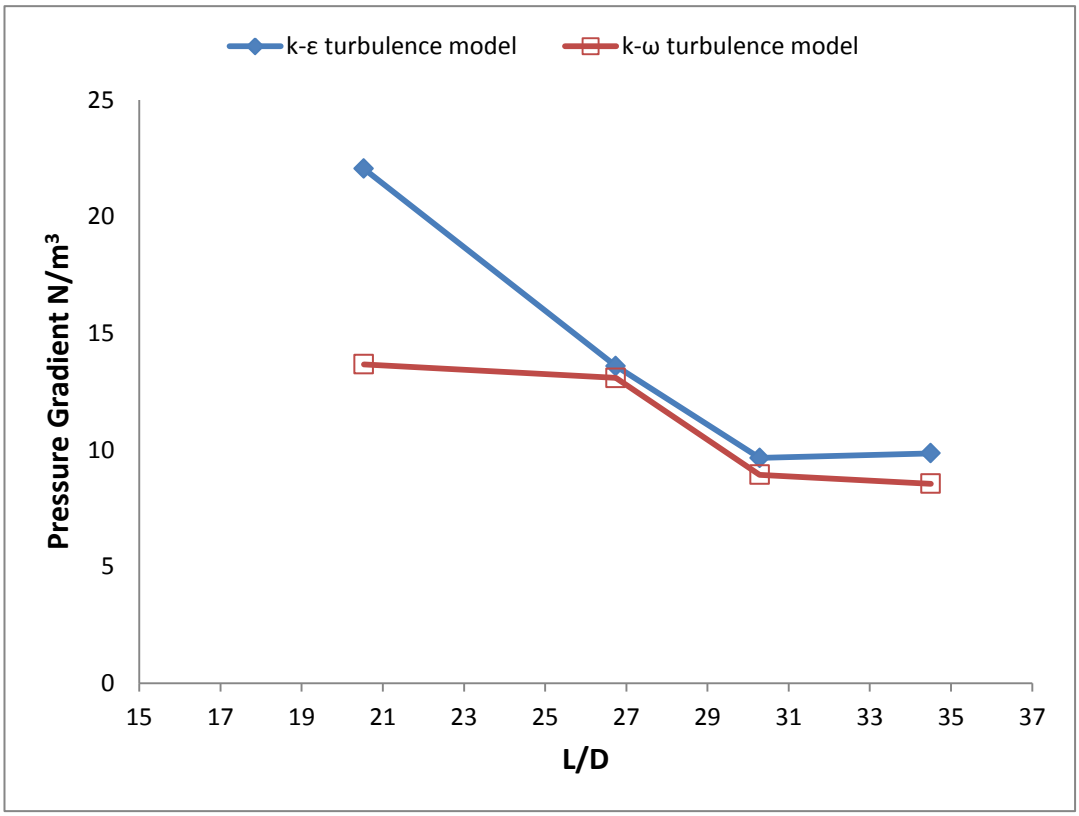

c) for 60 % water volume fraction

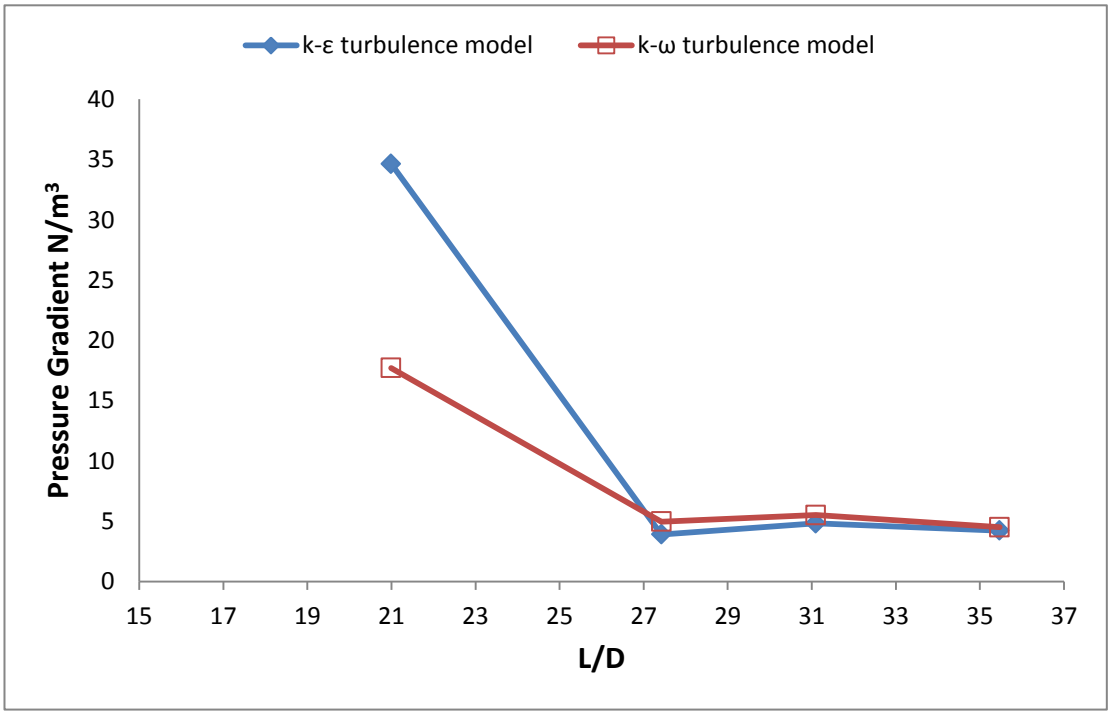

d) for 80 % water volume fraction

Figure 5.5 Pressure gradient for 0.2 m/s mixture velocity

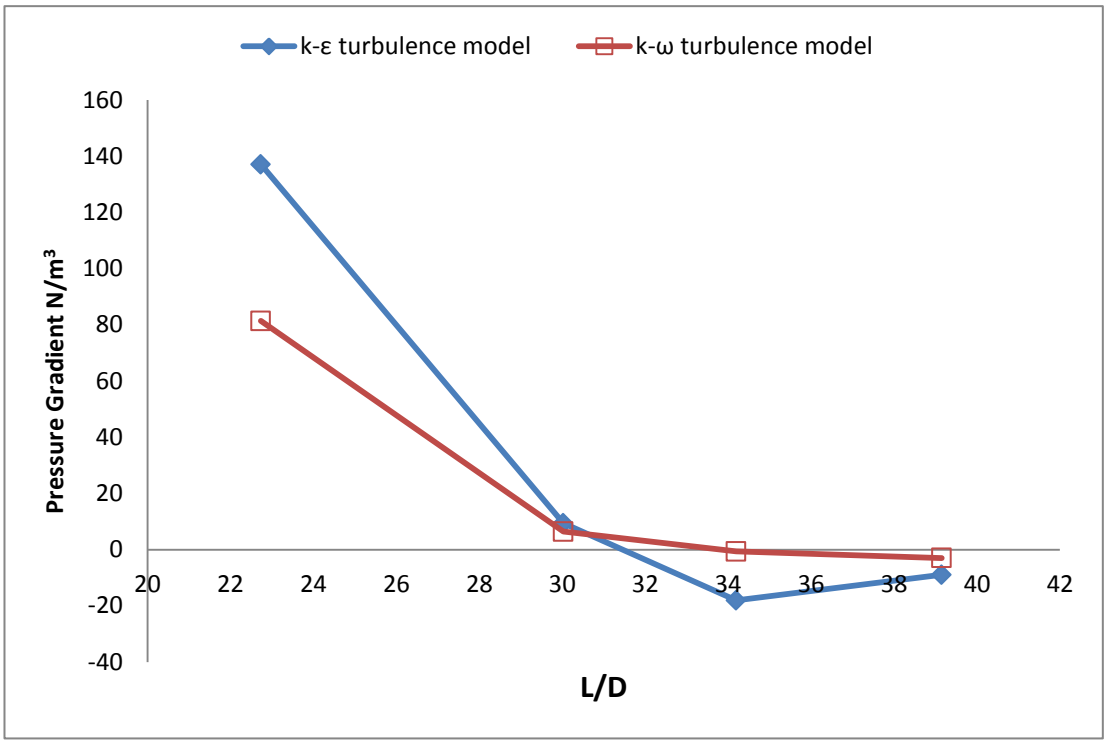

a) for 20 % water volume fraction

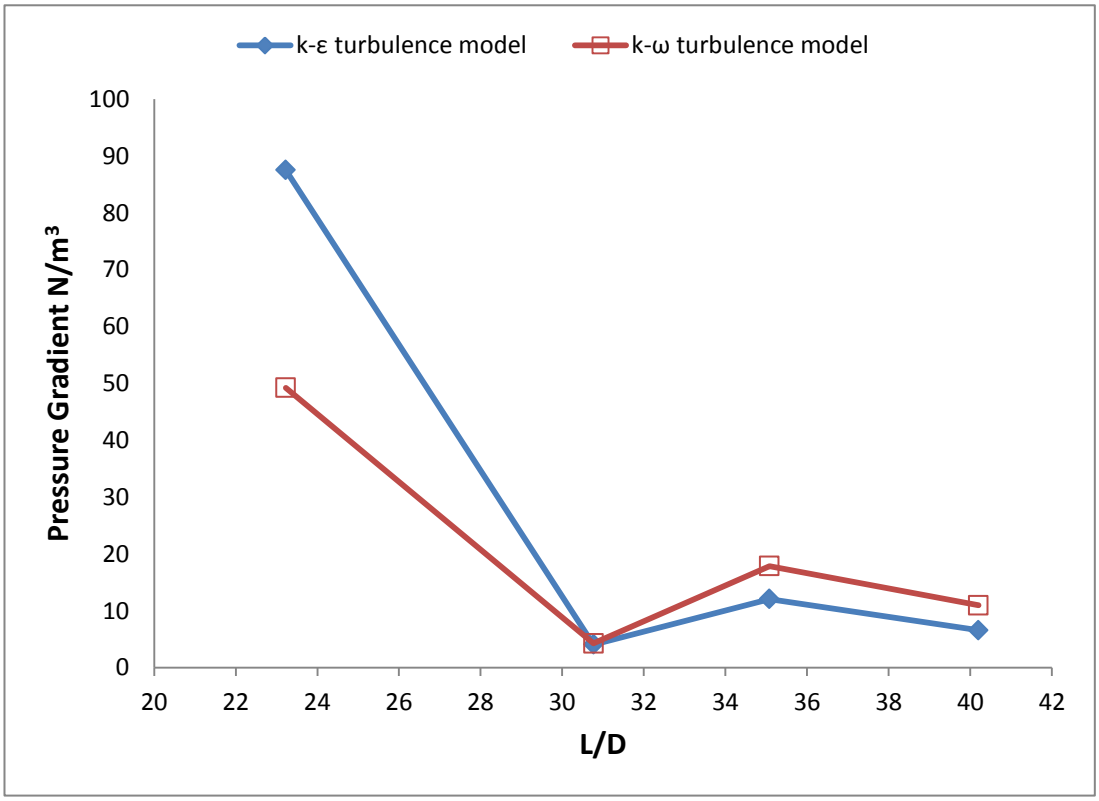

b) for 40 % water volume fraction

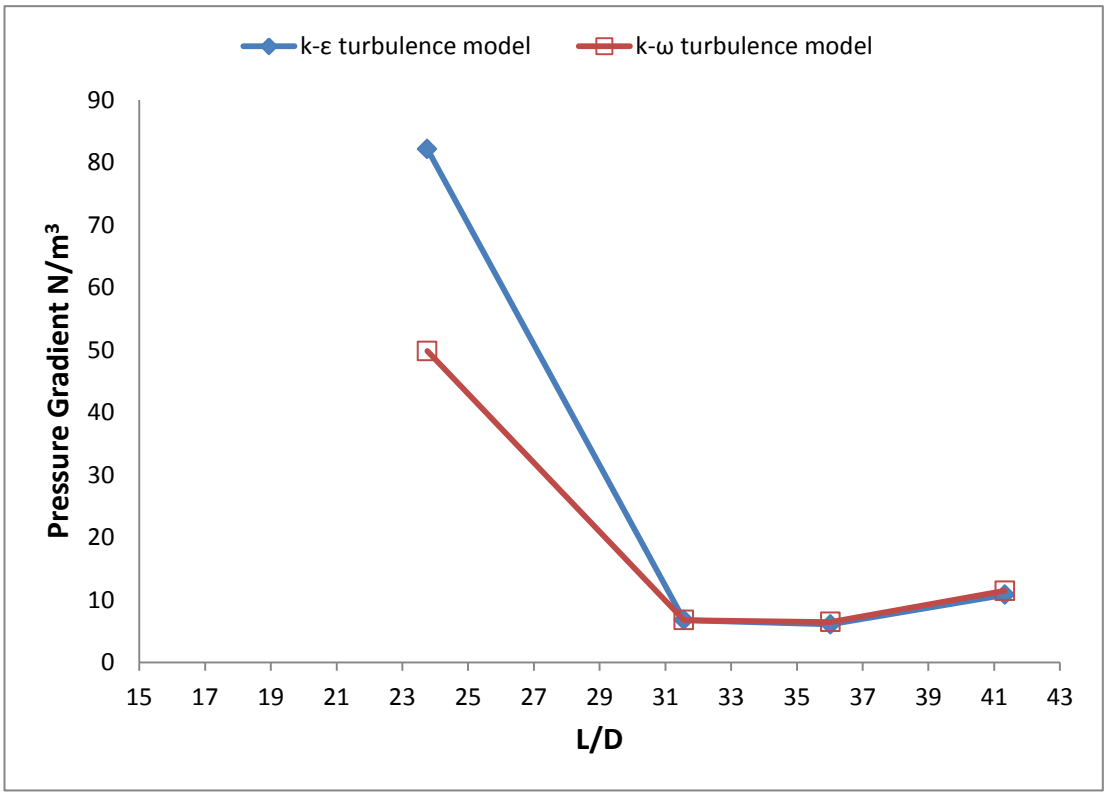

c) for 60 % water volume fraction

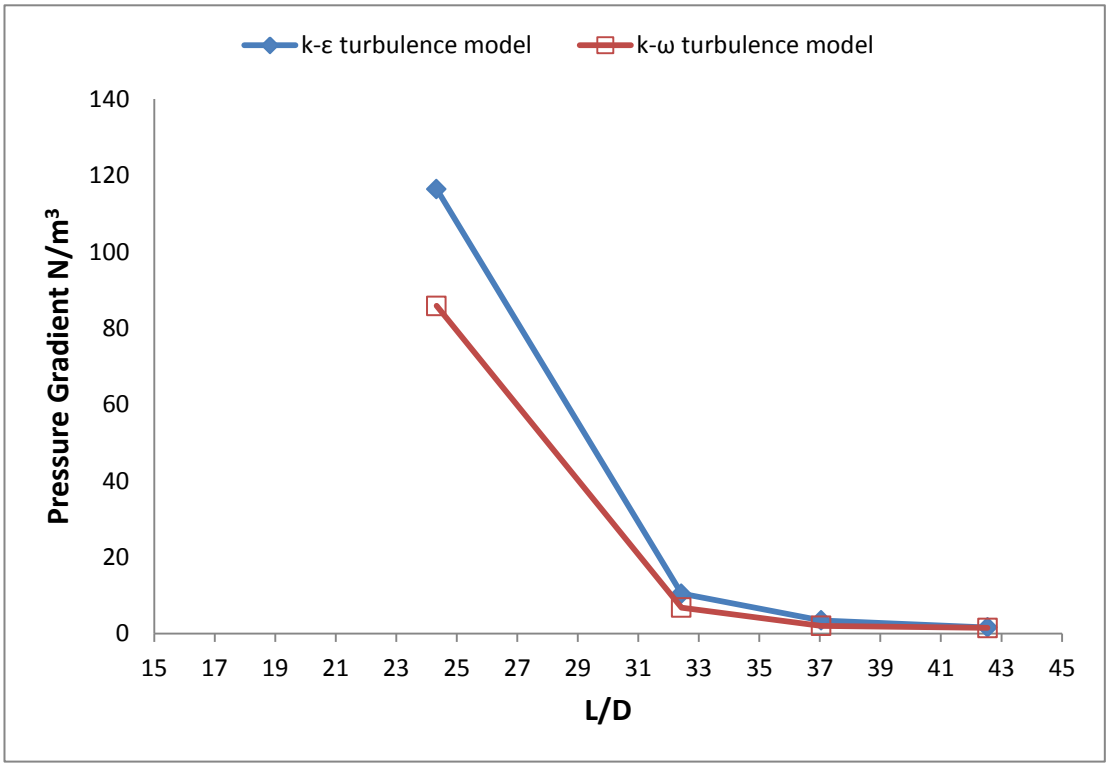

d) for 80 % water volume fraction

Figure 5.6 Pressure gradient for 0.5 m/s mixture velocity

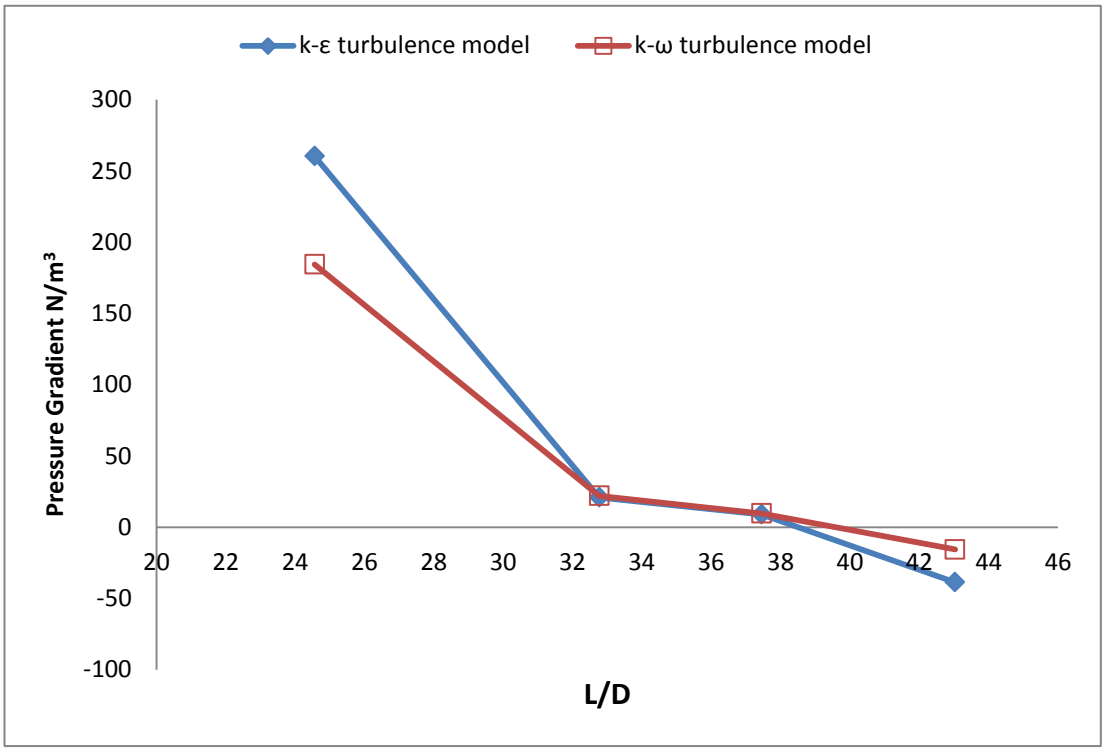

a) for 20 % water volume fraction

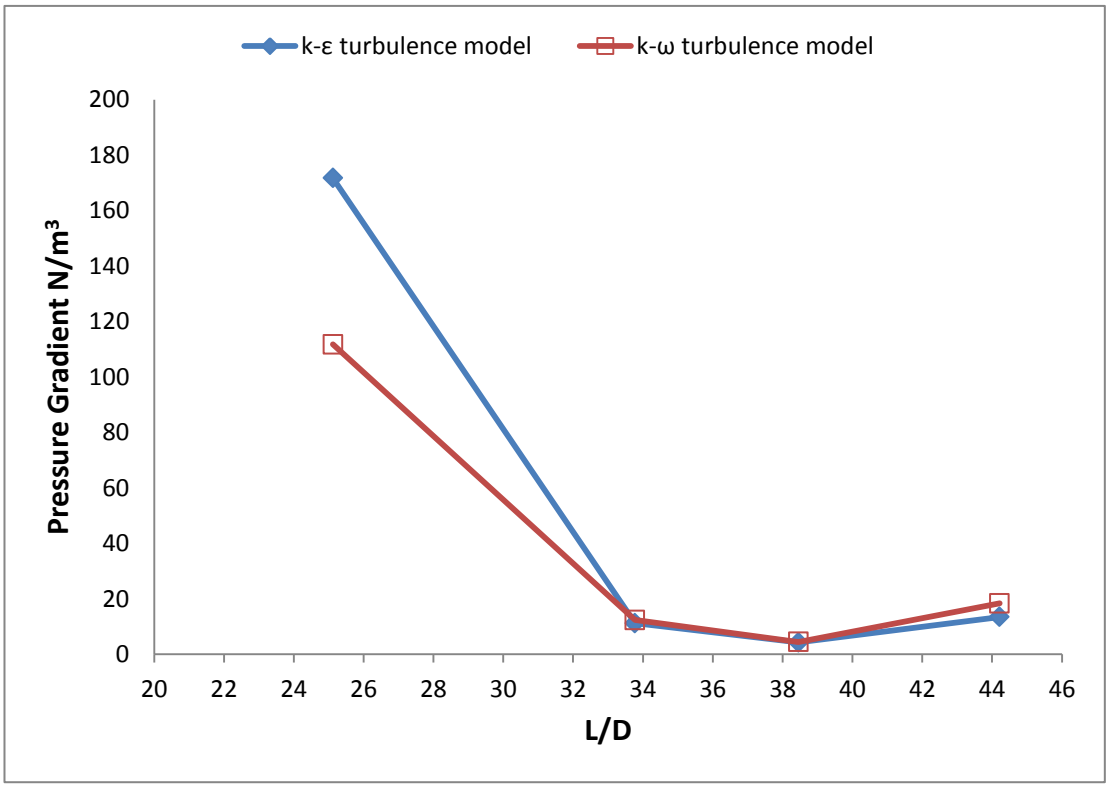

b) for 40 % water volume fraction

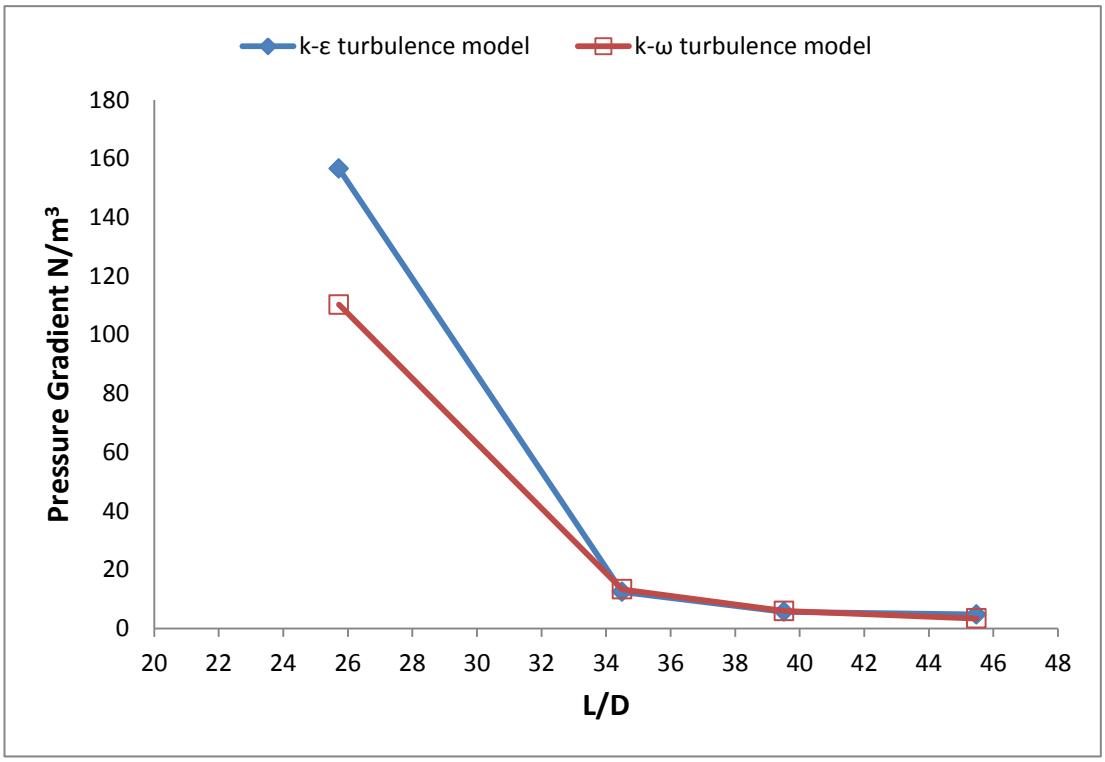

c) for 60 % water volume fraction

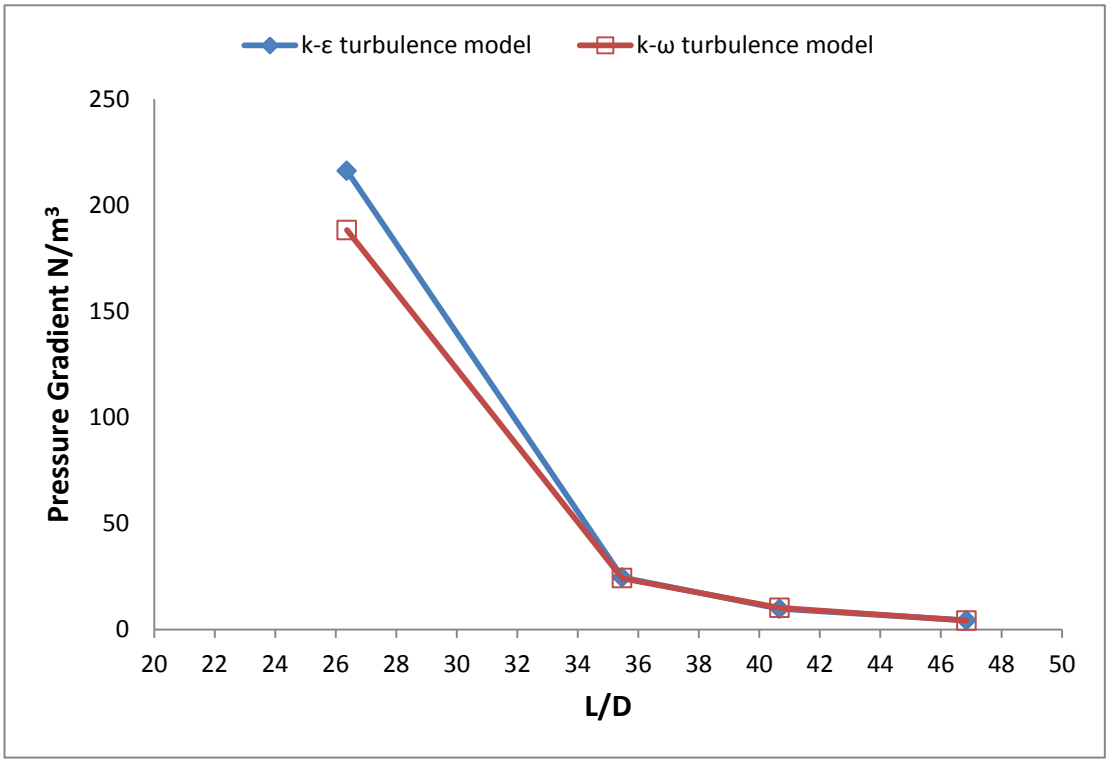

d) for 80 % water volume fraction

Figure 5.7 Pressure gradient for 0.8 m/s mixture velocity

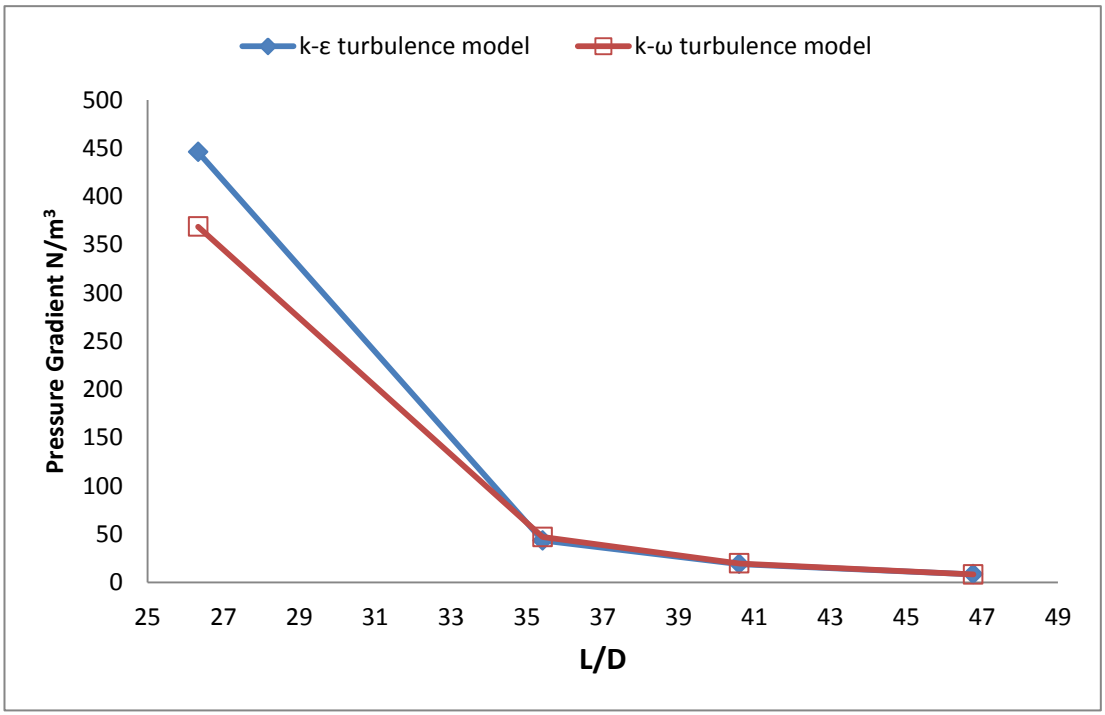

a) for 20 % water volume fraction

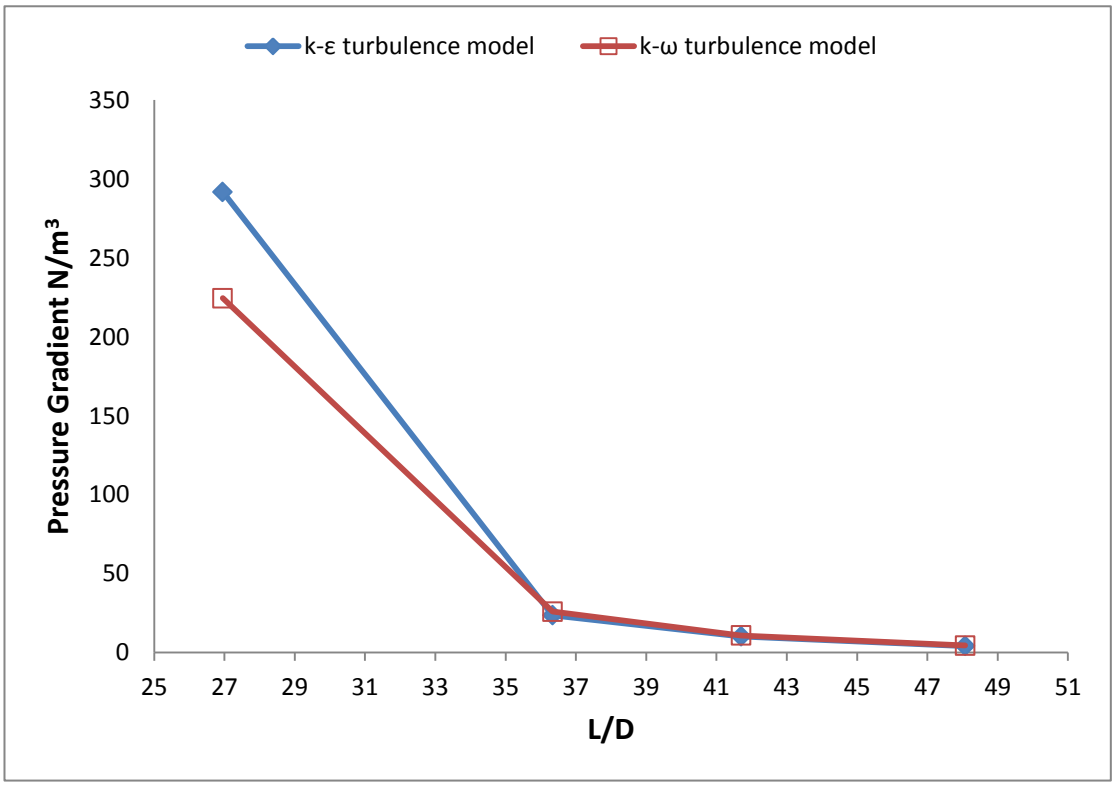

b) for 40 % water volume fraction

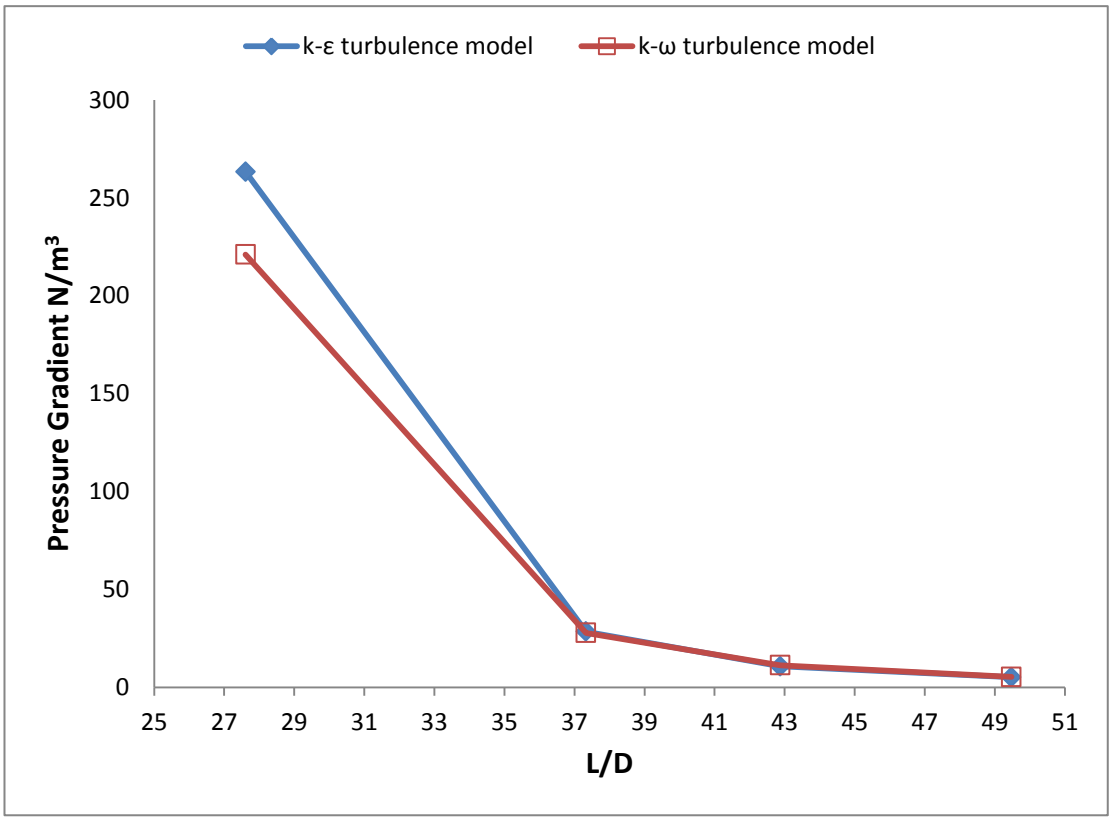

c) for 60 % water volume fraction

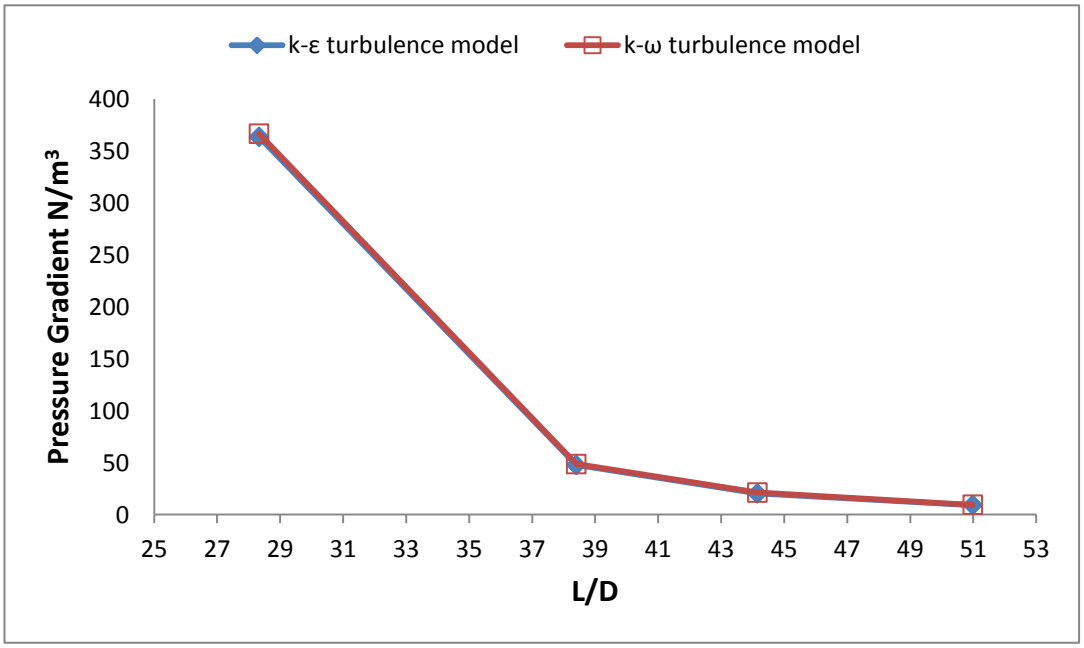

d) for 80 % water volume fraction

Figure 5.8 Pressure gradient for 1.2 m/s mixture velocity

5.4 Velocity profiles

The velocity profile diagrams illustrate the velocity change along the test section on the pipe. A few studies of oil-water two-phase stratified and stratified wavy flow has been reported on the mixture velocity profile. The velocity profiles for mixture velocity were introduced at L/D = 19.7139, L/D = 30.7676, L/D = 39.5146 and L/D = 50.9910 for 0.0254, 0.127, 0.254 and 0.508 m pipe diameters respectively (L is the developed length belonging to the different pipe diameter). The mixture velocity profile variation after the middle of pipe is very limited due to long of pipe, especially in the large diameters of pipe. For 0.2, 0.5, 0.8 and 1.2 m/s mixture velocities with 20 and 40 % water volume fraction ratio, the water phase tends to move slowly. The velocity profiles at the different parameters such as velocity, diameters and lengths of pipe for Realizable k-ε and Shear Stress Transition k-ω turbulence models are shown in Figures 5.9-5.12.

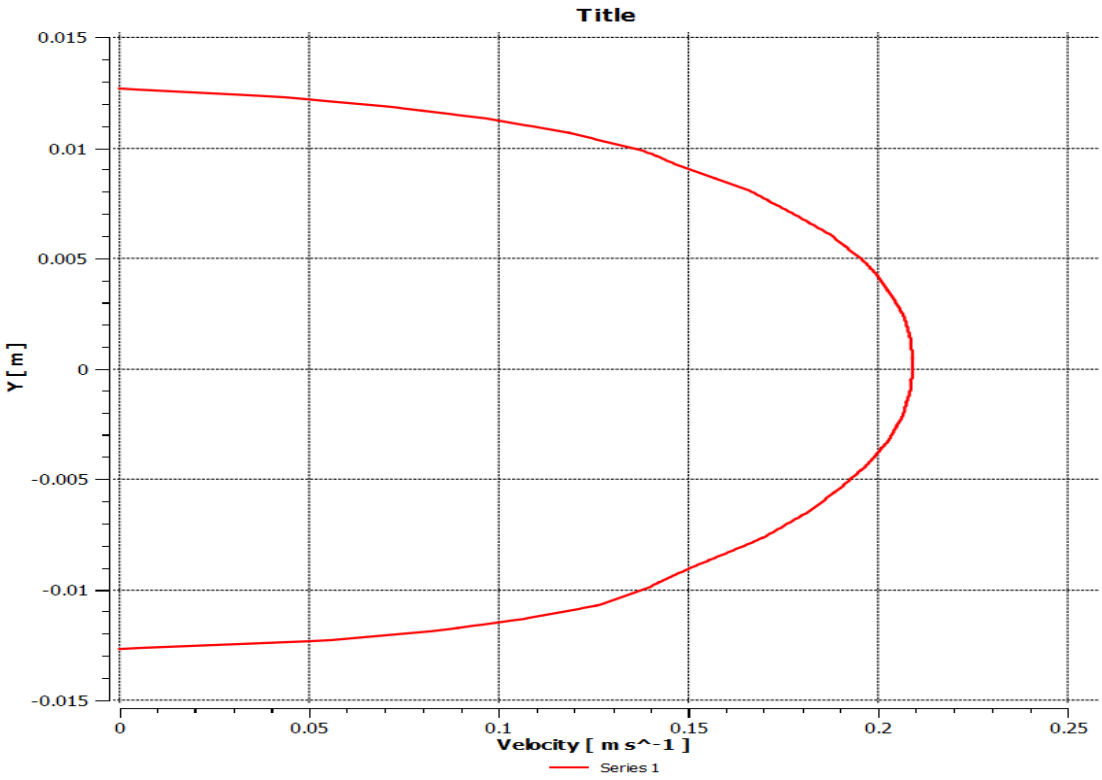

a) for L/D = 19.7139 (k-ε turbulence model)

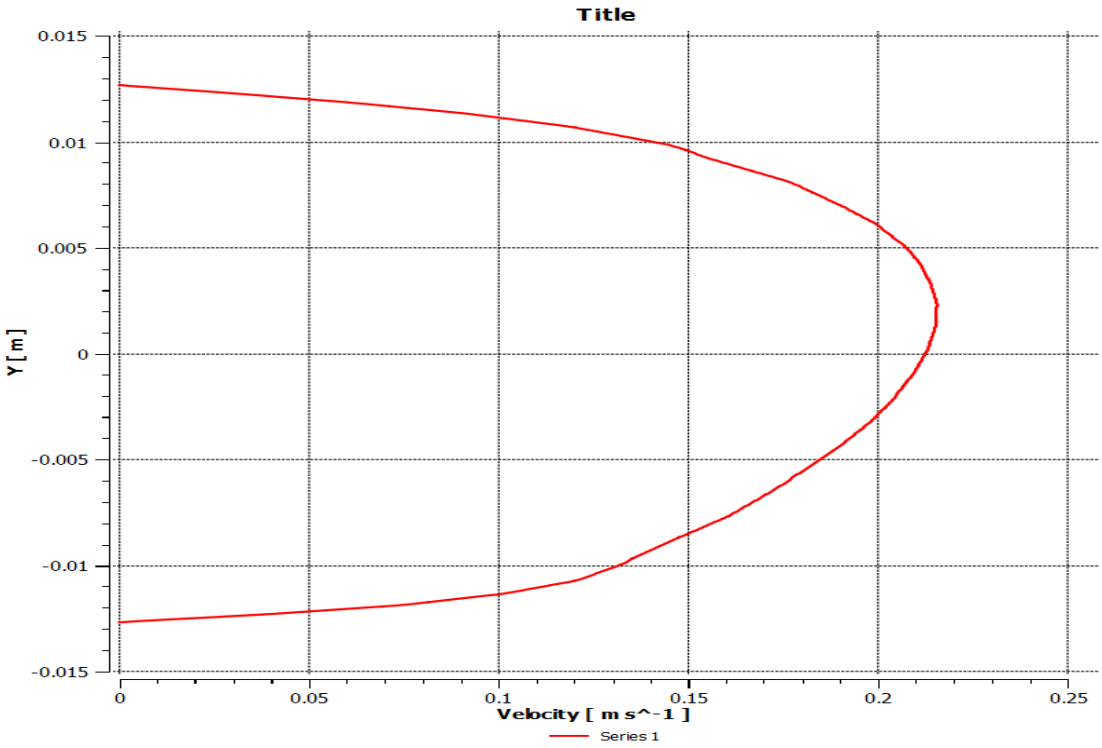

b) for L/D = 19.7139 (k-ω turbulence model)

Figure 5.9 Velocity profiles for 0.0254 m diameter pipe with 0.2 m/s mixture velocity

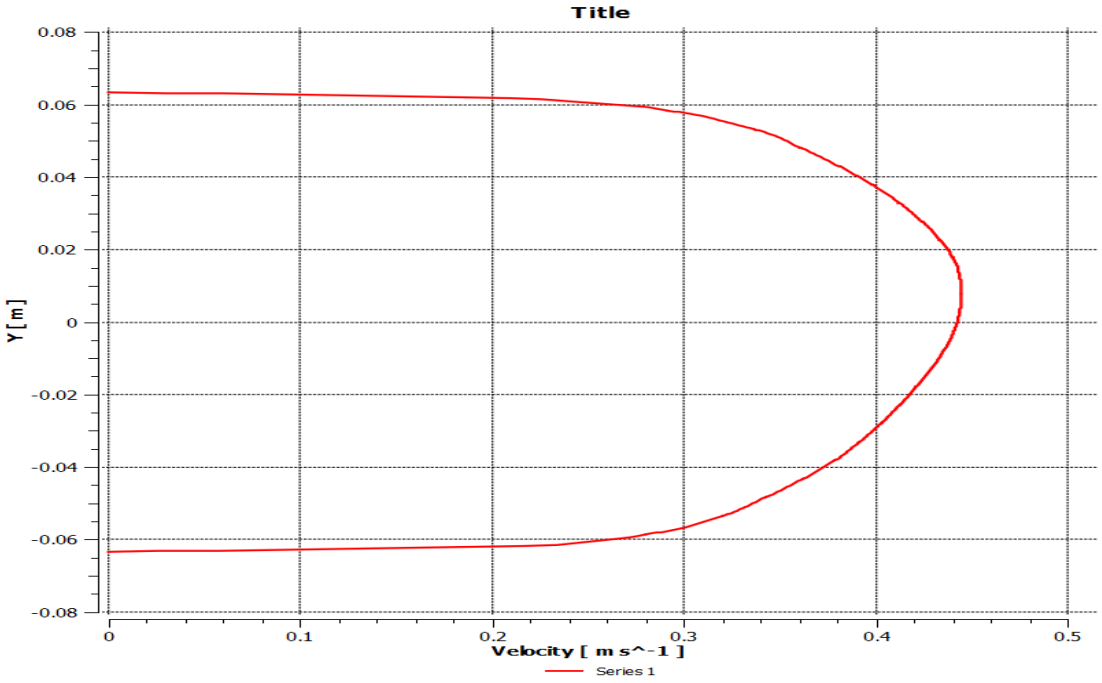

a) for L/D = 28.2677 (k-ε turbulence model)

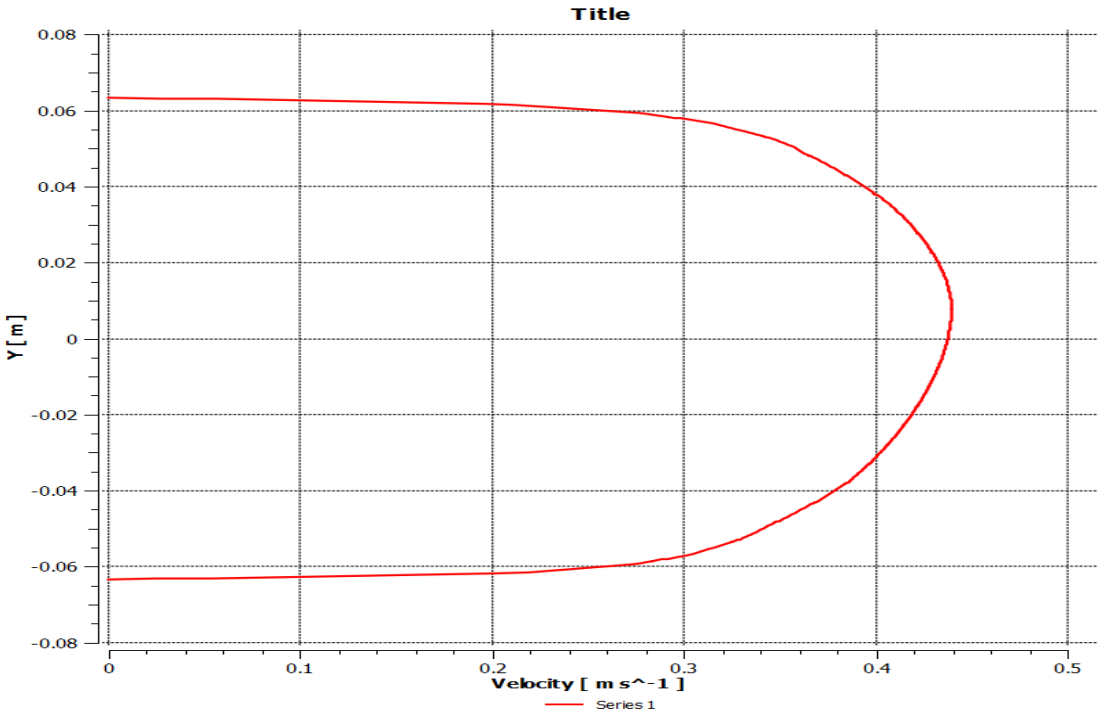

b) for L/D = 28.2677 (k-ω turbulence model)

Figure 5.10 Velocity profiles for 0.127 m diameter pipe with 0.5 m/s mixture velocity

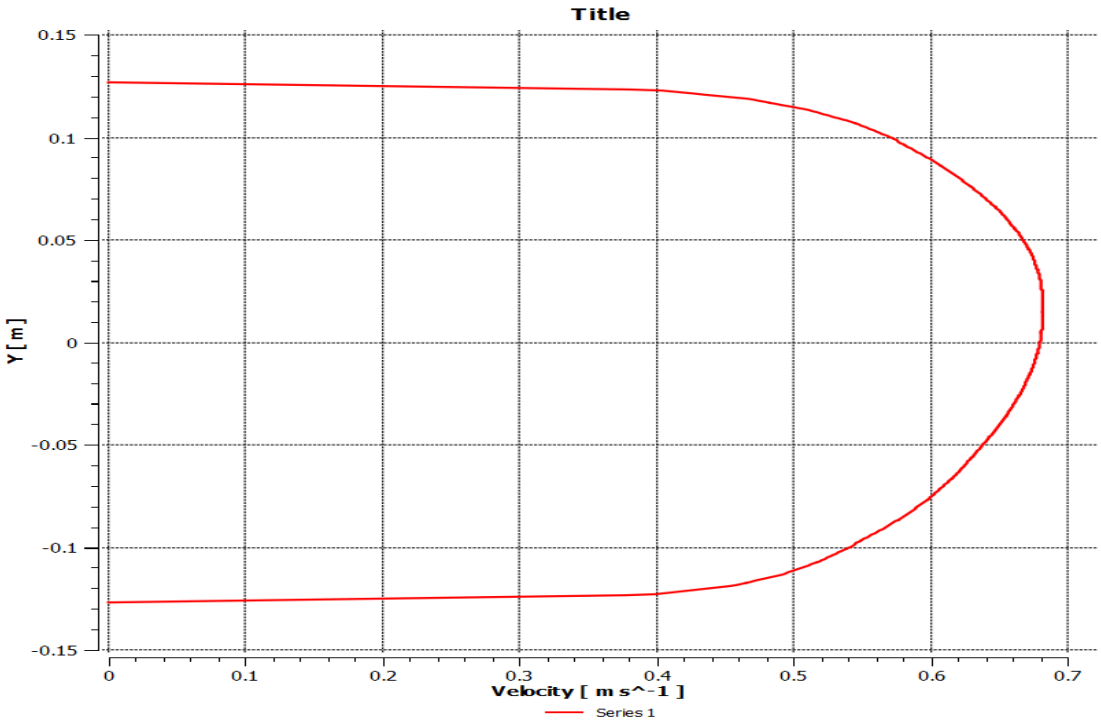

a) for L/D = 37.0145 (k-ε turbulence model)

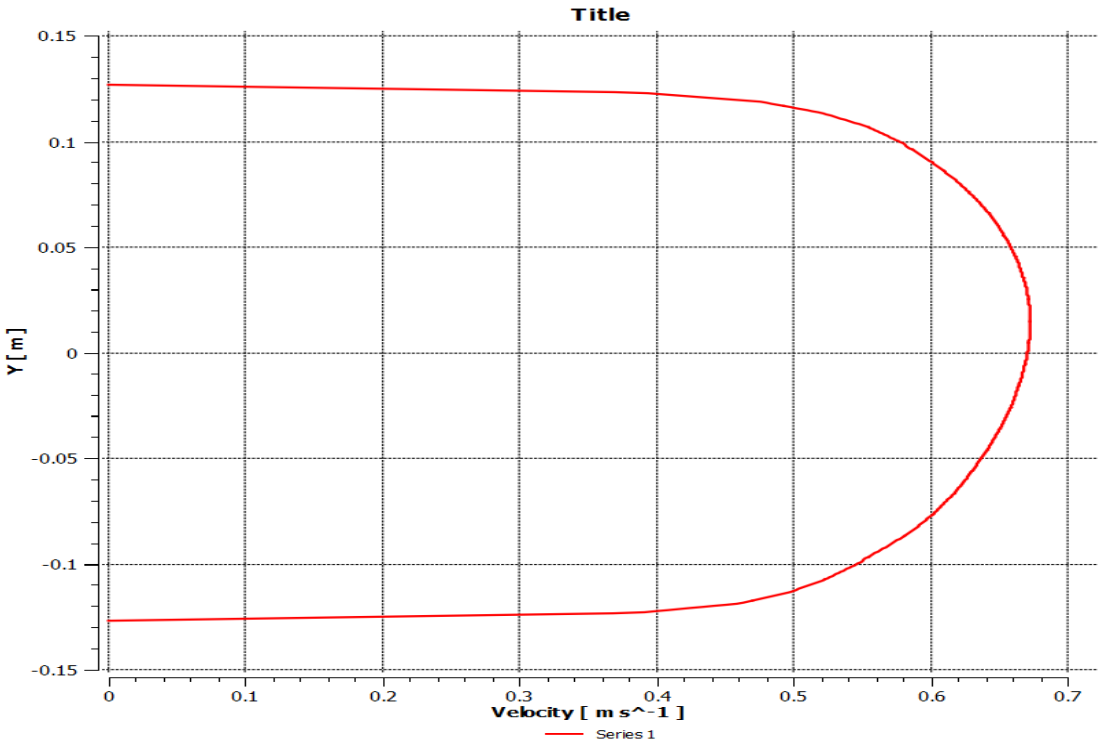

b) for L/D = 37.0145 (k-ω turbulence model)

Figure 5.11 Velocity profiles for 0.254 m diameter pipe with 0.8 m/s mixture velocity

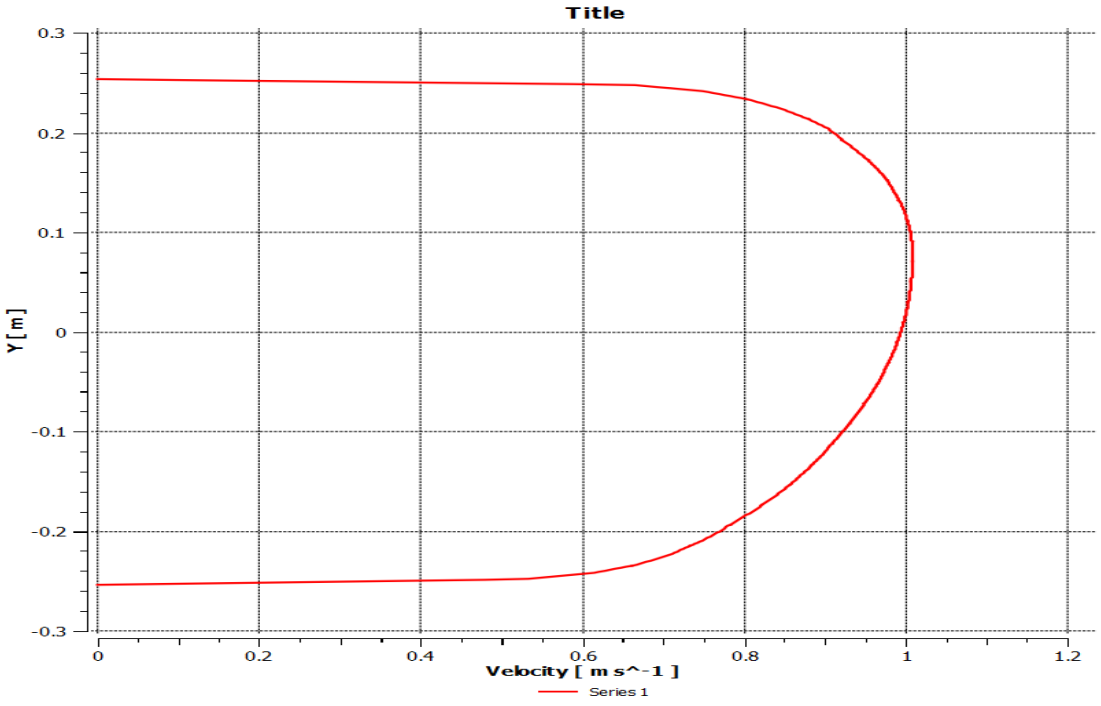

a) for L/D = 48.4909 (k-ε turbulence model)

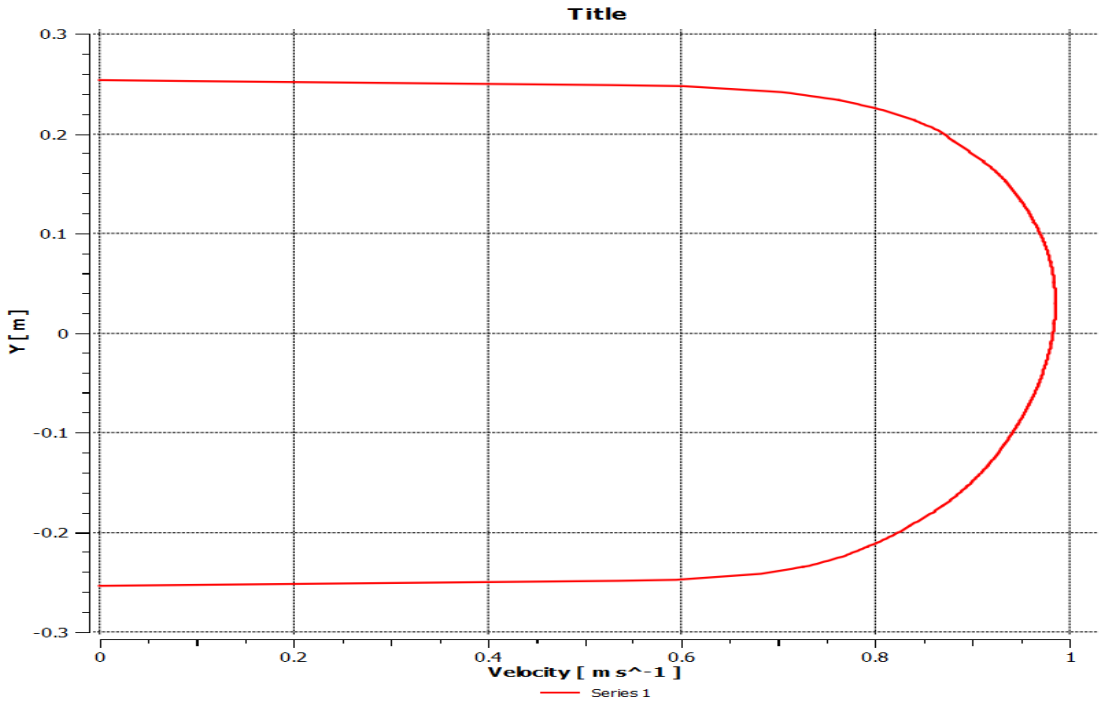

b) for L/D = 48.4909 (k-ω turbulence model)

Figure 5.12 Velocity profiles for 0.508 m diameter pipe with 1.2 m/s mixture velocity

5.5 Oil volume fraction

The counter plots of oil volume fraction are presented for some cases obtained by Realizable k-ε and Shear Stress Transition k-ω turbulence models. For each figure, different four planes were taken, two of them before the test section and the other two near test section as shown in Figures 5.13-5.20. In these figures, the oil layer is separated obviously with an interface, and a mixed region between the oil and water is numerically obtained by volume of fluid (VOF) model simulations. This result agrees well with the finding of Paulo et al. (2008).

The oil layer is separated clearly even with the high ratio of water volume fraction through 0.0254, 0.127, 0.254 and 0.508 pipe diameters for Realizable k-ε and Shear Stress Transition k-ω turbulence models because chosen the high optimum mesh size for all cases. The oil layer at 80 % water volume fraction through a 0.0254 pipe diameter did not predicted by Al-Yaari et al. (2009).

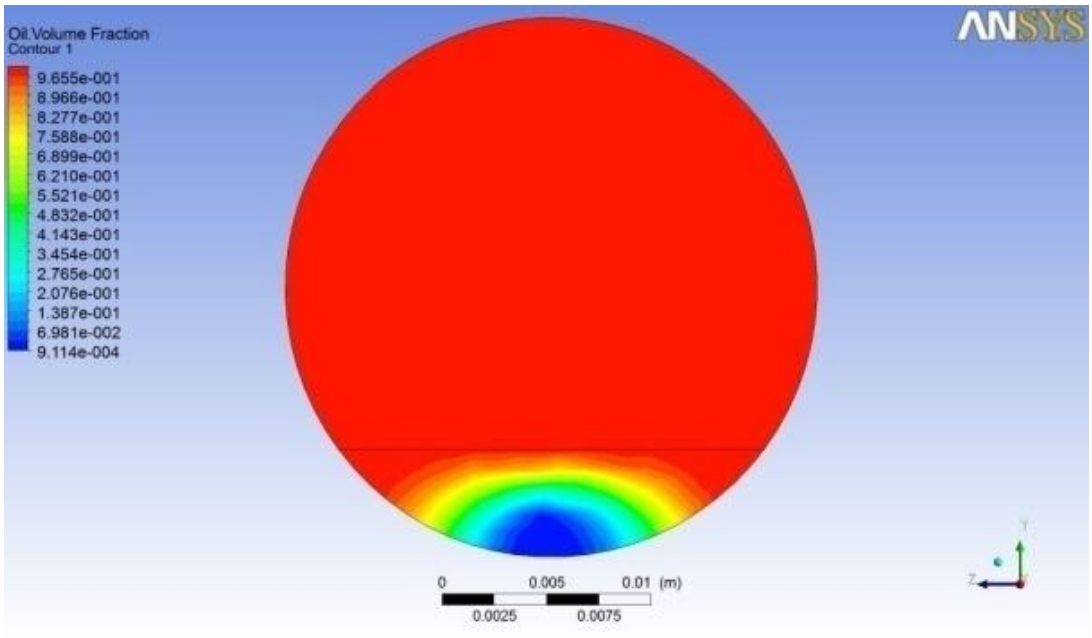

a) at L= 2.27 D from inlet

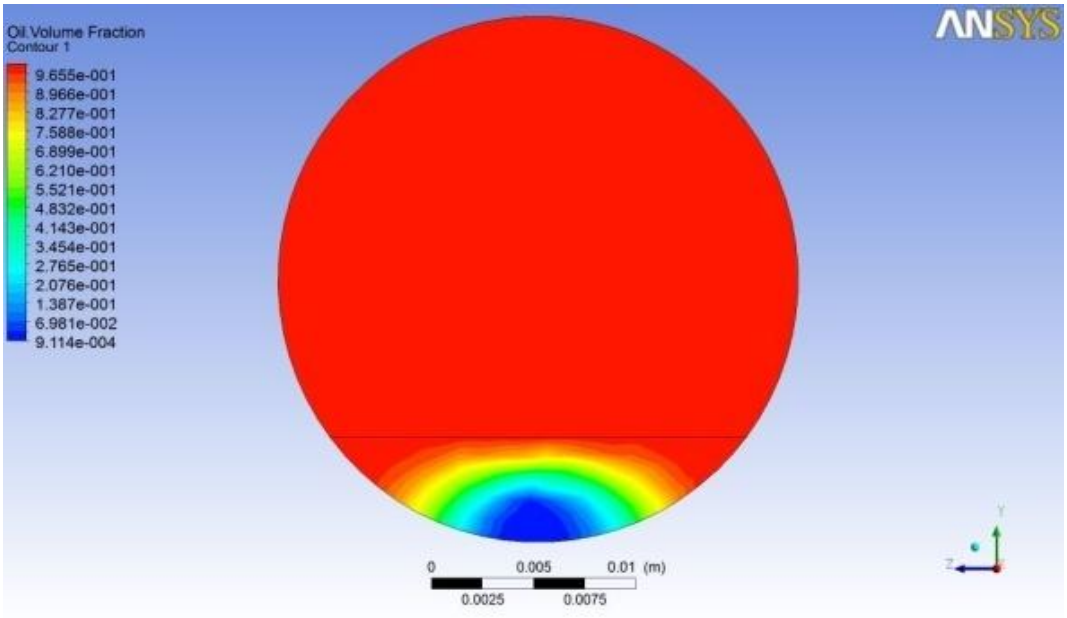

b) at L= 11.36 D from inlet

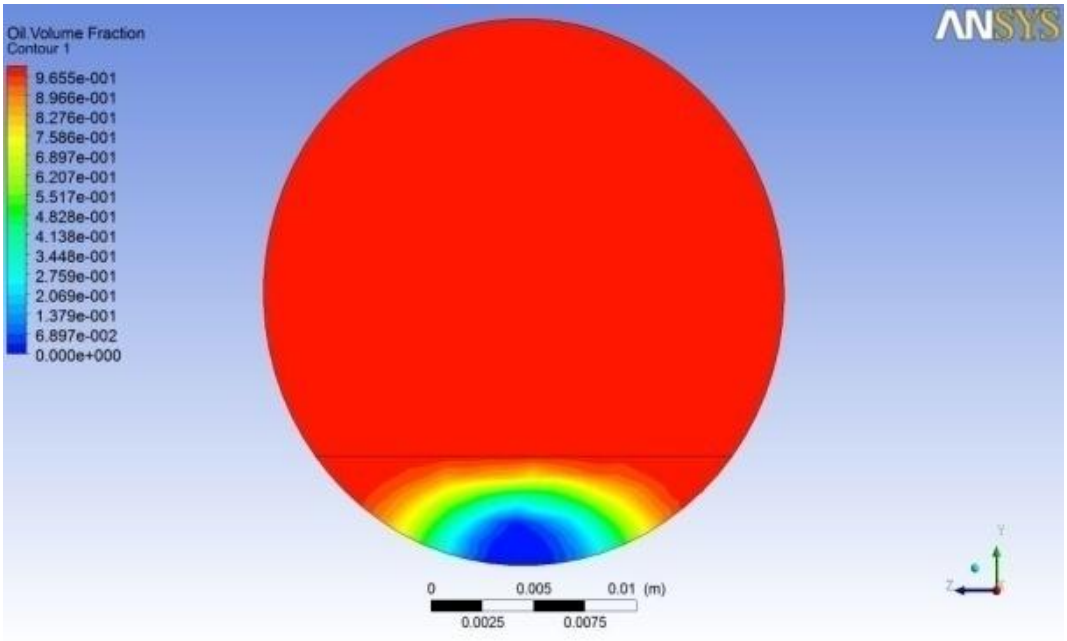

c) at L= 19.72 D from inlet

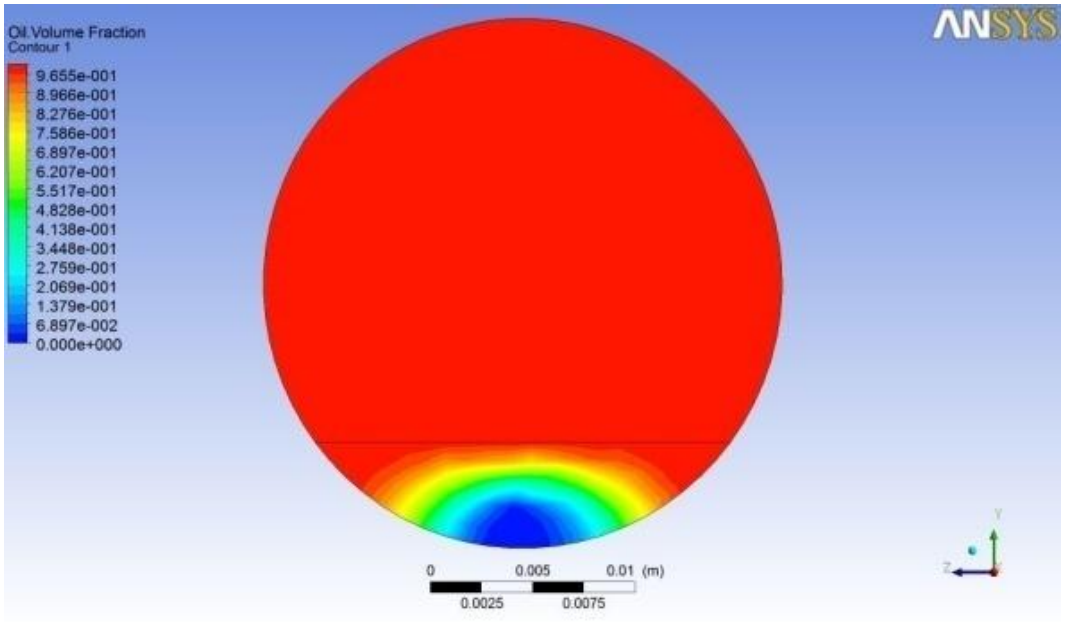

d) at L= 20.72 D from inlet

Figure 5.13 Oil volume fraction obtained by k-ε turbulence model for 0.5 m/s mixture velocity, 20 % water volume fraction and 0.0254 m diameter pipe

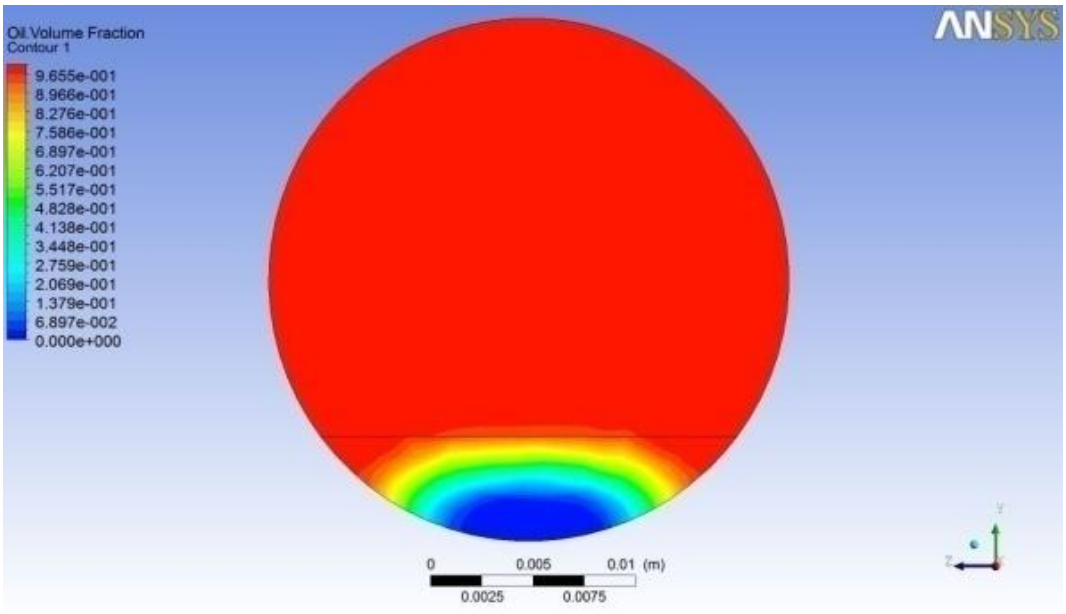

a) at L= 2.27 D from inlet

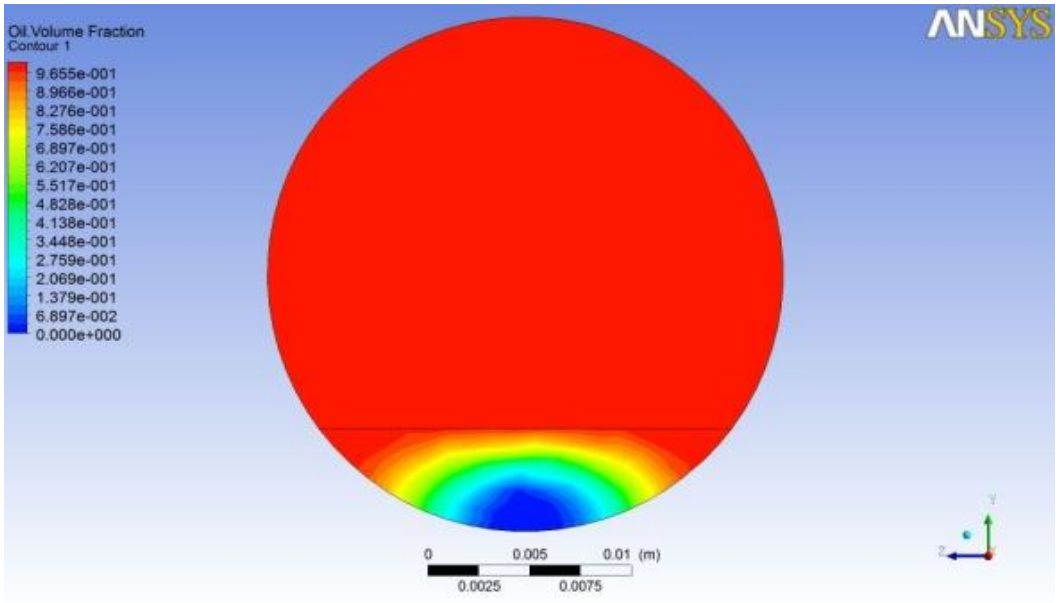

b) at L= 11.36 D from inlet

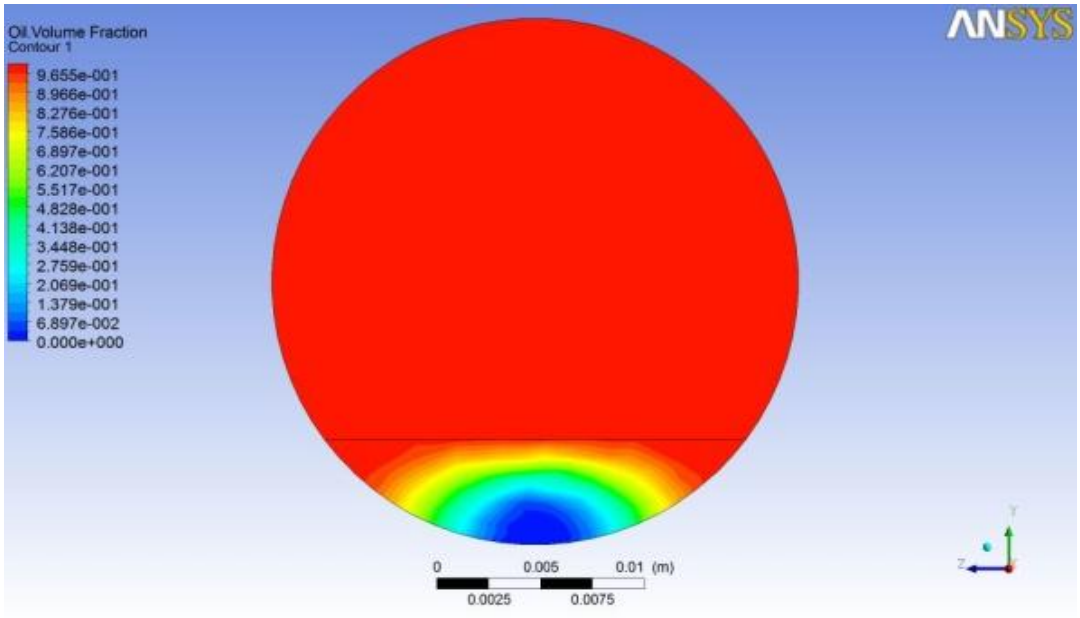

c) at L= 19.72 D from inlet

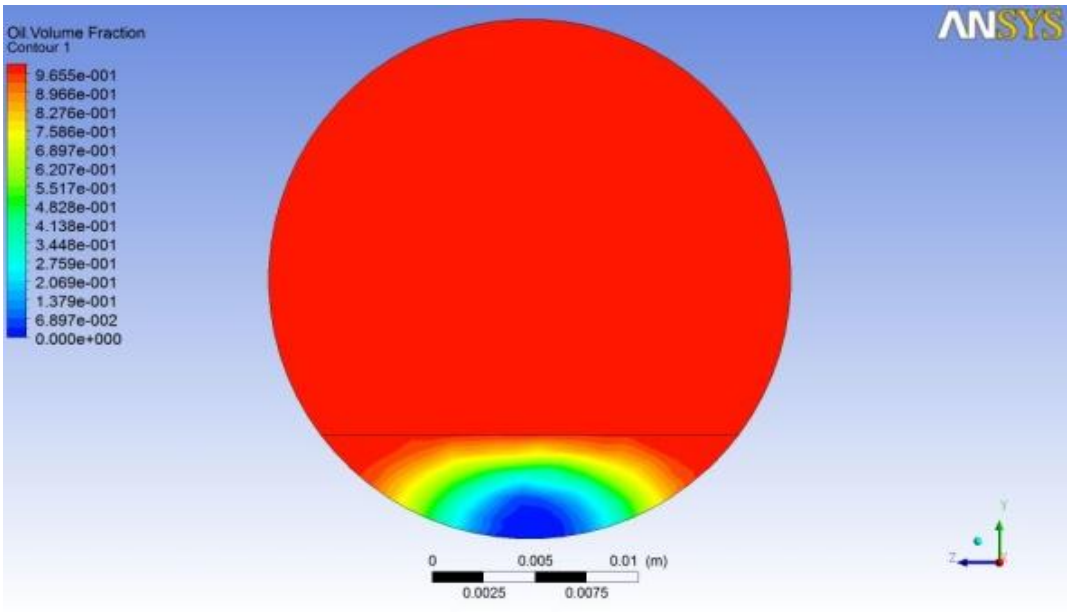

d) at L= 20.72 D from inlet

Figure 5.14 Oil volume fraction obtained by k-ω turbulence model for 0.5 m/s mixture velocity, 20 % water volume fraction and 0.0254 m diameter pipe

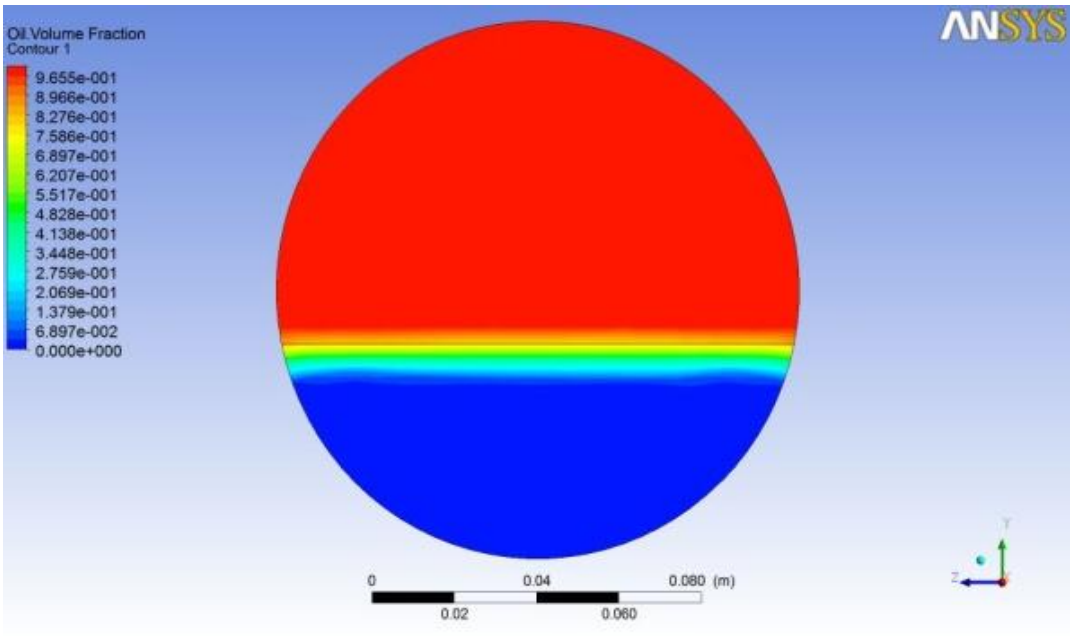

a) at L= 3.36 D from inlet

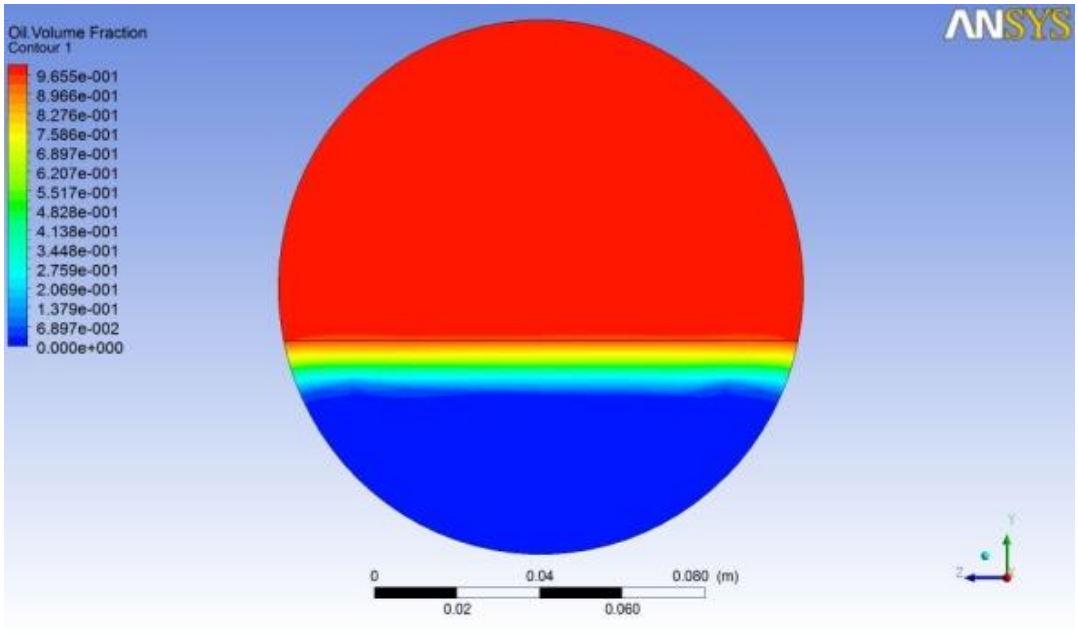

b) at L= 16.80 D from inlet

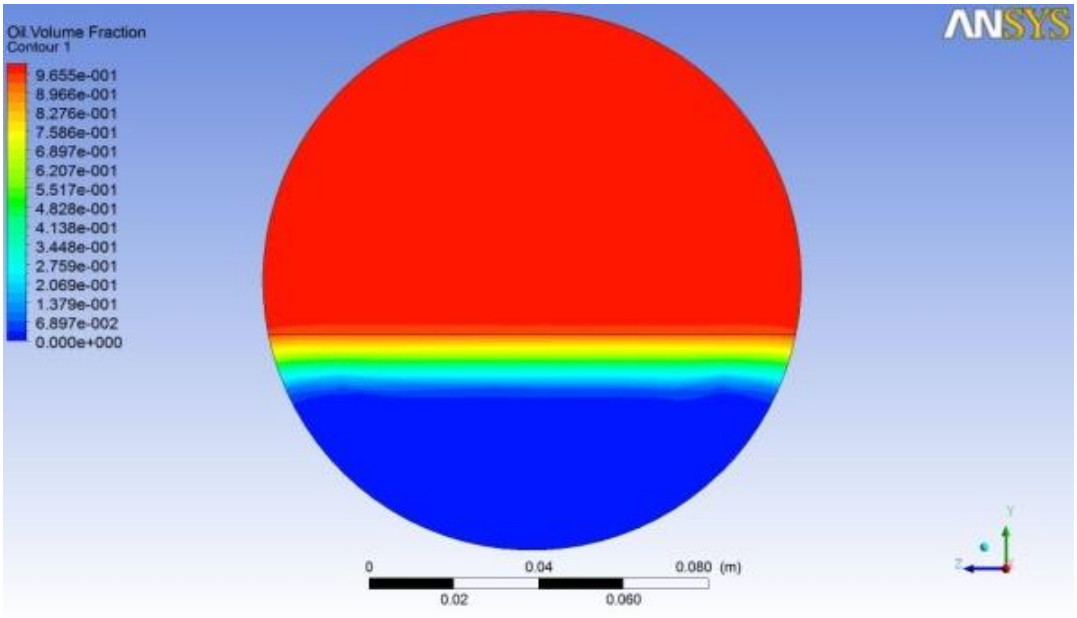

c) at L= 30.60 D from inlet

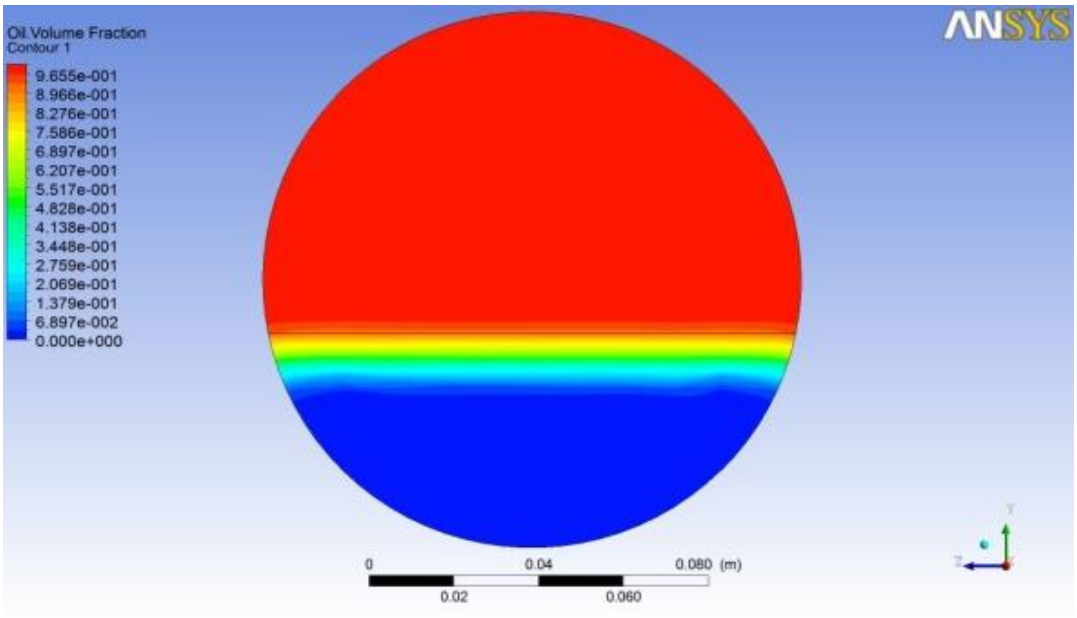

d) at L= 31.60 D from inlet

Figure 5.15 Oil volume fraction obtained by k-ε turbulence model for 0.8 m/s mixture velocity, 40 % water volume fraction and 0.127 m diameter pipe

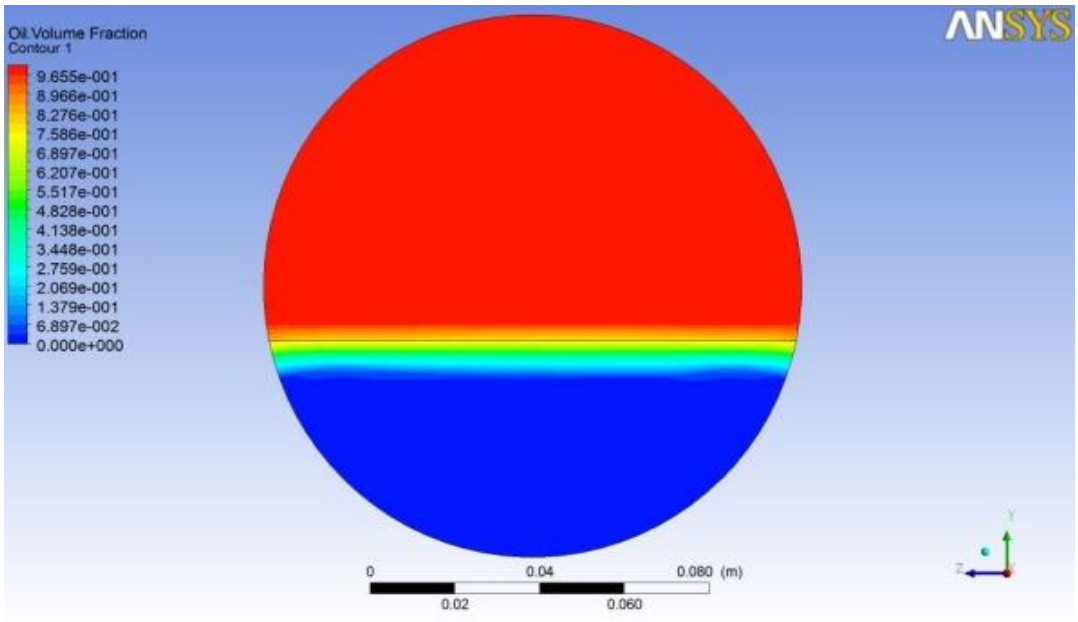

a) at L= 3.36 D from inlet

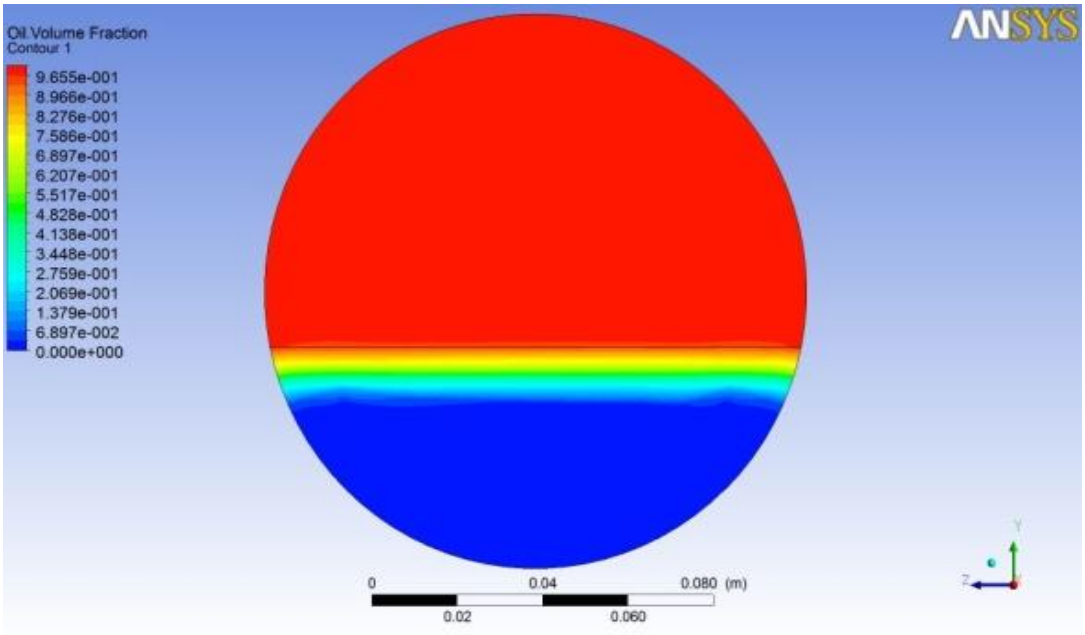

b) at L= 16.80 D from inlet

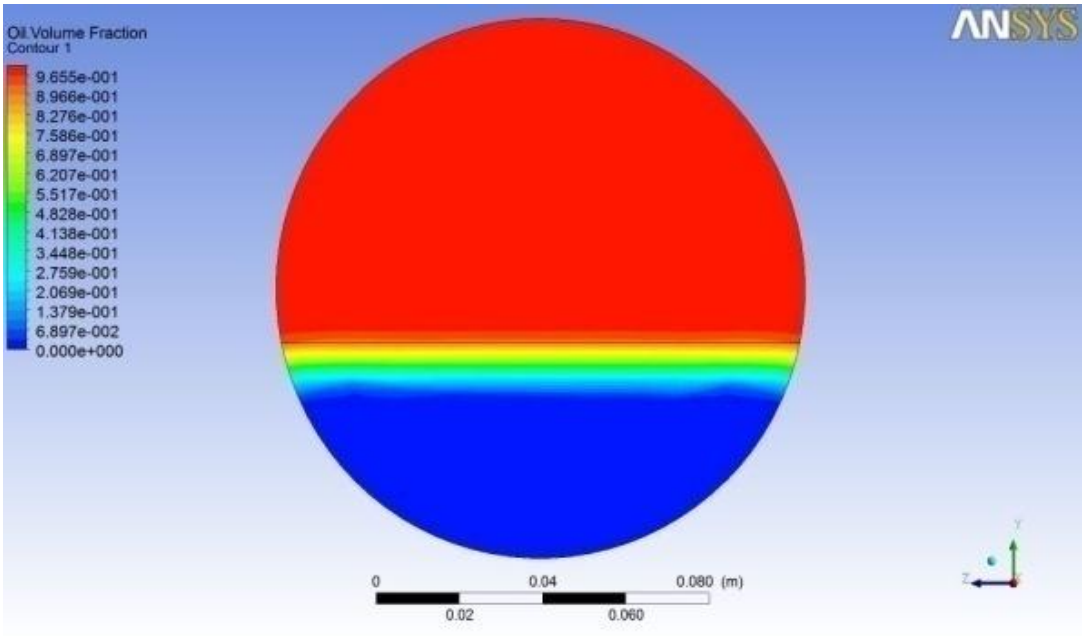

c) at L= 30.60 D from inlet

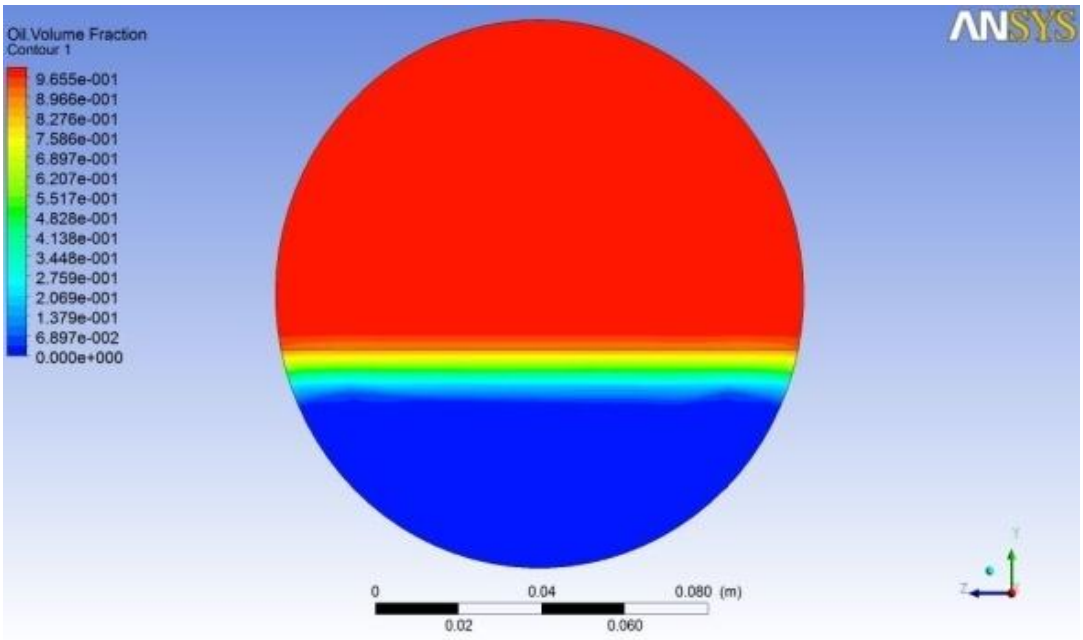

d) at L= 31.60 D from inlet

Figure 5.16 Oil volume fraction obtained by k-ω turbulence model for 0.8 m/s mixture velocity, 40 % water volume fraction and 0.127 m diameter pipe

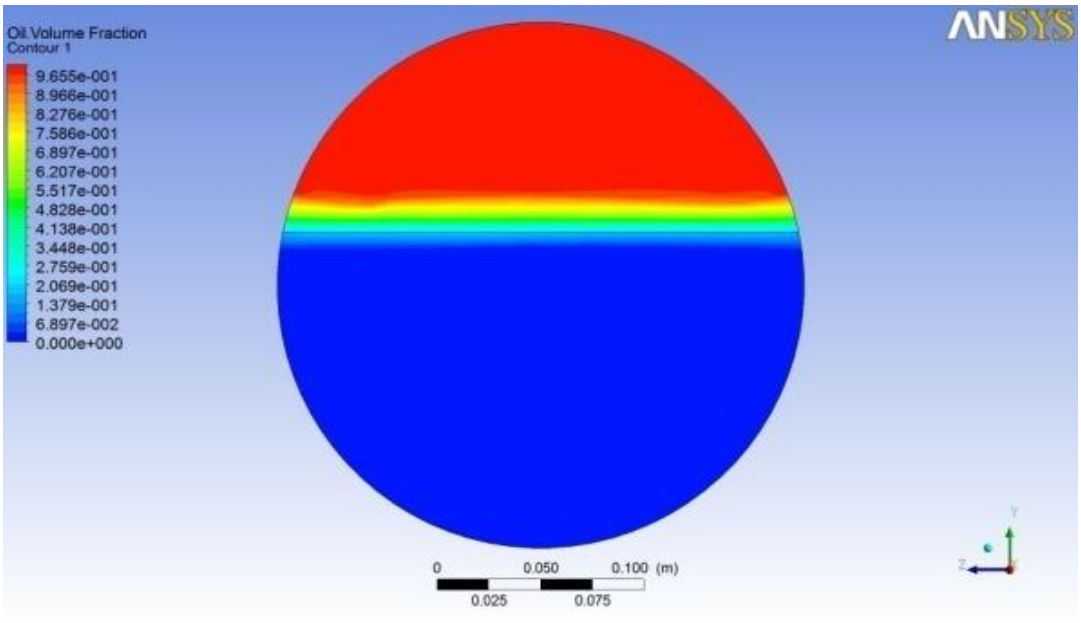

a) at L= 4.28 D from inlet

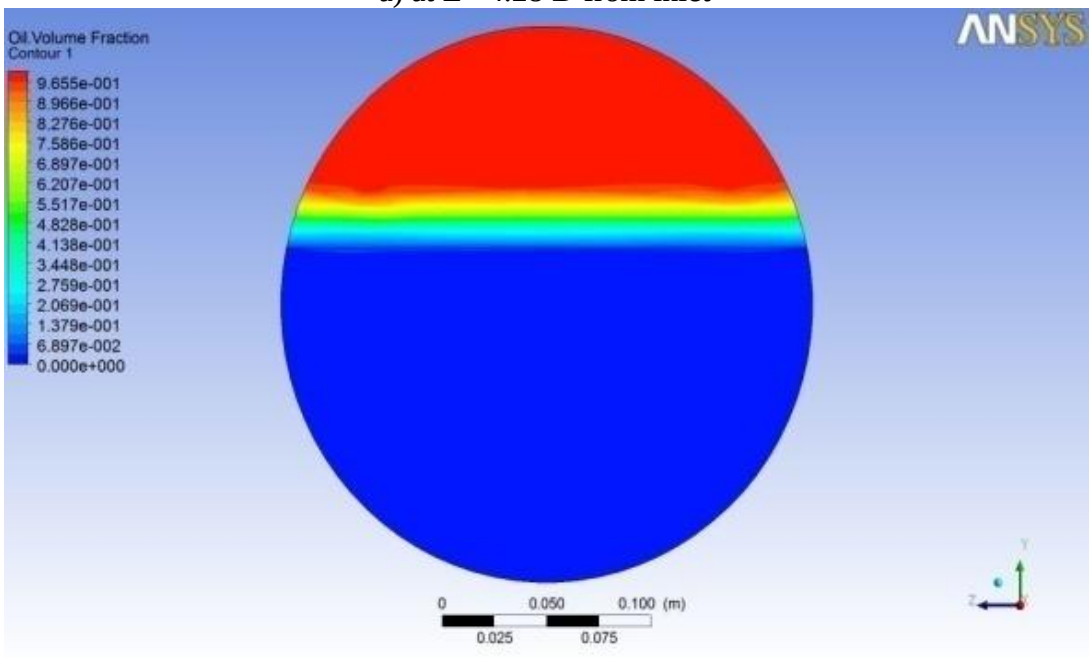

b) at L= 21.43 D from inlet

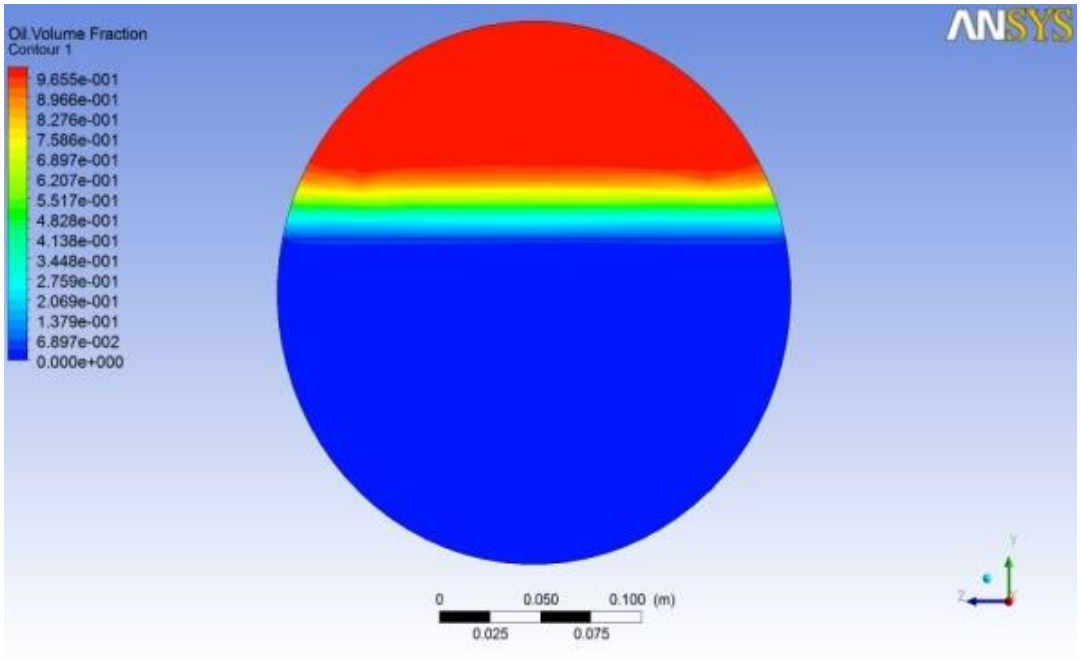

c) at L= 39.87 D from inlet

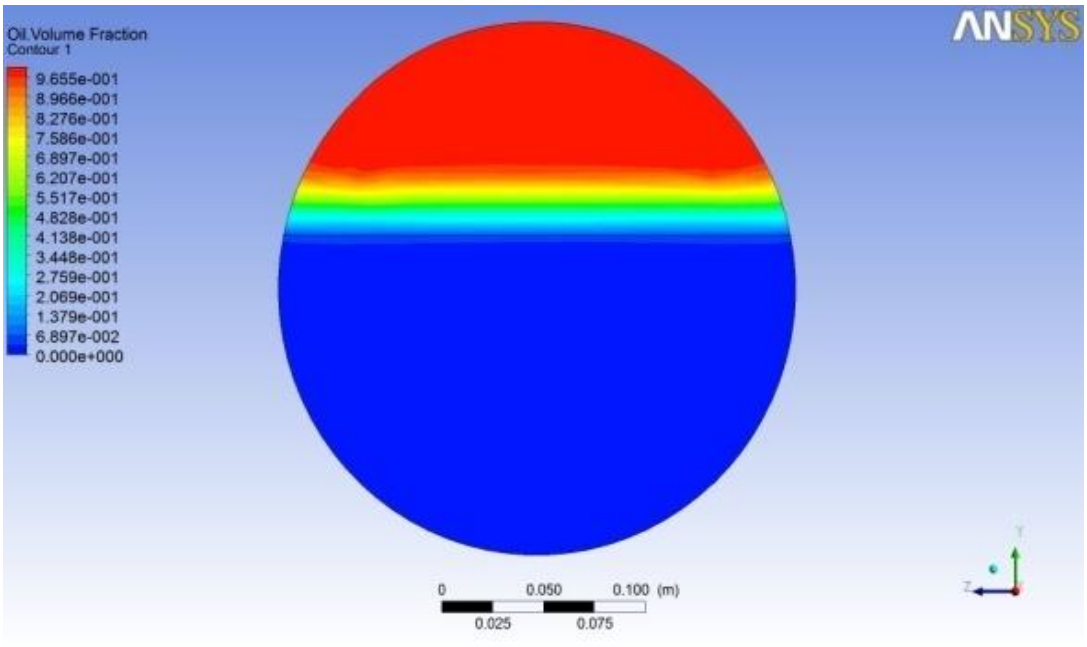

d) at L= 40.87 D from inlet

Figure 5.17 Oil volume fraction obtained by k-ε turbulence model for 1.2 m/s mixture velocity, 60 % water volume fraction and 0.254 m diameter pipe

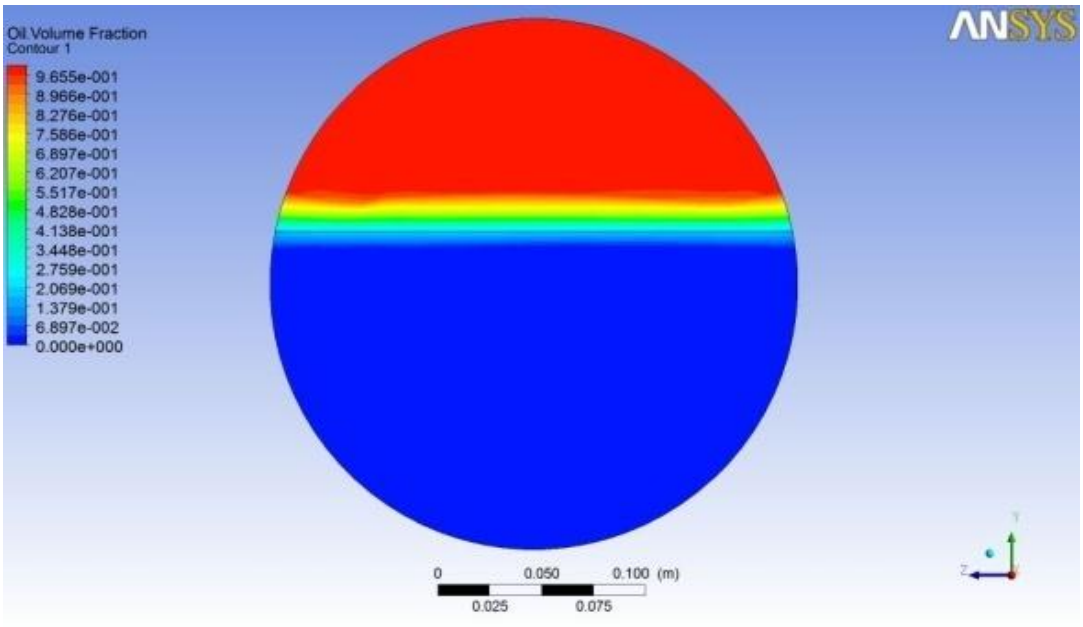

a) at L= 4.28 D from inlet

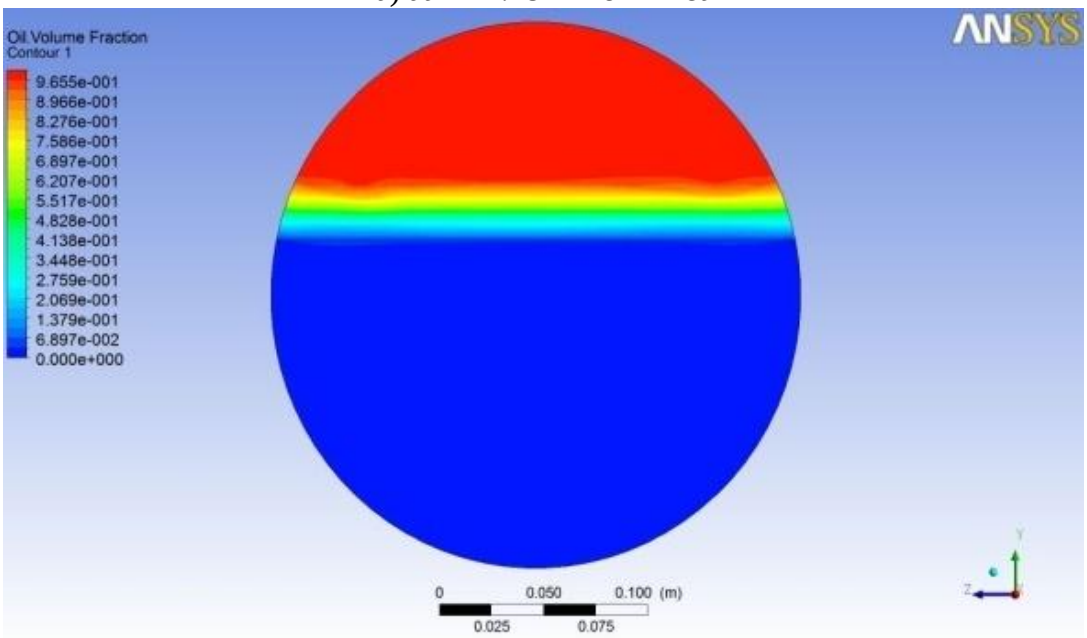

b) at L= 21.43 D from inlet

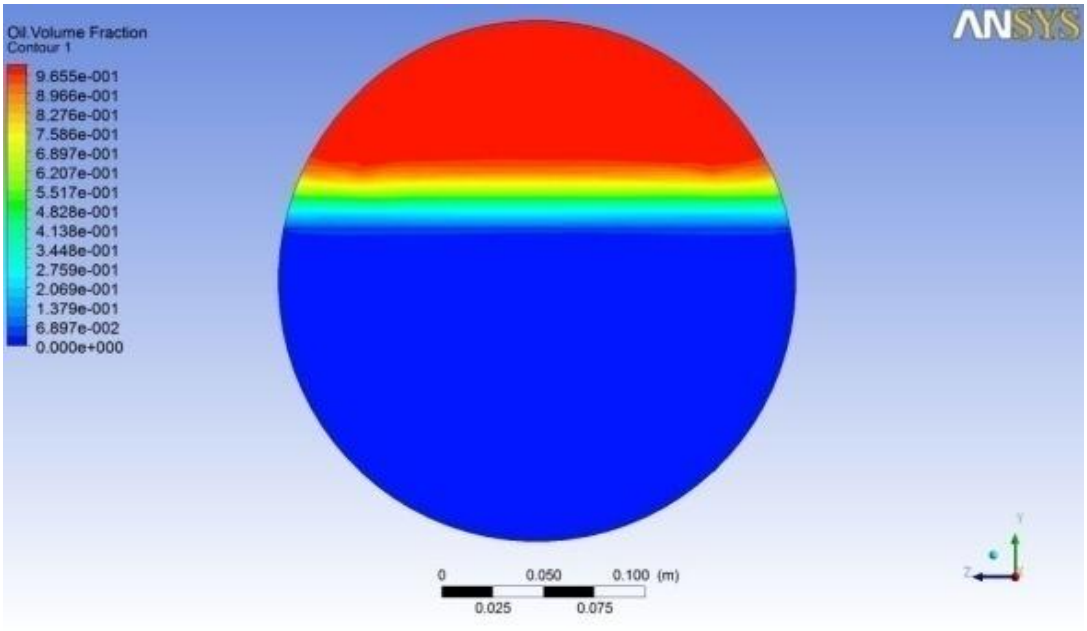

c) at L= 39.87 D from inlet

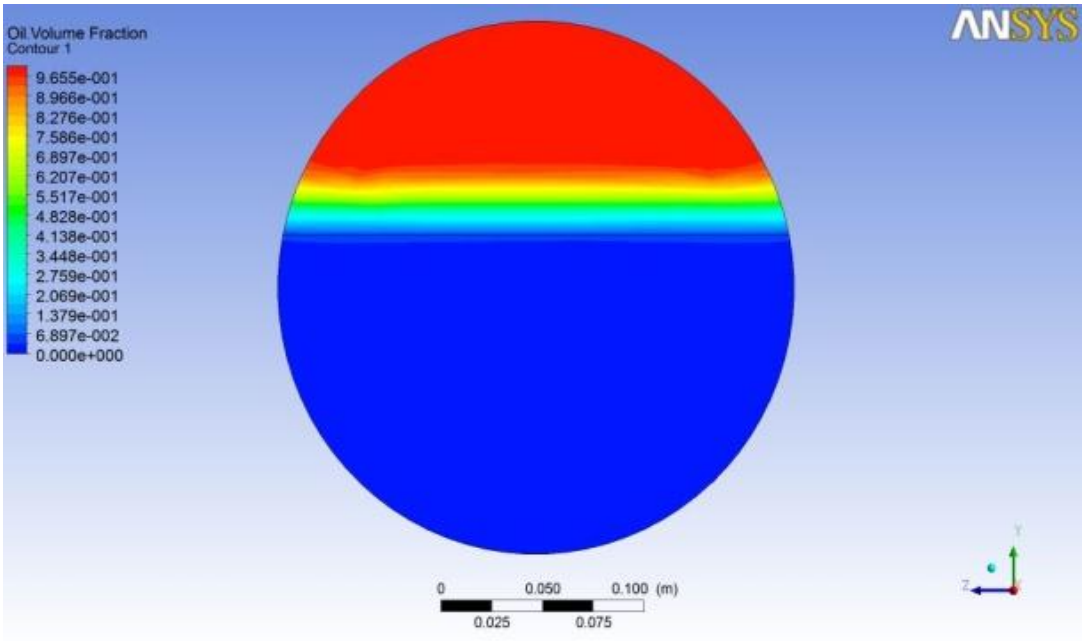

d) at L= 40.87 D from inlet

Figure 5.18 Oil volume fraction obtained by k-ω turbulence model for 1.2 m/s mixture velocity, 60 % water volume fraction and 0.254 m diameter pipe

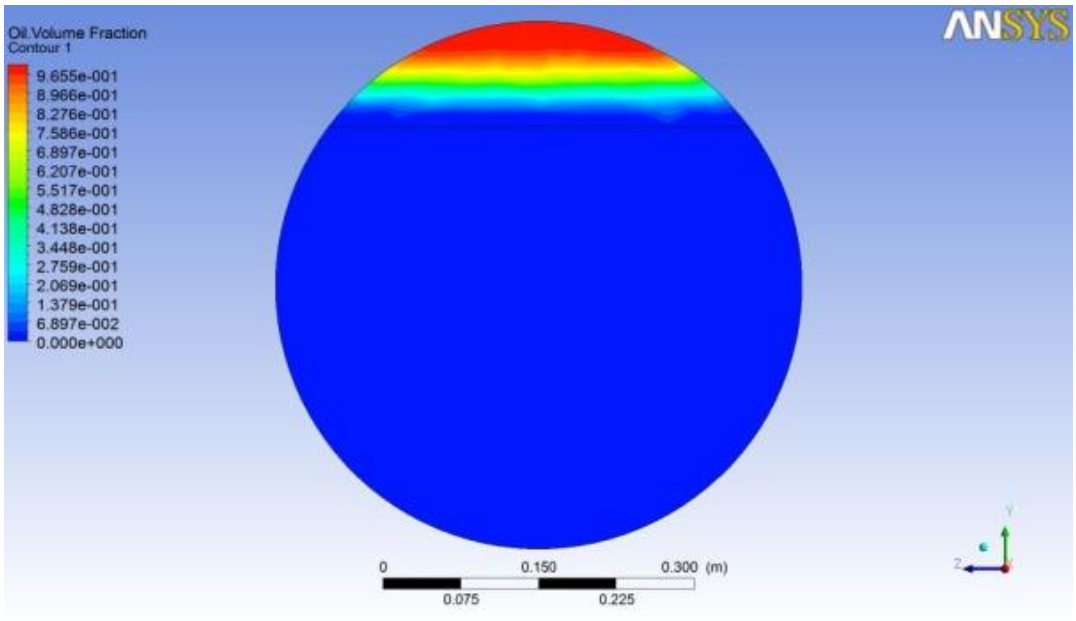

a) at L= 3.54 D from inlet

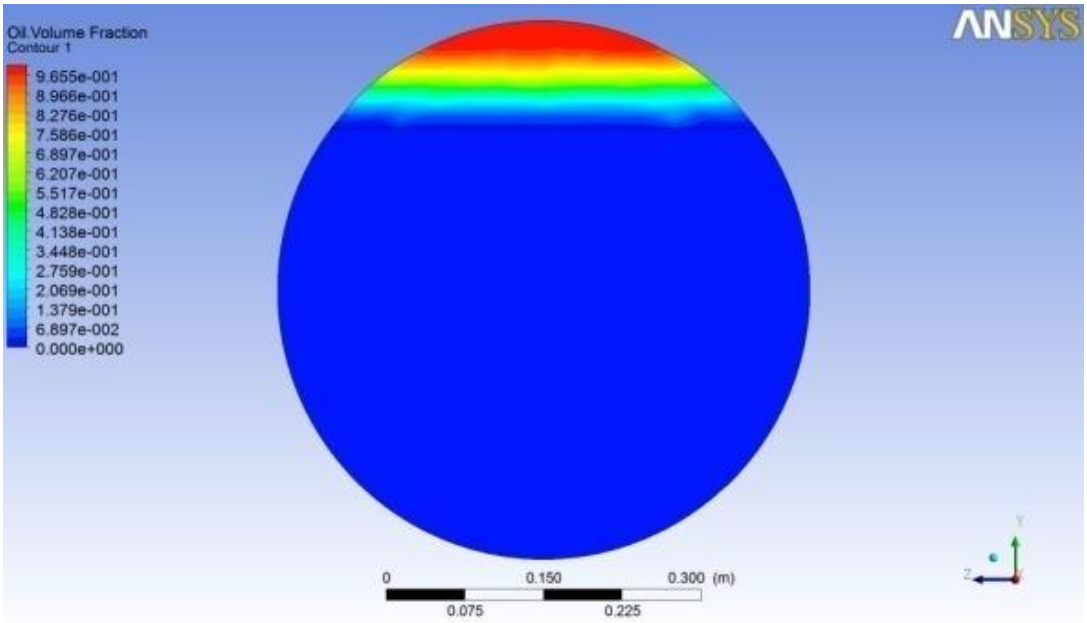

b) at L= 17.73 D from inlet

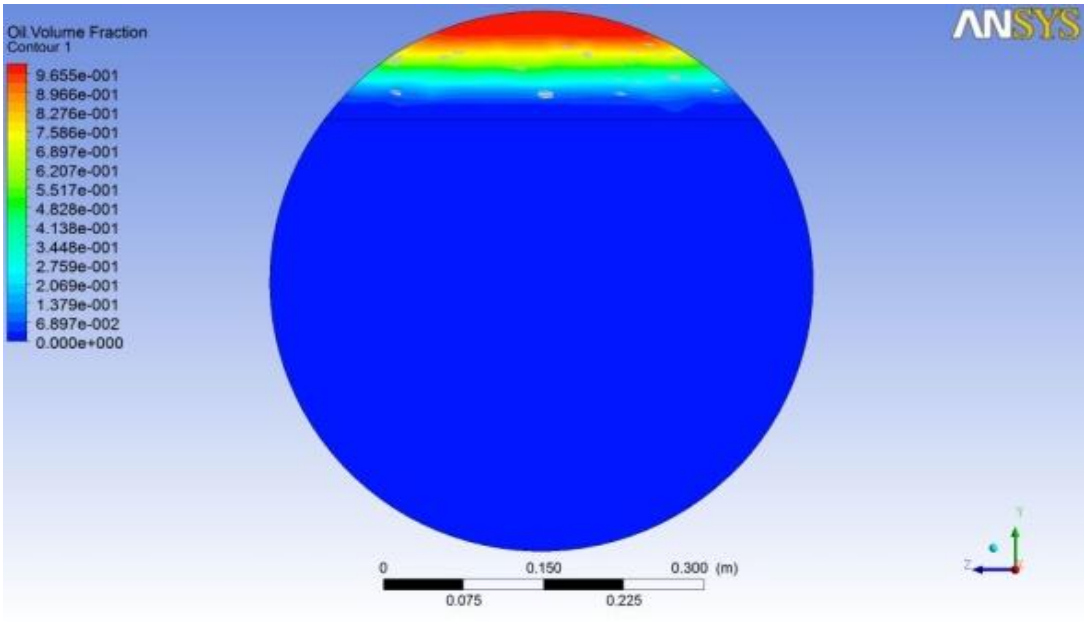

c) at L= 32.43 D from inlet

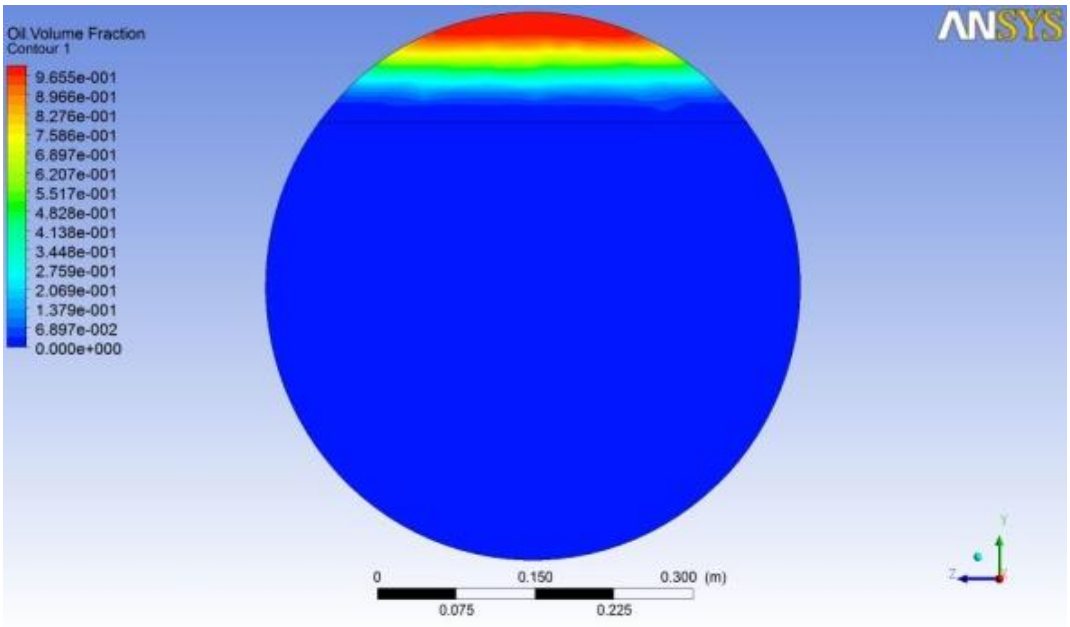

d) at L= 33.46 D from inlet

Figure 5.19 Oil volume fraction obtained by k-ε turbulence model for 0.2 m/s mixture velocity, 80 % water volume fraction and 0.508 m diameter pipe

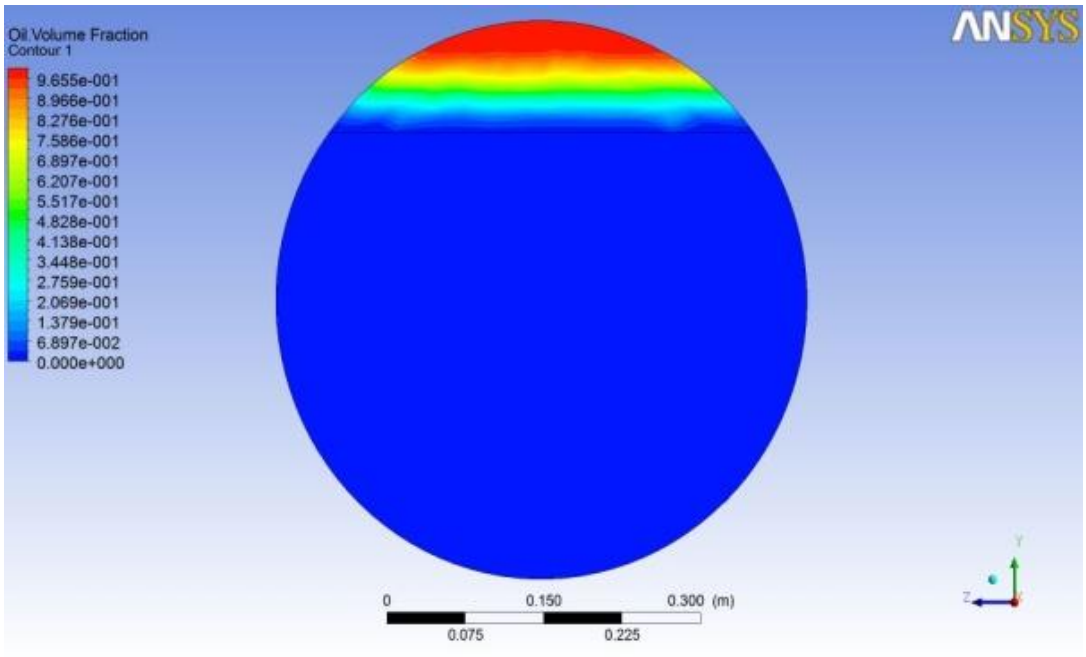

a) at L= 3.54 D from inlet

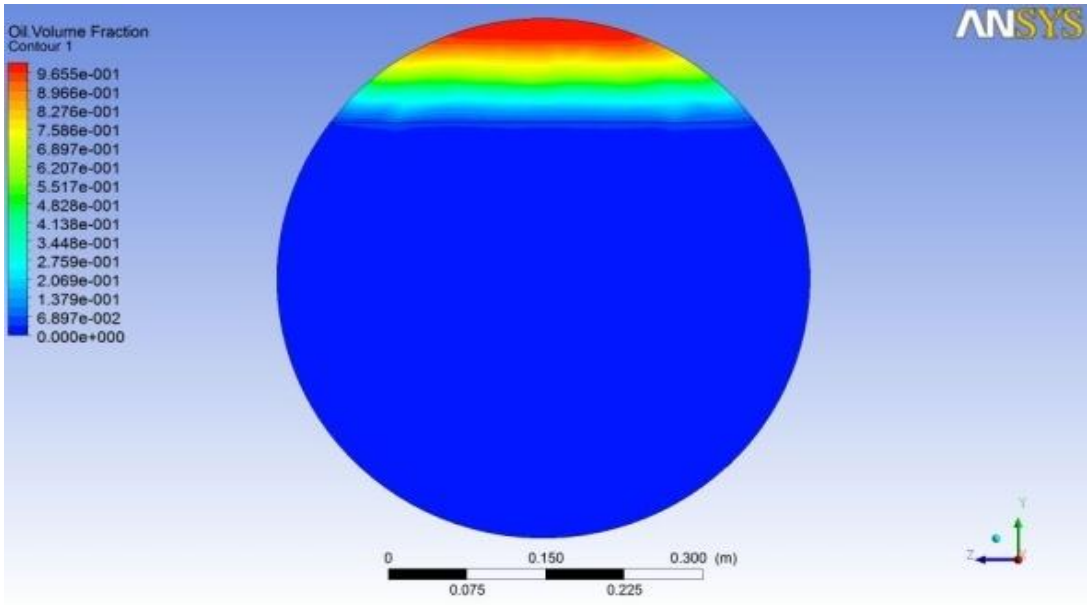

b) at L= 17.73 D from inlet

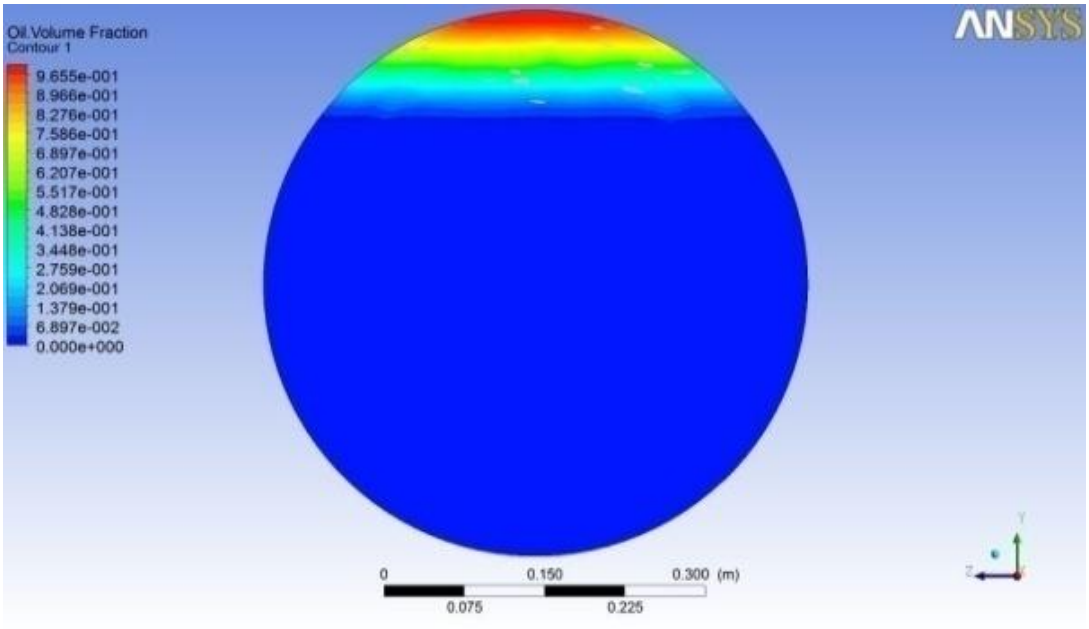

c) at L= 32.43 D from inlet

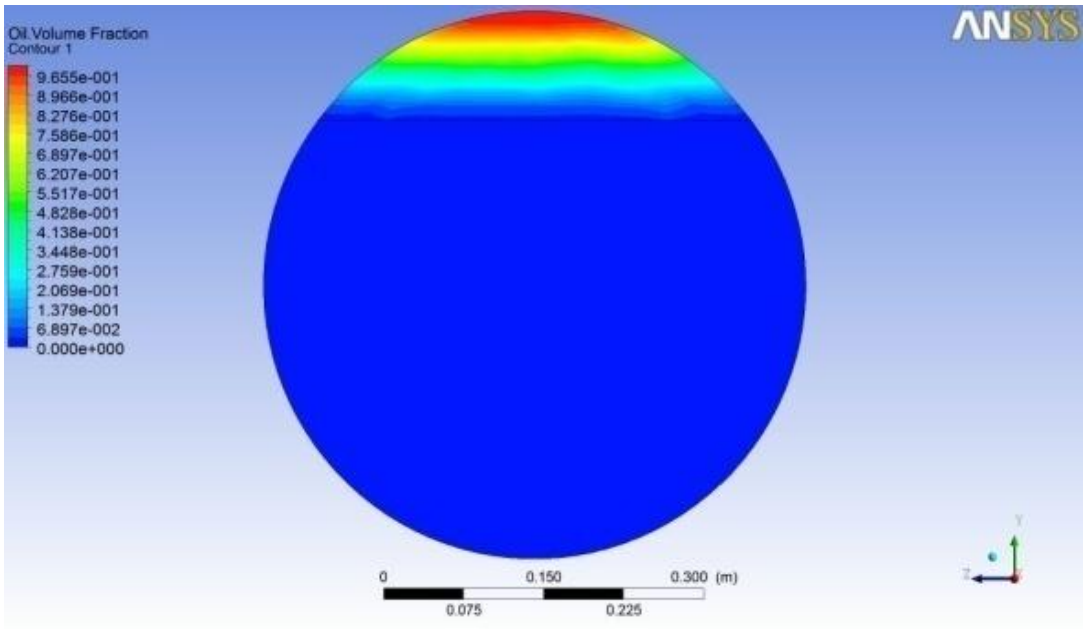

d) at L= 33.46 D from inlet

Figure 5.20 Oil volume fraction obtained by k-ω turbulence model for 0.2 m/s mixture velocity, 80 % water volume fraction and 0.508 m diameter pipe

5.6 Stratified and stratified wavy flows

The oil phase at the bottom of the pipe travels upwardly due to the gravity. Experimental studies in the literature proved that the stratified and stratified wavy flows occur at velocities between zero to 1.2 m/s. The stratified and stratified wavy flows of the oil-water phases was clearly observed with the interface between them for 0.2, 0.5, 0.8 and 1.2 m/s mixture velocity of oil-water flow in a 0.0254, 0.127, 0.254 and 0.508 m diameter pipe with 20, 40, 60 and 80 % water volume fraction by VOF method with Realizable k-ε and Shear Stress Transition k-ω turbulence models in ANSYS Fluent. These results agree with the studies of Hui Gao, (2002) and Al-Yaari et al. (2011).

For large diameters such as 0.254 m and 0.508 m, whenever the percentage of water phase close from oil phase such as 40 % and 60 % water volume fraction for Realizable k-ε and Shear Stress Transition k-ω turbulence models the stratified wavy flow that could be associated with local phase inversion from water continuous to oil continuous in the pipe was clearly observed. Figures 5.21 to 5.24 show the stratified and stratified wavy flow regimes.

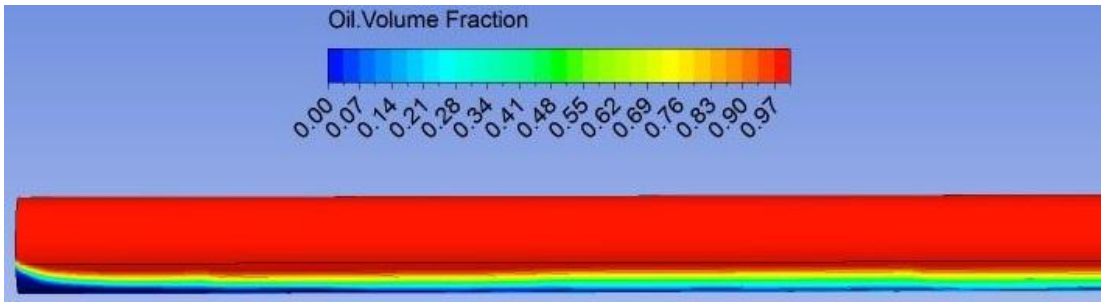

a) oil volume fraction distribution contours for 0.0254 m diameter pipe

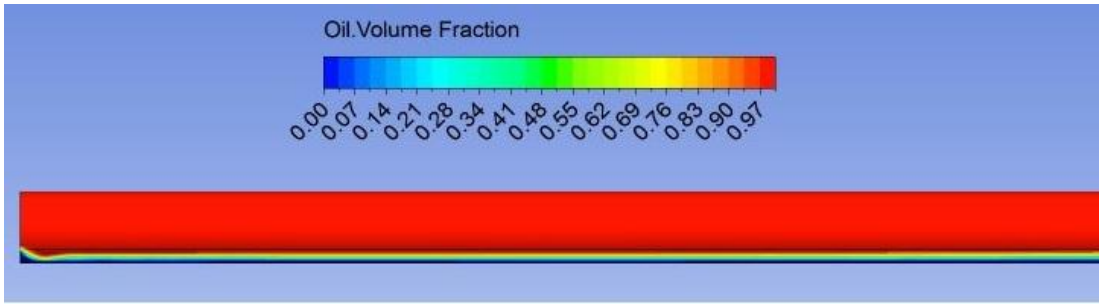

b) oil volume fraction distribution contours for 0.0.127 m diameter pipe

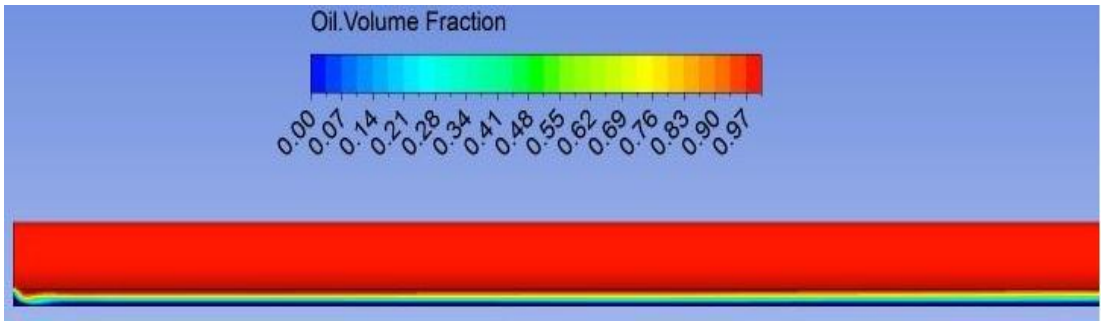

c) oil volume fraction distribution contours for 0. 254 m diameter pipe

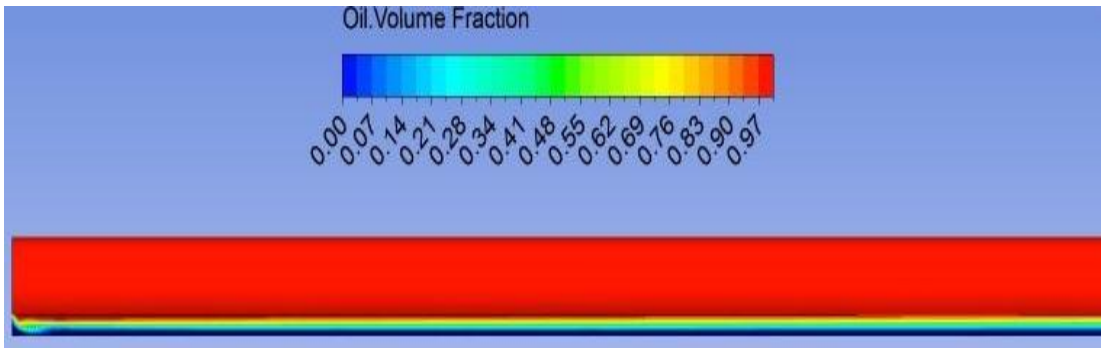

d) oil volume fraction distribution contours for 0.508 m diameter pipe

Figure 5.21 Stratified or stratified wavy flow regimes for 0.2 m/s mixture velocity with 20 % water volume fraction by k-ε turbulence model

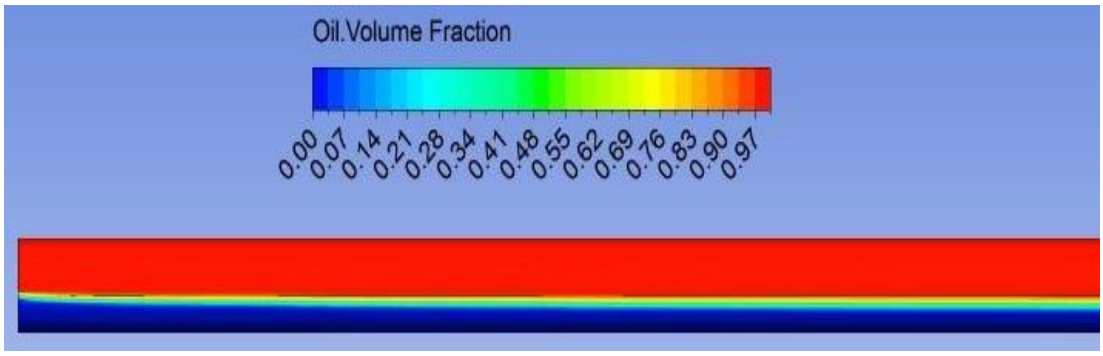

a) oil volume fraction distribution contours for 0.0254 m diameter pipe

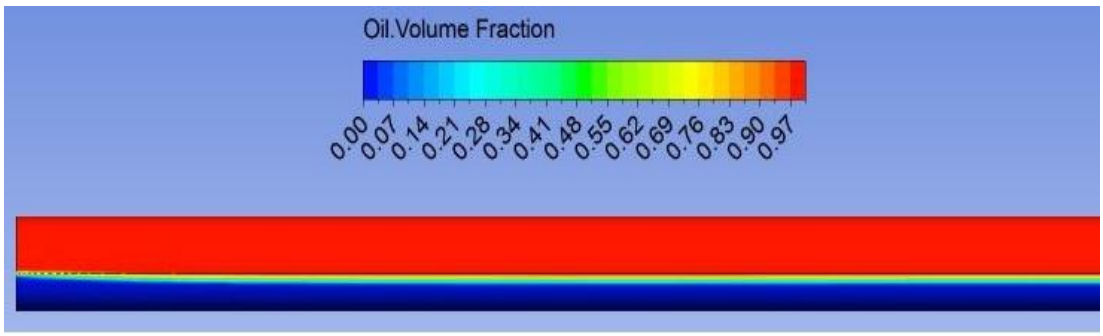

b) oil volume fraction distribution contours for 0.127 m diameter pipe

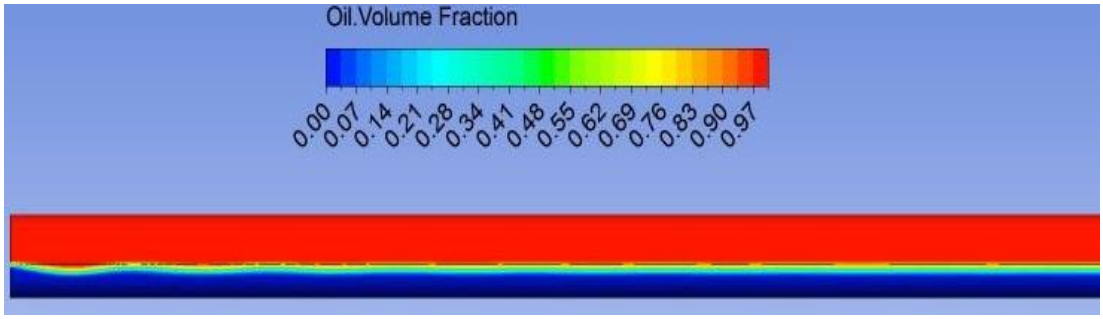

c) oil volume fraction distribution contours for 0. 254 m diameter pipe

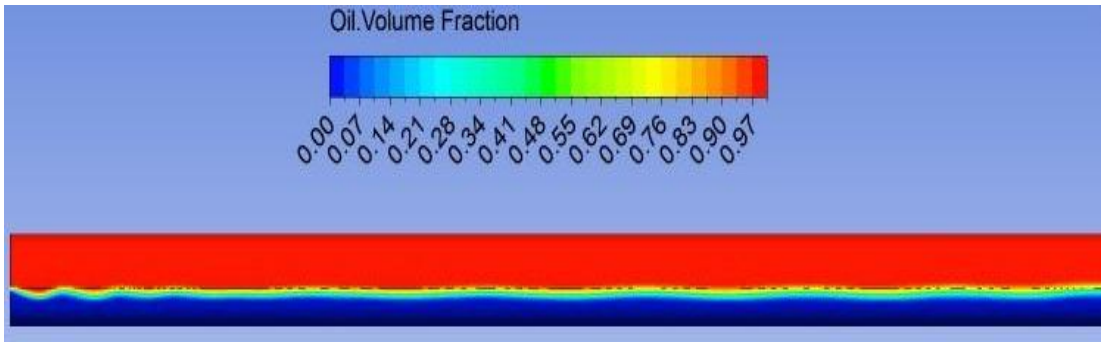

d) oil volume fraction distribution contours for 0.508 m diameter pipe

Figure 5.22 Stratified or stratified wavy flow regimes for 0.5 m/s mixture velocity with 40 % water volume fraction k-ε turbulence model

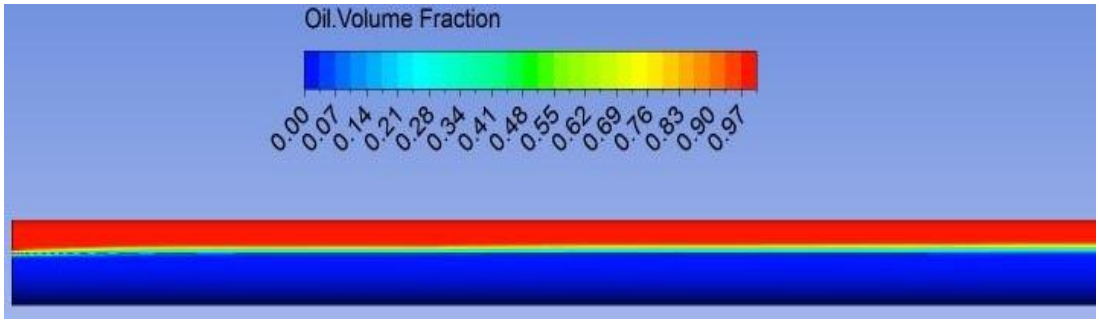

a) oil volume fraction distribution contours for 0.0254 m diameter pipe

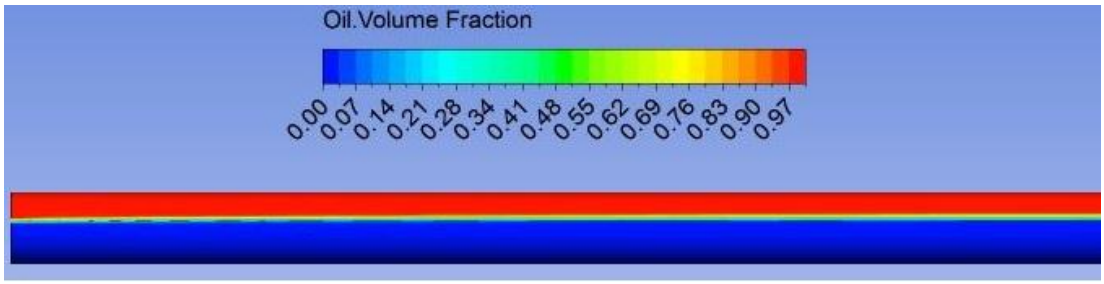

b) oil volume fraction distribution contours for 0.127 m diameter pipe

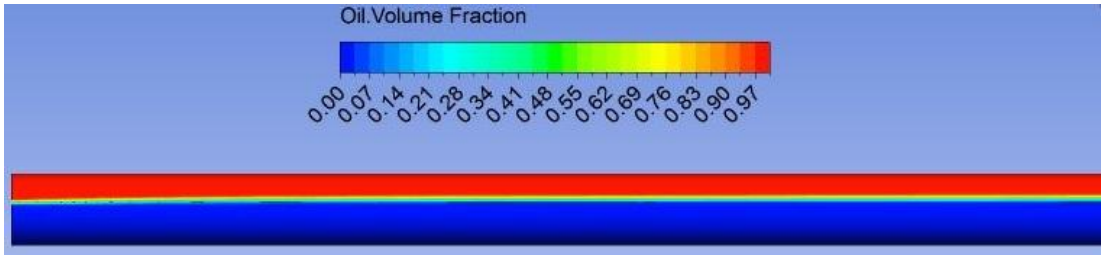

c) oil volume fraction distribution contours for 0. 254 m diameter pipe

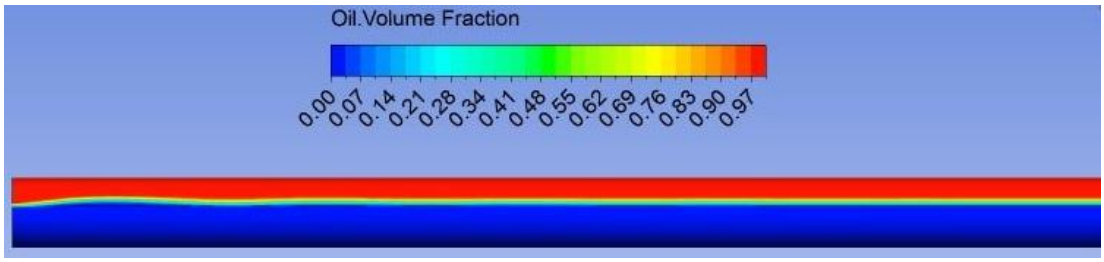

d) oil volume fraction distribution contours for 0.508 m diameter pipe

Figure 5.23 Stratified or stratified wavy flow regimes for 0.8 m/s mixture velocity with 60 % water volume fraction k-ε turbulence model

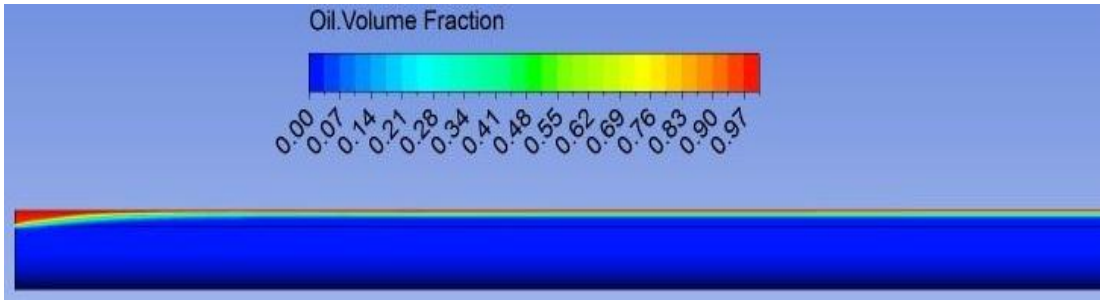

a) oil volume fraction distribution contours for 0.0254 m diameter pipe

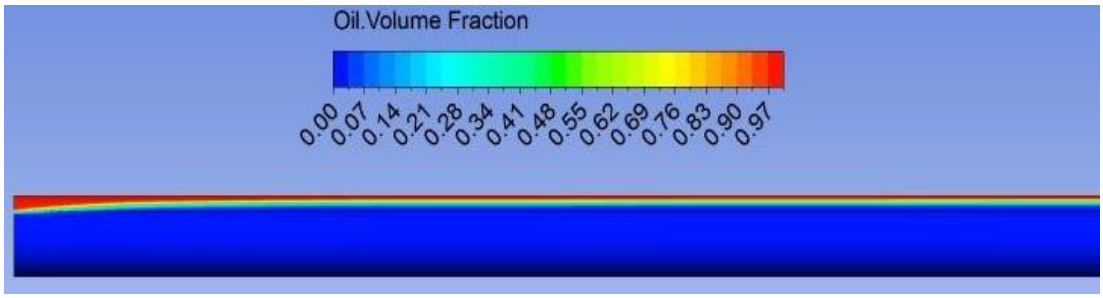

b) oil volume fraction distribution contours for 0.127 m diameter pipe

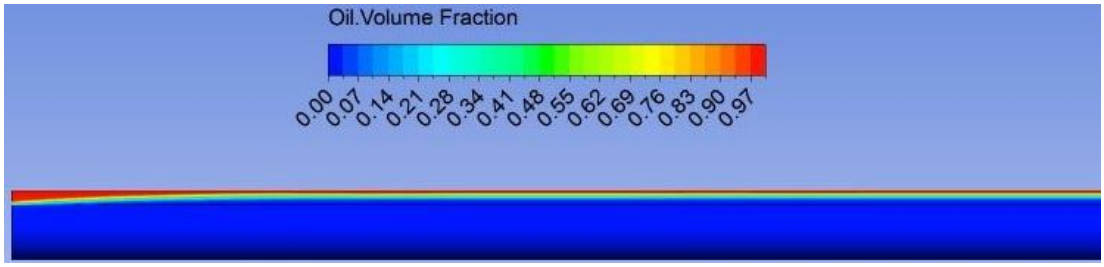

c) oil volume fraction distribution contours for 0. 254 m diameter pipe

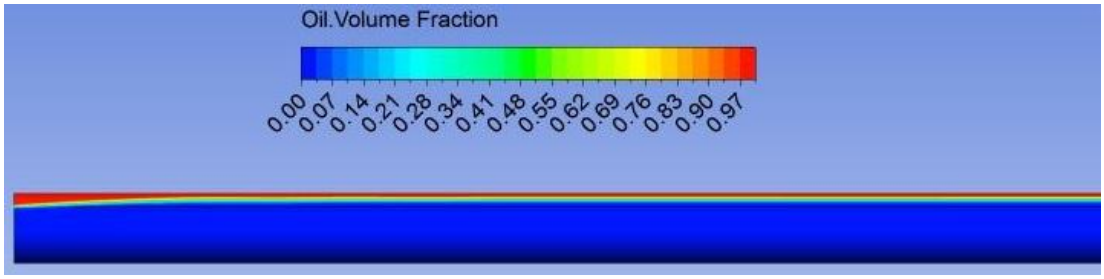

d) oil volume fraction distribution contours for 0.508 m diameter pipe

Figure 5.24 Stratified or stratified wavy flow regimes for 1.2 m/s mixture velocity with 80 % water volume fraction k-ε turbulence model

Table 5-1 Test section positions and pressure gradient results obtained by both turbulence models for 0.0254 m diameter pipe

No.	D	Mix. velocity	Water volume fraction	Mix. density	Mix. viscosity	Re	Fully dev. length	Pipe length	Point 1	Average Pressure at P1(k- ε)	Point 2	Average pressure at P2 (k- ε)	Pressure gradient (k- ε)	Pressure gradient (k- ω)	Mesh element
-	m	m/s	-	kg/m^3	mPa s	-	m	m	m	N/m^2	m	N/m^2	N/m^3	N/m^3	-
1	0.0254	0.20	0.20	823.640	0.001457	2872.51	0.2975	0.5007	0.4245	18.6143	0.4499	17.6892	36.4213	14.5945	208464
2	0.0254	0.20	0.40	867.280	0.001343	3280.06	0.3076	0.5108	0.4346	12.7601	0.4600	12.1850	22.6417	9.9646	220488
3	0.0254	0.20	0.60	910.920	0.001230	3762.79	0.3183	0.5215	0.4453	9.5502	0.4707	8.9900	22.0551	13.6693	237010
4	0.0254	0.20	0.80	954.560	0.001116	4343.57	0.3299	0.5331	0.4569	5.9781	0.4823	5.0982	34.6417	17.7165	218960
5	0.0254	0.50	0.20	823.640	0.001457	7181.26	0.3741	0.5773	0.5011	15.4404	0.5265	11.9582	137.0945	81.3898	248837
6	0.0254	0.50	0.40	867.280	0.001343	8200.16	0.3867	0.5899	0.5137	14.1781	0.5391	11.9553	87.5118	49.2205	236318
7	0.0254	0.50	0.60	910.920	0.001230	9406.96	0.4002	0.6034	0.5272	12.3171	0.5526	10.2303	82.1575	49.8425	258478
8	0.0254	0.50	0.80	954.560	0.001116	10858.93	0.4149	0.6181	0.5419	12.9165	0.5673	9.9592	116.4291	85.8110	273394
9	0.0254	0.80	0.20	823.640	0.001457	11490.02	0.4208	0.6240	0.5478	22.7871	0.5732	16.1731	260.3937	184.3701	257491
10	0.0254	0.80	0.40	867.280	0.001343	13120.26	0.4349	0.6381	0.5619	18.4961	0.5873	14.1286	171.9488	111.7677	294060
11	0.0254	0.80	0.60	910.920	0.001230	15051.14	0.4501	0.6533	0.5771	17.2966	0.6025	13.3192	156.5906	110.3031	305550
12	0.0254	0.80	0.80	954.560	0.001116	17374.29	0.4666	0.6698	0.5936	20.4869	0.6190	14.9961	216.1732	188.2598	282800
13	0.0254	1.20	0.20	823.640	0.001457	17235.03	0.4656	0.6688	0.5926	36.1484	0.6180	24.8169	446.1220	368.6890	262600
14	0.0254	1.20	0.40	867.280	0.001343	19680.39	0.4814	0.6846	0.6084	27.1768	0.6338	19.7645	291.8228	224.4213	241824
15	0.0254	1.20	0.60	910.920	0.001230	22576.71	0.4982	0.7014	0.6252	25.0764	0.6506	18.3879	263.3268	221.1220	324093
16	0.0254	1.20	0.80	954.560	0.001116	26061.44	0.5164	0.7196	0.6434	31.6787	0.6688	22.4412	363.6811	366.6693	239512

Table 5-2 Test section positions and pressure gradient results obtained by both turbulence models for 0.127 m diameter pie

No.	D	Mix. velocity	Water volume fraction	Mix. density	Mix. viscosity	Re	Fully dev. length	Pipe length	Point 1	Average Pressure at P1(k- ε)	Point 2	Average pressure at P2 (k- ε)	Pressure gradient (k- ε)	Pressure gradient (k- ω)	Mesh element
-	m	m/s	-	kg/m^3	mPa s	-	m	m	m	N/m^2	m	N/m^2	N/m^3	N/m^3	-
17	0.1270	0.20	0.20	823.640	0.001457	14362.53	2.2245	3.2405	2.8595	97.4782	2.9865	98.5636	-8.5465	3.3220	404322
18	0.1270	0.20	0.40	867.280	0.001343	16400.32	2.2995	3.3155	2.9345	72.6230	3.0615	71.7343	6.9976	6.2260	315864
19	0.1270	0.20	0.60	910.920	0.001230	18813.93	2.3798	3.3958	3.0148	38.4678	3.1418	36.7415	13.5929	13.0827	466697
20	0.1270	0.20	0.80	954.560	0.001116	21717.86	2.4668	3.4828	3.1018	16.5672	3.2288	16.0715	3.9031	4.9654	522695
21	0.1270	0.50	0.20	823.640	0.001457	35906.32	2.7972	3.8132	3.4322	94.2874	3.5592	93.0952	9.3874	6.4504	484704
22	0.1270	0.50	0.40	867.280	0.001343	41000.80	2.8915	3.9075	3.5265	67.2785	3.6535	66.7637	4.0535	4.2433	525816
23	0.1270	0.50	0.60	910.920	0.001230	47034.82	2.9925	4.0085	3.6275	40.3665	3.7545	39.5046	6.7866	6.7858	458980
24	0.1270	0.50	0.80	954.560	0.001116	54294.66	3.1018	4.1178	3.7368	15.7062	3.8638	14.3800	10.4425	6.7874	584374
25	0.1270	0.80	0.20	823.640	0.001457	57450.11	3.1459	4.1619	3.7809	56.5635	3.9079	53.9189	20.8236	21.9748	525140
26	0.1270	0.80	0.40	867.280	0.001343	65601.29	3.2520	4.2680	3.8870	58.1563	4.0140	56.7396	11.1551	12.3457	564876
27	0.1270	0.80	0.60	910.920	0.001230	75255.71	3.3656	4.3816	4.0006	38.2295	4.1276	36.6514	12.4260	13.3047	493308
28	0.1270	0.80	0.80	954.560	0.001116	86871.46	3.4885	4.5045	4.1235	20.2335	4.2505	17.1103	24.5921	24.1543	666124
29	0.1270	1.20	0.20	823.640	0.001457	86175.16	3.4815	4.4975	4.1165	42.0138	4.2435	36.5066	43.3638	47.0425	553008
30	0.1270	1.20	0.40	867.280	0.001343	98401.93	3.5989	4.6149	4.2339	51.0304	4.3609	48.0359	23.5787	25.8787	624424
31	0.1270	1.20	0.60	910.920	0.001230	112883.56	3.7246	4.7406	4.3596	41.3677	4.4866	37.7548	28.4480	27.7969	543994
32	0.1270	1.20	0.80	954.560	0.001116	130307.19	3.8607	4.8767	4.4957	29.4625	4.6227	23.4033	47.7102	48.7362	632800

Table 5-3 Test section positions and pressure gradient results obtained by both turbulence models for 0.254 m diameter pipe

No.	D	Mix. velocity	Water volume fraction	Mix. density	Mix. viscosity	Re	Fully dev. length	Pipe length	Point 1	Average Pressure at P1(k- ε)	Point 2	Average pressure at P2 (k- ε)	Pressure gradient (k- ε)	Pressure gradient (k- ω)	Mesh element
-	m	m/s	-	kg/m^3	mPa s	-	m	m	m	N/m^2	m	N/m^2	N/m^3	N/m^3	-
33	0.2540	0.20	0.20	823.640	0.001457	28725.05	5.2908	7.3228	6.5608	210.2655	6.8148	210.2755	-0.0394	7.6165	366272
34	0.2540	0.20	0.40	867.280	0.001343	32800.64	5.4692	7.5012	6.7392	150.5594	6.9932	148.5300	7.9898	10.5252	451617
35	0.2540	0.20	0.60	910.920	0.001230	37627.85	5.6602	7.6922	6.9302	63.9332	7.1842	61.4804	9.6567	8.9335	349444
36	0.2540	0.20	0.80	954.560	0.001116	43435.73	5.8670	7.8990	7.1370	31.4640	7.3910	30.2370	4.8307	5.5102	479412
37	0.2540	0.50	0.20	823.640	0.001457	71812.63	6.6528	8.6848	7.9228	181.0393	8.1768	185.6335	-18.0874	-0.6272	436240
38	0.2540	0.50	0.40	867.280	0.001343	82001.61	6.8772	8.9092	8.1472	134.5615	8.4012	131.4970	12.0650	17.8630	497777
39	0.2540	0.50	0.60	910.920	0.001230	94069.64	7.1173	9.1493	8.3873	83.2422	8.6413	81.6954	6.0898	6.4760	616121
40	0.2540	0.50	0.80	954.560	0.001116	108589.32	7.3774	9.4094	8.6474	27.9559	8.9014	27.0877	3.4181	1.9764	515338
41	0.2540	0.80	0.20	823.640	0.001457	114900.21	7.4823	9.5143	8.7523	167.7278	9.0063	165.4441	8.9909	9.6079	459792
42	0.2540	0.80	0.40	867.280	0.001343	131202.57	7.7346	9.7666	9.0046	132.3772	9.2586	131.3041	4.2248	4.4106	545664
43	0.2540	0.80	0.60	910.920	0.001230	150511.42	8.0047	10.0367	9.2747	78.0725	9.5287	76.6328	5.6681	5.9280	576294
44	0.2540	0.80	0.80	954.560	0.001116	173742.92	8.2972	10.3292	9.5672	31.1682	9.8212	28.6830	9.7843	10.2563	526015
45	0.2540	1.20	0.20	823.640	0.001457	172350.32	8.2805	10.3125	9.5505	99.7400	9.8045	94.8945	19.0768	19.7343	524560
46	0.2540	1.20	0.40	867.280	0.001343	196803.86	8.5598	10.5918	9.8298	110.0459	10.0838	107.4620	10.1728	10.7724	686322
47	0.2540	1.20	0.60	910.920	0.001230	225767.13	8.8587	10.8907	10.1287	75.1403	10.3827	72.4191	10.7134	11.2744	714016
48	0.2540	1.20	0.80	954.560	0.001116	260614.37	9.1823	11.2143	10.4523	38.9698	10.7063	33.7861	20.4083	21.3354	568936

Table 5-4 Test section positions and pressure gradient results obtained by both turbulence models for 0.508 m diameter pipe

No.	D	Mix. velocity	Water volume fraction	Mix. density	Mix. viscosity	Re	Fully dev. length	Pipe length	Point 1	Average Pressure at P1(k- ε)	Point 2	Average pressure at P2 (k- ε)	Pressure gradient (k- ε)	Pressure gradient (k- ω)	Mesh element
-	m	m/s	-	kg/m^3	mPa s	-	m	m	m	N/m^2	m	N/m^2	N/m^3	N/m^3	-
49	0.5080	0.20	0.20	823.640	0.001457	57450.11	12.5836	16.6476	15.1236	422.0725	15.6316	417.4394	9.1203	6.8222	826964
50	0.5080	0.20	0.40	867.280	0.001343	65601.29	13.0080	17.0720	15.5480	304.8678	16.0560	299.6988	10.1752	7.3281	862505
51	0.5080	0.20	0.60	910.920	0.001230	75255.71	13.4623	17.5263	16.0023	112.3992	16.5103	107.3929	9.8549	8.5512	1042578
52	0.5080	0.20	0.80	954.560	0.001116	86871.46	13.9541	18.0181	16.4941	56.4172	17.0021	54.2662	4.2343	4.5130	913273
53	0.5080	0.50	0.20	823.640	0.001457	143625.26	15.8231	19.8871	18.3631	371.9205	18.8711	376.4651	-8.9461	-2.9949	944208
54	0.5080	0.50	0.40	867.280	0.001343	164003.22	16.3567	20.4207	18.8967	271.8017	19.4047	268.4668	6.5648	10.9612	1064252
55	0.5080	0.50	0.60	910.920	0.001230	188139.27	16.9279	20.9919	19.4679	155.4783	19.9759	149.9741	10.8350	11.4715	1353729
56	0.5080	0.50	0.80	954.560	0.001116	217178.65	17.5464	21.6104	20.0864	53.4872	20.5944	52.6927	1.5640	1.4514	1020230
57	0.5080	0.80	0.20	823.640	0.001457	229800.42	17.7960	21.8600	20.3360	367.2105	20.8440	386.8732	-38.7061	-15.5961	1077152
58	0.5080	0.80	0.40	867.280	0.001343	262405.15	18.3961	22.4601	20.9361	289.4539	21.4441	282.6280	13.4368	18.3169	1809540
59	0.5080	0.80	0.60	910.920	0.001230	301022.84	19.0385	23.1025	21.5785	163.4122	22.0865	161.0143	4.7203	3.3705	1521862
60	0.5080	0.80	0.80	954.560	0.001116	347485.83	19.7341	23.7981	22.2741	54.1304	22.7821	51.9122	4.3665	4.2291	1136274
61	0.5080	1.20	0.20	823.640	0.001457	344700.63	19.6945	23.7585	22.2345	310.0115	22.7425	305.7705	8.3484	8.2372	1081104
62	0.5080	1.20	0.40	867.280	0.001343	393607.72	20.3587	24.4227	22.8987	256.5443	23.4067	254.4765	4.0705	4.3652	1332330
63	0.5080	1.20	0.60	910.920	0.001230	451534.26	21.0696	25.1336	23.6096	152.0004	24.1176	149.4159	5.0876	5.2772	1323270
64	0.5080	1.20	0.80	954.560	0.001116	521228.75	21.8394	25.9034	24.3794	60.6349	24.8874	56.0339	9.0571	9.3876	1161300

5.7 Conclusions

This study including the effect of some new large diameters such as 0.127, 0.254 and 0.508 m on pressure gradient in horizontal pipe with different water volume fraction such as 20, 40, 60 and 80 %, different mixture velocities such as 0.2, 0.5, 0.8 and 1.2 m/s.

The results reveal that the choice of large diameters for oil-water stratified flow has a critical effect on the pressure gradient. The studies of Angeli and Hewitt, (1999), Al-Yaari et al. (2009) and Sandra et al. (2008) didn't including the large diameters effect on the pressure gradient. Realizable k-ε and Shear Stress Transport k-ω turbulence models are also compared to experimental data in literature. Generally, the pressure gradient is found by the Shear Stress Transport k-ω model better than those found by Realizable k-ε turbulence model.

CHAPTER 6

CONCLUSIONS

6.1 Conclusion

In the present thesis, a research is conducted to have an understanding on the oil-water stratified or stratified wavy flow phenomenon in horizontal steel pipes. The study provides a framework with using ANSYS FLUENT commercially available CFD simulation software in order to take the advantage of using of a CFD and selected volume of fluid (VOF) oil-water phases model. From the post processing results of stratified or stratified wavy flow analyses by realizable k-ε and shear stress transition k-ω turbulence model, the following conclusions have been evaluated.

- The diameter (D), water volume fraction (α) and mixture velocity (υ_m) can clearly influence the pressure gradient for a two-phase oil-water mixture in a horizontal steel pipe. The pressure gradient increases as considerably for a small diameter pipe such as 0.0254 m with increasing mixture velocity. However, the pressure gradient for a large diameter pipe more than 0.127 m decreases and stabilizes with high mixture velocities. This is caused by the flow in a large diameter and long length of pipe. As a result of this research and previous experimental studies in the literature showed that pressure gradient increasing with the pipe diameter.
- The two-phase oil-water stratified flow includes difficulties in the specification and introduction of the flow field geometry. To represent the

stratified flow and stratified wavy flow by CFD, phase volume fraction determination plays a significant role. The stratified flow is clearly detected in the cases for velocities between 0.2 m/s and 1.2 m/s. The stratified wavy flows have been detected for 0.5 and 0.8 m/s mixture velocities with 40 % and 60 % water volume fractions by Realizable k-ε and Shear Stress Transition k-ω turbulence models.

- The pressure gradient is found by the Shear Stress Transport k-ω model better than those is found by Realizable k-**ε** turbulence model.

- The oil volume fraction distribution and oil-water layers are predicted for all flow conditions and turbulence models used in this study. Mesh independence studies were performed to ensure that the computed results were independent of the chosen mesh.

6.2 Future Works

The two phase flow, especially oil-water flow in a horizontal pipe are very popular and continuously in progress. The studies in this field by ANSYS FLUENT software are very limited.

In this study, simulation and analysis were performed for oil fields. However, numerical and analyses experimental studies should be performed for an extraction station and transportation of oil. Moreover, the other regimes (slug, plug, etc....), in long pipes and large diameter pipes over 0.5 m can be studied by CFD simulation, as future works.

REFERENCES

Anand B. Desamala, Anjali Dasari, Vinayak Vijayan, Bharath K. Goshika, Ashok K. Dasmahapatra, and Tapas K. Mandal. (2013). CFD Simulation and Validation of Flow Pattern Transition Boundaries during Moderately Viscous Oil-Water Two-Phase Flow through Horizontal Pipeline. World Academy of Science, Engineering and Technology, 73.

Angeli P., G.F. Hewitt. (1998). Pressure gradient in horizontal liquid-liquid Flows. *International Journal of Multiphase Flow*, **24,** 1183-1203.

Angeli P., G.F. Hewitt. (1999). Flow structure in horizontal oil-water flow. *International Journal of Multiphase Flow*, **26,** 1117-1140.

Al-Yaari M., A. Soleimani, B. Abu-Sharkh, U. Al-Mubaiyedh, A. Al-sarkhi. (2009). Effect of drag reducing polymers on oil–water flow in a horizontal pipe. *International Journal of Multiphase Flow*, **35,** 516–524.

Al-Wahaibi Talal. (2012). Pressure gradient correlation for oil–water separated flow in horizontal pipes. *Experimental Thermal and Fluid Science*, **42,** 196–203.

ANSYS package help, version 14.0 (2011).

Bakker A. (2001). Realize grate benefits from CFD. Fluid Solids Handling, March, pp 45-53.

Berger, R. C., and Stockstill, R. L. (1999). A finite-element system for flows.

Carlos F. Torres. (2006). Modeling of oil-water flow in horizontal and near horizontal pipes. Ph. D. The Graduate School, the University of Tulsa.

Charles H. Newton, Masud Behnia (2000). Numerical calculation of turbulent stratified gas-liquid pipe flows. *International Journal of Multiphase Flow*, **26,** 327-337.

DeJesus, J.M. (1997). An experimental and numerical investigation of two-phase slug flow in a vertical tube. Ph. D. thesis, University of Toronto, Canada.

Florian R. Menter. (1994). Improved Two-Equation k-ω Turbulence Models for Aerodynamic Flows. NASA Technical Memorandum 103975.

Fluent User Services Center, (2013). www.fluentusers.com.

Fritz J. and Dolores H. Russ (2001). Study of oil-water flows in large diameter horizontal pipelines. Ph.D. College of Engineering and Technology, Ohio University.

Graham. B. Wallis. (1969). One-dimensional two-phase flow. By McGraw-Hill.

Ityokumbul M. T., N. Kosaric, W. Bulani. (1994). Gas hold-up and liquid mixing at low and intermediate gas velocities I. Air-water system. The chemical engineering journal, Volume **53,** Issue 3, February, Pages 167‑172.

Hua Shi, J.Y. Cai, and W.P. Jepson. (1999). Oil-water distribution in large diameter horizontal pipelines. Multiphase Flow and Heat Transfer, Proc .of the Fourth International Symposium Aug. 22-24, Xi'an China.

Hui Gao, Han-Yang Gu and Lie-Jin Guo. (2002). Numerical study of stratified oil–water two-phase turbulent flow in a horizontal tube. *International Journal of Heat*

and Mass Transfer, **46,** 749–754.

http://esi-cfd.com/esi-users/turb_parameters.

Jepson W. P., R. E. Taylor. (1993). Slug flow and its transition in large diameter horizontal pipes. *International Journal of Multiphase Flow* Vol. **19.** NO.3, pp. 411-420.

Ing-yuXu, Ying-xiang Wu, Fei-feiFeng, Ying Chang and Dong-hui Li. (2008). Experimental investigation on the slip between oil and water in horizontal pipes. Experimental Thermal and Fluid Science, **33,** 178–183.

John R. Thome. (2010). Engineering data book III. By Wolverine Tube, Inc. All rights reserved.

Langley Research Center of NASA. (2013). Turbulence Modeling Resource. http://turbmodels.larc.nasa.gov/wilcox.html.

Launder, B., and Spalding, D. (1974). The numerical computation of turbulent flows, Computer Methods in Applied Mechanics and Engineering, **3,** 269-289.

Lockhart, R.W. and Martinelli, R.C. (1949). Proposed Correlation of Data for Isothermal Two-Phase, Two-Component Flow in Pipes. Chem. Eng. Prog., **45,** pp. 39-48.

Lovick J., P. Angeli. (2004). Experimental studies on the dual continuous flow pattern in oil–water flows. *International Journal of Multiphase Flow*, **30,** 139–157.

Luis Mora Vallejo and Jacobo Zegri Reiriz. (2011). A theoretical and experimental study of horizontal air-water two-phase flow with a spool piece.

Manchester Center for Nonlinear Dynamics, (2013). http://www.mcnd.manchester.ac.uk/pictures.php.

Mohammed A. Al-Yaari and Basel F. Abu-Sharkh. (2011). CFD Prediction of Stratified Oil-Water Flow in a Horizontal Pipe. *Asian Transactions on Engineering* (ATE ISSN: 2221-4267), Volume **01**, Issue 05.

Mouza A.A., Paras S. V.and Karaelas A. J. (2001). CFD code application to wavy stratified gas-liquid flow. Institution of chemical engineering.

Mukhtar Abdulkadir. (2011). Experimental and Computational Fluid Dynamics (CFD) Studies of Gas-Liquid Flow in Bends. Ph. D. Department of Chemical and Environmental Engineering, University of Nottingham.

Newton C. H., M. Behnia. (2001). A numerical model of stratified wavy gas–liquid pipe and flow. Chemical Engineering Science, **56**, 6851–6861.

Paulo A.B. de Sampaioa, Jose L.H. Faccinia,b, Jian Su. (2008). Modeling of stratified gas–liquid two-phase flow in horizontal circular pipes. International Journal of Heat and Mass Transfer, **51**, 2752–2761.

Pope, S.B. (2000). Turbulent flow. Cambridge: Cambridge University Press.

Rashmi G. Walvekar , Thomas S.Y. Choong, S.A. Hussain, M. Khalid, T.G. Chuah. (2009) Numerical study of dispersed oil–water turbulent flow in horizontal tube. *Journal of Petroleum Science and Engineering*, **65,** 123–128.

Ramos-Banderas, A., Morales, R. D., Sanchez-Perez, R., Garcia-Demedices, L., and Solorio-Diaz, G. (2005). Dynamics of two-phase downwards flow in submerged entry nozzles and its influence on the two-phase flow in the mold. International

Journal of Multiphase Flow, **31,** 643-665.

Russell, T.W.R. Hodgsen, G.W. and Govier, G.W. (1959). Horizontal Pipeline Flow of Mixtures of Oil and Water. Can. J. Chem. Eng., **37,** pp. 9-17.

Sandra C.K. De Schepper, Geraldine J. Heynderickx , Guy B. Marin. (2008). CFD modeling of all gas–liquid and vapor–liquid flow regimes predicted by the Baker chart. *Chemical Engineering Journal*, **138,** 349–357.

Siti A. slina Hussain, Soo Mee Khuan. (2009) CFD model for determining local phase fraction oil-water dispersion in turbulent flow.

Steel pipe wall thicknesses & weights. (2013). www.standardne.com.

Valls. A. (2000). Three phase gas-oil-water pipe flow. Ph.D. Dissertation, Imperial College, University of London.

Venkatesan M., Sarit K. Das, A.R. Balakrishnan. (2011). Effect of diameter on two-phase pressure drop in narrow tubes. *Experimental Thermal and Fluid Science*, **35,** 531–541.

Versteeg, H. K., Malalasekera, W. (2007). An Introduction to Computational Fluid Dynamics.2nd Edition, UK.

Veronica Miller. (2010). Dynamic modeling and environmental analysis of hydrokinetic energy. Ph. D. Thesis University of Pittsburgh.

White F. (1997). Fluid Mechanics. By McGraw-Hill.

Xiao-XuanXu. (2007). Study on oil–water two-phase flow in horizontal pipelines. *Journal of Petroleum Science and Engineering*, **59,** 43–58.

Yemada Taitel, A. E. Dukler. (2004). A model for predicting flow regime transitions in horizontal and near horizontal gas-liquid flow.

Yih, C. (1967). Instability due to Viscosity Stratification. J. Fluid Mech., **27,** pp. 337-352.

Yuling LÜ, LiminHE, Zhengbang HE, Anpeng WANG. (2012). A Study of Pressure Gradient Characteristics of Oil-Water Dispersed Flow in Horizontal Pipe.